



# ScuDo

Scuola di Dottorato ~ Doctoral School  
WHAT YOU ARE, TAKES YOU FAR



Doctoral Dissertation  
Doctoral Program in Electrical, Electronics and Telecommunications Engineering  
(33<sup>th</sup> Cycle)

# Synthetic models of distribution gas networks in low-carbon energy systems

**Enrico Vaccariello**

\* \* \* \* \*

## Supervisors

Prof. Igor S. Stievano

Prof. Pierluigi Leone

## Doctoral Examination Committee:

Prof. Sami Barmada, Università di Pisa

Prof. Flavio Canavero, Politecnico di Torino

Prof.ssa Flavia Grassi, Referee, Politecnico di Milano

Prof. Antonino Laudani, Università degli Studi Roma Tre

Prof. Walter Zamboni, Referee, Università degli Studi di Salerno

Politecnico di Torino

June 2021

This thesis is licensed under a Creative Commons License, Attribution - Noncommercial - NoDerivative Works 4.0 International: see [www.creativecommons.org](http://www.creativecommons.org). The text may be reproduced for non-commercial purposes, provided that credit is given to the original author.

I hereby declare that the contents and organisation of this dissertation constitute my own original work and does not compromise in any way the rights of third parties, including those relating to the security of personal data.

.....

Enrico Vaccariello

15<sup>th</sup> June 2021

# Summary

Gas networks are crucial assets in today's energy supply chain and are currently playing a key complementary role in the on-going decarbonization of energy systems. On the one hand, gas infrastructures are excellent candidates to provide strategic flexibility and reliability to future energy systems based on variable renewable sources of energy. On the other hand, switching from fossil natural gas to renewable or low-carbon gases is an unavoidable condition to keep the infrastructure running.

Increasing attention is therefore being devoted by policymakers, industrial players and academics, to the deployment of "green" gases in existing gas grids. Hydrogen and biomethane constitute the most promising options for an affordable decarbonization of the gas sector. Their integration into the grids comes with technical and operational challenges, as well as with opportunities of cross-sectorial couplings with, for example, the power grid.

The distributed injection of alternative gases – especially hydrogen – in pure form or blended with natural gas, affects the system hydraulics, changes the thermophysical properties of the transported fuel and raises concerns of safety at the end-users' appliances and of material compatibility within the infrastructure. On the other hand, significant benefits may derive by the deployment of low-carbon gases in the context of multi-energy systems where the electrical and gas grids interact through coupling technologies like power-to-gas.

Extensive research is therefore being carried out to assess the behaviour of gas grids in presence of distributed injections of alternative fuels, verify the compliance with gas quality prescriptions and hydraulic limits (e.g., pressures and velocities), and test new management schemes for both gas networks and integrated electricity and gas grids.

Most of the simulation studies, however, derive their results from only one or a limited number of network models. The findings of these works are therefore

affected by a substantial case-specificity, which partially limits their validity and prevents their generalisation to other case studies.

To overcome this limitation, the present work proposes a tool for the synthetic generation of statistically similar gas network models, readily deployable for simulation applications at distribution-level systems. The main purpose of the tool is enabling the execution of simulative experiments over several (virtually infinite) case studies, with evident benefits in terms of validity and extendibility of the results. Attention is given to both topological and technical realism of the synthetic network models.

A topological approach supported by complex networks and system theoretical tools is undertaken to provide a structural characterization of gas grids, described with a graph-based representation. Structural information is therefore deployed to calibrate and validate a probabilistic generator of synthetic topologies, capable of delivering complex network structures with multiple pressure tiers. Network models are subsequently finalized by assigning technical specifications. This is addressed by means of a custom technical designer performing the correct and realistic sizing of distribution systems according to arbitrary design parameters.

The tool proves to successfully generate thousands of finished models of synthetic networks. A subset of synthetic grids is therefore deployed to study the effect of injecting hydrogen in distribution gas networks. Increasing penetrations of hydrogen are considered, and the impacts on the system hydraulics and gas quality are derived statistically.

The tool effectively enables a novel methodology for network simulations and offers a powerful support to studies with a systematic and generalized approach. Further perspective applications look promising and will contribute to a broader assessments of gas grids in low-carbon and integrated energy environments.

# Table of Contents

<b>1</b>	<b>Table of Contents .....</b>	<b>III</b>
<b>1</b>	<b>Introduction.....</b>	<b>1</b>
1.1	Background.....	1
1.2	Current role of gas and perspective uses in low-carbon energy systems.....	3
1.3	Modelling of gas networks in low-carbon scenarios .....	7
1.4	Uses of synthetic grid models for energy network analyses .....	10
1.5	Motivations, objectives, and structure of the work.....	12
<b>2</b>	<b>Topological modelling of distribution gas networks .....</b>	<b>15</b>
2.1	Introduction .....	15
2.1.1.1	<i>Description of the case studies .....</i>	<i>17</i>
2.2	Topological properties of distribution gas grids .....	20
2.2.1	Degree related topological properties .....	20
2.2.2	Length related topological properties .....	21
2.2.2.1	<i>Pipeline lengths .....</i>	<i>22</i>
2.2.2.2	<i>Average path length.....</i>	<i>22</i>
2.2.3	Clustering of nodes .....	23
2.2.3.1	<i>Global clustering coefficient .....</i>	<i>23</i>
2.2.4	Loops related topological properties.....	24
2.2.4.1	<i>Number of cycles .....</i>	<i>25</i>
2.2.4.2	<i>Length and location of cycles .....</i>	<i>26</i>

<b>2.3</b>	<b>Generation of statistically similar topologies of distribution gas grids</b>	<b>28</b>
2.3.1	Description of case study: multi-level distribution gas grid.....	30
2.3.2	Spatial distribution of nodes in the synthetic network.....	30
2.3.2.1	<i>Spatial distribution of the synthetic nodes</i> .....	31
2.3.2.2	<i>Identification of subnetwork islands</i> .....	32
2.3.3	Establishment of basic connectivity: formation of tree .....	34
2.3.4	Network reinforcement: creation of cycles.....	34
2.3.4.1	<i>Street-level networks</i> .....	35
2.3.4.2	<i>Long-range distribution networks</i> .....	35
2.3.5	Links among the pressure levels.....	36
<b>2.4</b>	<b>Model evaluation .....</b>	<b>37</b>
2.4.1	Methods for assessing the structural similarity.....	38
2.4.1.1	<i>Comparison of degree distributions</i> .....	39
2.4.1.2	<i>Comparison of line length distributions</i> .....	39
2.4.2	Topological properties of synthetic networks.....	40
2.4.2.1	<i>Level 1 (4<sup>th</sup> species)</i> .....	40
2.4.2.2	<i>Level 2 (6<sup>th</sup> species)</i> .....	42
2.4.2.3	<i>Level 3 (7<sup>th</sup> species)</i> .....	42
<b>2.5</b>	<b>Concluding remarks.....</b>	<b>43</b>
<b>3</b>	<b>Technical design of distribution gas grids.....</b>	<b>45</b>
<b>3.1</b>	<b>Design criteria for gas distribution systems: standards and best practices .....</b>	<b>45</b>
3.1.1	Estimation of gas demand.....	47
3.1.2	System layout and pipeline locations.....	47

3.1.3	Hydraulic design .....	48
<b>3.2</b>	<b>Gas network technical designer .....</b>	<b>51</b>
3.2.1	Purpose of the algorithm.....	51
3.2.2	Structure of the algorithm .....	54
3.2.3	Oversizing the networks .....	56
3.2.4	Design of multi-source and multi-pressure systems .....	57
<b>4</b>	<b>Structural and hydraulic properties of synthetic gas network models.....</b>	<b>60</b>
4.1	Generation of synthetic case studies .....	60
4.2	Case A: constraint-free generation of synthetic networks .....	64
4.3	Case B: generation of synthetic networks with technical and topological constraints .....	68
4.4	Case C: a-posteriori selection of the synthetic networks .....	71
4.5	Application to other reference case studies .....	74
<b>5</b>	<b>Statistical assessment of the injection of hydrogen in distribution gas grids .....</b>	<b>78</b>
5.1	Introduction .....	78
5.2	Rationale for the study and methodology .....	82
5.3	Effect of blending hydrogen in distribution gas grids .....	87
5.3.1	Case A: effect of hydrogen injection nearby the NG source .....	88
5.3.2	Case B: effect of hydrogen injection at arbitrary locations in the grid	
	94	
5.4	Concluding remarks.....	99
<b>6</b>	<b>Conclusions.....</b>	<b>101</b>

# List of Tables

Table 1. Description of the original set of distribution systems used for the study. .....	18
Table 2. Description of the system <i>islands</i> extracted and used for the topological analysis.....	19
Table 3. Summary of the structural properties of the investigated gas networks..	28
Table 4. Selected values of $\alpha$ , $\beta$ and $\gamma$ for the reference distribution network.....	37
Table 5. Summary of the structural properties of the synthetic and the reference gas networks, for each pressure level of the network. ....	41
Table 6: Definition of pressure tiers of gas distribution systems for several European Countries. High-pressures are included when specific definitions within the distribution system are applied. Source: adapted from [86]. ....	46
Table 7: Classification and operational bounds of medium and low-pressure networks according to Italian legislation and standards. ....	49
Table 8: Diameter sizes from real-world Italian distribution systems.....	52
Table 9: Inputs required by the tool for the technical design of distribution gas networks.....	53
Table 10. Design parameters used for the technical sizing of the synthetic networks.....	63
Table 11. Limits to volume concentrations of hydrogen in natural gas according to international legislations [93]. ....	79
Table 12. NG quality constraints as from Italian legislation [94]. ....	80
Table 13. Properties of the statistically similar networks used in the study and input parameters deployed for their technical sizing. ....	83

# List of Figures

Figure 1. Structure and workflow of the thesis.....	14
Figure 2. Degree distributions by pressure tiers of investigated real-world gas networks.....	21
Figure 3. Length distributions of pipelines belonging to different pressure tiers of investigate networks. Lengths are computed as point-to-point Euclidean distances between the connected nodes. Lengths are in m and their logarithm is natural logarithm.....	22
Figure 4. Variation of the average path length in <i>meters</i> (A) and <i>hops</i> (B) in the sampled networks, in function of the network size – total length (A) and number of nodes (B). .....	23
Figure 5. Number of cycles of gas distribution grids against total network length. ....	25
Figure 6. Comparison of network loops (highlighted in orange) in (A) MP system (4 <sup>th</sup> <i>species</i> ) and (B) LP system (7 <sup>th</sup> <i>species</i> ). .....	26
Figure 7. Comparison of cycle lengths in medium pressure (4 <sup>th</sup> <i>species</i> ) and low pressure (7 <sup>th</sup> <i>species</i> ) systems. ....	27
Figure 8. Relation between node degrees and average distance from 10 closest neighbours for nodes in LP (7 <sup>th</sup> <i>species</i> ) networks .....	27
Figure 9. High-level diagram of the algorithm designed for the generation of synthetic network topologies. ....	29
Figure 10. Real-world distribution gas grid adopted as reference case study. ....	30
Figure 11. Real nodes of the gas network and synthetic nodes generated using GMM for each pressure level. Numbers of GMM components are 50, 36 and 11 in Levels 1, 2 and 3. ....	32

Figure 12. Clusters of synthetic nodes detected for (a) Level 2 and (b) Level 3, displayed with different colours. The nodes of Level 2 and 3 are the same as displayed in Figure 11.....	33
Figure 13. (a) Close-up of a stand-alone synthetic island of Level 2; (b) connection of the island to the upper network level by means of reduction stations (b). Connections within the island were generated with parameters $\alpha = 28 (m)$ , $\beta = 326 (m)$ and $\gamma = 116 (m)$ .....	36
Figure 14. Sensitivity of level-1 network topologies to the choice of parameter $\alpha$ . .....	37
Figure 15. Sample of one out of 100 multi-level synthetic gas networks generated by the algorithm with the parameter selection of Table 4. ....	38
Figure 16. Degree distributions by pressure tiers of synthesized gas networks.....	40
Figure 17. Length distributions of pipelines belonging to different pressure tiers in synthesized networks. Lengths are computed as point-to-point Euclidean distances between the connected nodes. Lengths are in m and their logarithm is natural logarithm.....	40
Figure 18: Distribution of diameter sizes by pressure tier, as from the sample of real-world Italian distribution grids. ....	52
Figure 19: Diagram of the algorithm accomplishing the technical design of distribution gas networks with given topology and target operational restrictions. Conditions imposed for the identification of the pipelines are highlighted.....	59
Figure 20. Time required for the creation of finished network models with increasing number of network nodes. Results refer to 20 different executions for each network size.....	61
Figure 21. Real-world MP distribution grid used as reference. The width of the edges (pipelines) of the graph is proportional to the diameter values. For comparison: the largest pipeline (connected to the source node) has a diameter of 0.25 m. ....	61
Figure 22. Process for the creation of ten thousand finished gas network model .	64

Figure 23. Ten random samples out of the 10,000 networks generated in the constraint-free synthetization process.....	65
Figure 24. Cumulative gas loads against their distance from the supply node. The chart includes the information for the real-world network used as reference, for comparison.....	66
Figure 25. Structural properties and fluid-dynamic response of synthetic networks generated by the algorithm in the constraint-free process. Cumulative distribution functions (CDF) of diameters, pressures and velocities are illustrated as overlaid histograms. Boxplots are added for a complete description of the CDF values. ...	67
Figure 26. Ten random samples out of the 10,000 networks generated in the constrained synthetization process.....	69
Figure 27. Cumulative gas loads against their distance from the supply node. The patterns of gas consumption within the synthetic networks are constrained to follow the behaviour of the reference real-world gas grid, as visible from the fine agreement of the grey curves and the reference red line. ....	70
Figure 28. Structural properties and fluid-dynamic response of synthetic networks generated by the algorithm in the constrained process. Cumulative distributions functions (CDF) of diameters, pressures and velocities are illustrated as overlaid histograms. Boxplots are added for a complete description of the CDF values. ...	70
Figure 29. Statistical distribution (CDF) of pressures in the 10,000 synthetic networks generated in Case A (see panel C in Figure 24). Colours indicate the fit between the curves and the target reference, expressed by the two-sample KS statistic (KSstat2).....	72
Figure 30. Resulting selection of the networks featuring the most similar pressure distributions to the target reference ( $KSstat2 \leq 0.2$ ). See Figure 28 for comparison. ....	73
Figure 31. Anonymized twin of the reference network of Figure 20, featuring similar hydraulic behaviour (pressure profile).....	73
Figure 32. Results obtained with the application of the tool to first alternative network. Panel A illustrates the reference real-world grid; panel B illustrates a	

sample of 4 synthetic networks; panels C, D, E, F provide the statistical structural and hydraulic properties of the synthetic grids. ....	76
Figure 33. Results obtained with the application of the tool to second alternative network. Panel A illustrates the reference real-world grid; panel B illustrates a sample of 4 synthetic networks; panels C, D, E, F provide the statistical structural and hydraulic properties of the synthetic grids. ....	77
Figure 34. Variation of thermophysical properties of hydrogen-methane blends with volume concentrations of H <sub>2</sub> : (A) HHV, (B) specific gravity, (C) Wobbe index.....	81
Figure 35. Diagram of the statistical study on H <sub>2</sub> injection in distribution gas grids. ....	87
Figure 36. Distribution of H <sub>2</sub> concentrations received by consumption nodes: fraction of load nodes for which the received H <sub>2</sub> molar concentration exceeds a given value. Hydrogen injection is constrained close to NG source. ....	89
Figure 37. Tracking of gas quality for four sample networks featuring increasing levels of H <sub>2</sub> injections. H <sub>2</sub> injection point is constrained close to the source of NG. ....	91
Figure 38. Evolution of average (panel A) and maximum (panel B) gas velocity in pipelines with increasing H <sub>2</sub> concentrations. H <sub>2</sub> injection point is constrained close to NG source. ....	92
Figure 39. Evolution of average (panel A) and minimum (panel B) nodal pressures with increasing H <sub>2</sub> concentrations. H <sub>2</sub> injection point is constrained close to NG source. ....	92
Figure 40. Evolution of higher heating value (panel A), specific gravity (panel B) and Wobbe Index (panel C) of blend with highest concentration of H <sub>2</sub> received by load nodes. H <sub>2</sub> injection point is constrained close to NG source. ....	93
Figure 41. Distribution of H <sub>2</sub> concentrations received by consumption nodes: fraction of load nodes for which the received H <sub>2</sub> molar concentration exceeds a given value. H <sub>2</sub> injection point is freely placed in the grid.....	95

Figure 42. Tracking of gas quality for four sample networks featuring increasing levels of H <sub>2</sub> injections. H <sub>2</sub> injection point is freely placed close to the source of NG.....	96
Figure 43. Evolution of average (panel A) and maximum (panel B) gas velocity in pipelines with increasing hydrogen concentrations. H <sub>2</sub> injection point is freely placed in the grid.....	97
Figure 44. Evolution of average (panel A) and minimum (panel B) nodal pressures with increasing hydrogen concentrations. H <sub>2</sub> injection point is freely placed in the grid.....	97
Figure 45. Evolution of higher heating value (panel A), specific gravity (panel B) and Wobbe Index (panel C) of blend with highest concentration of H <sub>2</sub> received by load nodes. H <sub>2</sub> injection point is freely placed in the grid.....	98



# Chapter 1

## Introduction

### 1.1 Background

The ongoing transition towards a low carbon emissions energy system involves a deep transformation in the whole supply chain of energy, where *flexibility*, i.e., the capability to readily adapt to uncertain conditions, is key to integrating new and diversified energy sources, vectors, and market solutions.

At present time, the electricity sector has undoubtedly undergone the fastest shift to renewable energy sources (RES). The installed capacity of electrical renewable sources of energy more than doubled since 2010, reaching 2.5 TW of installed capacity in 2019, almost half of which (47%) from variable sources like solar photovoltaics (PV) and wind [1]. Additional efforts are required for a deep decarbonization of the power sector. Nevertheless, renewables already accounted for 26% of worldwide electricity generation in 2019 and covered 37% of production in Europe [2].

These results have been enabled by several supporting policies put in place in the effort to limit the climate-change related temperature rises to 1.5°C above pre-industrial levels – as internationally agreed in Paris in 2015 [3]. Further ambitious targets and novel support mechanisms are being issued, as the new decade to 2030 and the Covid-19 health and economic crisis call for an update of the decarbonization agendas. With the binding objectives set by the Directive 2018/2001/EC [4], the European Union commits to satisfy 32% of its gross final energy consumption with renewables, targeting reductions in greenhouse gas

(GHG) emissions for 45% with respect to 1990 levels in the framework of the *Clean Energy for all Europeans* Package [5]. Additionally, climate objectives for 2030 will be formally pushed to 55% reduction of GHG emissions by June 2021, in view of a detailed implementation of the plans announced by the European Commission in September 2020 [6].

In line with the current trends, the power sector is expected to play a pivotal role in the achievement of EU and international ambitious targets, integrating large quantities of RES and gaining increased market shares. Projections elaborated in several institutional energy outlooks, realized with a diversity of tools, inputs and purposes, agree that the decarbonization of the energy systems will necessarily involve a particularly high penetration of renewables in electricity [7]. For a 30% of renewable energy share in gross energy production, RES are expected to penetrate in the power sector by 50%. The International Energy Agency (IEA) foresees a RES contribution of 40% in the 2030 worldwide electricity mix, if the objectives of the currently issued policies are met without further fortifications (*STEPS* scenario in *World Energy Outlook 2020*) [8]. In Europe, latest objectives indicated by the European Commission [6] envisage a minimum share of renewable electricity generation equal to 65% by 2030.

Although electricity will most certainly have a central role in the future energy mix, a full system electrification supported by electric RES (E-RES) would be hardly achievable, nor would it be desirable in terms of overall system resilience [8]. The accommodation of significant shares of E-RES poses concerns of stability and quality of supply both in transmission and distribution (T&D) grids. Additionally, it necessarily involves massive investments in grid expansions and high costs associated to hourly and seasonal storage capacity. As power electronics interface RES-E plants with the networks, transmission systems feature decreasing system inertia, becoming vulnerable to the frequent supply-demand mismatches driven by the generation from variable renewables (V-RES). The consequent challenges related to system balancing at different time scales require foreseeing additional back-up thermal capacity and (inter)connection reinforcements [9], faster frequency response [10], as well as load shifting and shedding [11]. Furthermore, issues related to thermal limits violations, over voltages, reverse power flows, phase unbalances and increased system losses are

emerging in distribution grids (i.e., medium and low-voltage) with high shares of distributed generation (DG) [12–14].

Challenges related to a widespread system electrification are not purely of infrastructural nature, but rather derive from technological limits too. The current electrical power technology portfolio is in fact mostly unsuitable for numerous energy-intensive sectors like shipping, aviation, heavy-duty transport and industrial processes including steel and cement production. [8,15].

This picture suggests that the transformation should extend well beyond electricity, embracing sectors like heating and cooling, fuels and transports that, despite their weighty role in today's energy uses and related emissions, are currently lagging behind in the path of decarbonization. For a higher affordability and resilience of a low-carbon system, the transition should be unfolded in the framework of a diversified multi-energy system, where energy subsectors and the related infrastructures interact at various levels (including community, district and Country layers) [16].

## **1.2 Current role of gas and perspective uses in low-carbon energy systems**

Natural gas (NG) represents a major backbone of today's energy system. Worldwide gas consumption has recorded a significant increase in the last decade. With 3379 million tons of oil equivalent (Mtoe), NG accounted for 23% of the world total primary energy consumption in 2019 [8]. According to the most recent figures of IEA (referred to 2018), more than 40% of the natural gas supplies are deployed in the power generation sector, being responsible for 23% of the production of electricity worldwide [17]. The largest part of the remaining supplies is consumed by industrial (37%) and residential users (30%). Minor shares are deployed in commercial and services (13%) and transport (7%) sectors.

In Europe, NG accounts for 37% of the total energy demand in the residential sector, covering almost half (45%) of the space heating needs of dwellings [18]. Significant differences are found amidst European Countries, as UK, Germany, Italy, France and The Netherlands account for more than 80% of EU-28 NG consumption for residential heating [19].

Despite the uncertainties that the oil and gas (O&G) sector faces as a result of the ongoing Covid-19 crisis – which led to a significant decrease in the demand

and to consequent price reductions that are expected to affect the sector for years to come – latest projections of IEA foresee that NG may still play a crucial role in the energy transition of the next two decades [8]. The actual demand of gas will significantly depend on the policies that will be implemented. Nevertheless, NG still covers at least 24% and 23% of global primary energy demand in 2030 and 2040 respectively and, in all the scenarios, a growth of consumptions to 2030 is projected.

One of the principal drivers of the worldwide increase in the NG consumption relies in the installment and reconversion of gas-fired power plants, in partial substitution of the coal generation fleet. Not only gas-fired power plants provide lower emission factors to the power grid, but they also respond to the increasing necessity of putting in place a highly flexible back-up fleet with a fast response to RES variations [9,20,21]. The process already broadly took place in USA and Europe, where it is likely to decline along the next decade. However, a substantial boost is projected in the Chinese market and other emerging economies, along with a massive deployment of gas in the industrial sector [8]. In this regard, natural gas is functional to the integration of variable E-RES, counterbalancing their intrinsic variability.

The deployment of NG, however, cannot be an end in itself. The IEA estimates that in the future two decades the CO<sub>2</sub> emissions avoided by switching to NG from other carbon-intensive fuels may be heavily outweighed by the reductions obtained by switching away from natural gas [8]. Strategies for the decarbonization of the gas sector have therefore been drawn by the industry and policymakers, in the effort to preserve the future role of the gas grid infrastructure in a low-carbon system. The principal outlined paths involve a substantial reconversion to renewable gases (e.g., hydrogen and biomethane), the deployment of carbon capture and storage (CCS) technologies and an enhanced integration with other energy subsectors.

The perspective achievement of a higher integration among energy subsystems has gained an increased momentum in the latest years, and has been formally implemented in the European policies towards climate neutrality through the European Strategy for Energy System Integration [22]. In this framework, the gas infrastructure should reinforce and create new links with other sectors (e.g., electricity grids), provide a complementary support to the integration of

renewables, and facilitate the decarbonization of heating, transport, and other subsectors where infrastructural limits may prevent the electrification of end-uses. If the conditions to decarbonize and repurpose the gas networks in a *net-zero* Europe are met, yearly savings may amount up to 217 billion euros with respect to the alternative reconversion (e.g., electrification) of most of today's gas-based energy uses (as estimated by the *Gas for Climate* consortium [23]). Gas systems, in fact, constitute valuable assets with a pivotal capacity of transporting energy, an unequalled flexibility (provided by storage facilities and the intrinsic compressibility of gas), and geographical pervasiveness, extension and capillarity (approximately 1.7 million km of pipelines in Europe, most of which at distribution level [23]).

One of the most promising coupling options among the power and gas sectors, as indicated in the European Strategy for Energy System Integration [22], is represented by electrolysis. Electrolysers produce a gaseous fuel, namely hydrogen, exploiting electrical power. Among the possible options, hydrogen produced in this way can be deployed as an industrial feedstock or as a fuel for mobility [15]. In other cases, it can substitute conventional gaseous fuels (e.g., methane) in pure, blended or methanised (i.e., synthetic natural gas, SNG) forms [24,25]. The key benefits of using hydrogen instead of fossil gases is that there are no CO<sub>2</sub> emissions at its point of use. Furthermore, its whole fuel supply chain features net-zero emissions when the fuel production is based on renewable-powered electrolysis or traditional processes coupled with CCS (mostly steam methane reforming, SMR, although alternative feedstocks and technologies are available) [26]. The practice of injecting and distributing hydrogen within the existing gas networks in blended form is suggested in the European Hydrogen Strategy, especially in a transitional and scaling up stage [27,28]. Hydrogen is already being deployed in the gas pipelines in more than 20 ongoing power-to-gas (PtG) projects [24,25,29] and the number of pilot and full-scale demonstrators is expected to raise in the next future, as the European Commission envisages up to 470 billion euros of investments and several funding programmes for the hydrogen sector [27,30].

In the framework of a gas sector heavily relying on renewable gases, IEA estimates that the global yearly demand of hydrogen may amount to 18 Mt (600 TWh) in 2030, raising to 75 Mt (2500 TWh) in 2040 [8]. Projected values for

2040 correspond to approximately 6% of energy supplied by NG in 2019. More ambitious scenarios outlined by mixed private and public consortia in the gas, hydrogen and fuel cell sector envision up to 1710 TWh [23] and 2250 TWh [31] by 2050 in European Union, respectively representing 38% and 51% of the energy currently (2019) consumed in EU under the form of NG.

Whether these ambitions will be actually met depends on the combined and reciprocal effect of supportive policies, price evolution of fossil fuels and reduction of technology costs. In the latter regard, electrolytic hydrogen production costs may be abated down to 1.8 \$/kg by 2030<sup>1</sup>, if policy and research efforts towards the establishment of economies of scale are put in place [8].

The deployment of hydrogen may require significant modifications to the existing infrastructure, especially at transmission level, due to material incompatibilities that may arise in steel pipelines (embrittlement issues) and storage facilities, enhanced leaks, changes in condition monitoring, as well as reductions of system capacity with possible hydraulic complications [26,32–34]. Further issues arise from the lower calorific value of hydrogen with respect to NG, which causes higher gas velocities, and therefore enhanced pressure drops, to deliver the same thermal power to the end-users.

The impacts on the existing infrastructure could be considerably limited when biomethane is instead deployed in networks as a substitute of fossil natural gas. Network compatibility, technology maturity and high production potentials make of biomethane the most promising complementary alternative to hydrogen in the decarbonization of the gas sector. Biomethane is derived from organic feedstocks that, in most cases, are subject to a process of anaerobic digestion (AD). The gas mixture produced from the AD process – i.e., the biogas – is typically composed of predominant fractions of CH<sub>4</sub> (40-75%) and CO<sub>2</sub> (25-60%), plus trace compounds that can vary based on the feedstock [35]. A further step is therefore required to obtain a gas with similar properties as NG transported in the networks, consisting in the separation of the CO<sub>2</sub> fraction from the mixture. This process is broadly known as upgrading.

---

<sup>1</sup> Assuming that the electrolyser works at full operating hours, with consequent lower system sizes and capital costs. This assumption may hold in a limited number of cases, since the operation of several facilities may be restricted to hours with cheap grid electricity prices, or to times of availability of variable renewables coupled with the H<sub>2</sub> production site.

In its early stages, and still today, the biogas sector has been mostly developed around the generation of electricity. Data for the European market indicate that total installed capacity of biogas power generation units amounted to 11 GW in 2018, distributed in about 18,200 plants [36]. In the meantime, due to the increased demand the development of renewable gases, the number of biomethane production plants in EU is rapidly growing, amounting to 729 units in 2020 (+51% with respect to 2018). This trend may lead to the grid injection of 1170 TWh/year of biomethane by 2050 [37], constituting 26% of NG energy consumed in 2019. Further policy support is however required to unleash this underlying potential, as IEA foresees that, in absence of reinforcements of currently stated policies (“STEPS” scenario in World Energy Outlook 2020 [8]), biomethane production in Europe may be limited to around 150 TWh by 2040 (representing about 3% of current NG consumption). Pressures from industrial lobbies are also being applied to enhance the development of biomethane in EU, proposing a binding target of 11% renewable gas by 2030 (8% being biomethane and 3% hydrogen) [38].

As for today, the use of biomethane within natural gas networks in EU must comply with the standard EN 16723:2016 [39], on the quality requirements for uses in transport and injection into natural gas grids. These recently issued quality standards, together with country-specific rewarding mechanisms – see, for instance, Italian certificates of release [40] –, established a clearer and attractive framework, which led to significant sectorial developments [41].

### **1.3 Modelling of gas networks in low-carbon scenarios**

The forthcoming escalation of the use of hydrogen, biomethane and other green gases within the gas networks requires assessing the readiness of the existing infrastructures to unconventional operational schemes.

Different scales are adopted to assess the suitability of gas systems to a diversity of gas sources. An extensive research branch has focused the response of materials, pipelines and non-pipeline elements, to identify the most vulnerable physical components along the gas supply chain. Potentially constraining sensitiveness to hydrogen has been identified in NG underground storage facilities, vehicle compressed natural gas (CNG) tanks and engines, gas chromatographs and leak detection devices, domestic end-use appliances

(especially the ones prior to GAD<sup>2</sup>), as well as in steel pipelines due to embrittlement effect [34,42–44].

Adopting a higher-level system-wide perspective, further extensive research delivered insights on the behaviour of gas infrastructures in presence of renewable gases, putting attention to the modelling and the analysis of the gas network. The hydraulic response of the networks in presence of unconventional gas blends, with possible distributed injections of fuels, constitutes part of the information typically gathered by these studies. Results allow to identify risks of noncompliance to operational restrictions (e.g., minimum and maximum pressures and maximum velocities). Furthermore, as the simulated scenarios may involve multiple sources of different gases, gas network simulation tools should offer the capability to map the quality (e.g., composition and thermophysical properties) of gas transported within the networks. This is of crucial importance to predict local violations of gas quality constraints, and to account for composition and thermophysical differences (e.g., heating value) among the network users for proper gas metering and billing.

Accordingly, quality tracking gas network simulation tools have been proposed in several contributions. A detailed mathematical description of the models is provided in the studies [45] and [46], both focusing steady-state applications. The study in [45] investigates the effect of injecting hydrogen (in pure and blended form) and upgraded biogas in a gas distribution system. Simulations are executed on a fictitious low-pressure (LP) simple grid model and discuss the way that the injection of alternative fuels affects the nodal pressures (effects may change with the location of the injection), as well as the gas quality. It is also proven that levels of hydrogen of 10% vol – i.e., beyond the limits set by UK legislation – may still comply with other quality restrictions, like the Wobbe index. A full reconversion to hydrogen of a real-world medium-pressure (MP) and LP distribution system is modelled in ref. [32] (in the framework of H21 Leeds Citygate project). No hydraulic issues emerge from the analyses, apart from pressure and velocity violations in a limited set of nodes and pipelines, that may be addressed with limited efforts.

---

<sup>2</sup> The Gas Appliances Directive (GAD) – i.e., Directive 2009/142/EC – led to the publication of standard EN 437:1995 [97] (currently updated by EN 437:2019) on the test conditions of appliances burning gaseous fuels. According to the standard, appliances must be tested and ensure correct functioning with CH<sub>4</sub>-H<sub>2</sub> blends with 23% of hydrogen (i.e., reference test gas G222).

Similar information is targeted in reference [46]. The proposed model proves to effectively handle non-trivial networks characterized by non-pipeline elements like pressure regulator stations and compressors. As a further value, the model is non-isothermal and thus suitably describes gas temperature changes induced by Joule-Thomson effect, heat exchanges with the soil, compressions and expansions. Results obtained for a high-pressure (HP) regional network operated at two pressure tiers indicate that the deployment of hydrogen and synthetic – or *substitute* – natural gas (SNG) enhances pressure drops along the pipelines, with consequent higher compression costs. It is also showed that deploying upgraded biomethane with CO<sub>2</sub> content of 5% leads to negligible changes in gas quality.

Other steady-state analyses of distribution systems are presented in references [47] and [48]. The study in [47] addresses the introduction of up to 10%vol of hydrogen in a low-pressure natural gas grid. Simulations are executed with a commercial software and suggest that, at the above conditions, minimum higher heating value (HHV) requirements may be slightly violated at certain nodes. In reference [48], a complex MP distribution system with two gas infeed sites (or *city gates*) is deployed as simulation testbed. Hydrogen admixtures up to 20% are modelled in correspondence of one of the city gates. The study evidences that the deployment of hydrogen leads to significantly higher pressure drops and that concentrations of 10%vol H<sub>2</sub> raise compliance issues against Polish requirements on HHV. The contribution also offers a comprehensive description of modelling and solution approaches to natural gas network studies.

The option of injecting biogas into the gas network is explored in ref. [49], where gas quality limits were considered to assess the maximum allowable injection of biogas within a medium-pressure distribution grid. Further insights are given in [50], proposing the modulation of supply pressures in distribution systems to accommodate larger distributed intakes of biomethane.

In the framework of electrical and gas grids coupled by power-to-gas (PtG) technology, a transient assessment of a MP gas network is provided in ref. [51] where the injection of electrolytic hydrogen produced from excess renewables is modelled. Besides assessing disturbances on pressures and velocities, the work relates the occurrence of gas quality violations to the penetration of RES in the electrical grid. Emphasis is given to the benefits deriving from a proper location for the injection site, as well as from a suitable injection profile along the day.

Most of extensive remaining research around the coupling of NG and power grids through PtG has been carried out on a transmission scale (regional and National) and explore the extent to which electrolyzers may be deployed to improve the dispatchability of renewables and feed the natural gas network with hydrogen (see for instance [52,53]).

What emerges from the available literature is that the research landscape is rich in studies, models and methodologies around the simulation and analysis of gas networks in presence of alternative fuels. It is also noticeable that, however, some difficulties may be encountered to gather a generalized understanding on the effect of green gases in gas grids. In most cases, simulated scenarios are in fact hardly comparable, involving different types of networks (e.g., pressure tiers, number of gas sources, etc.) and admixture levels of alternative gases.

Additionally and most importantly, as a common practice, all the existing contributions adopt single network models (either real-world or fictitious) as testbeds for fluid-dynamic simulations. The response of these networks is significantly influenced by their topology and several other factors among which the location of NG source(s) and loads and of the distributed injection of gas.

It can be therefore inferred that available studies are affected by an intrinsic case-specificity that may limit the extent of their validity and prevent generalized statistical outputs. As better discussed in the next sections, the major contribution of this work relies in overcoming this limitation by offering a tool for the generation of a large number of fictitious (*synthetic*) and realistic network models, to be deployed for simulation purposes. Although this constitutes an unprecedented application to gas networks, the idea of producing synthetic network models to support infrastructural studies is inspired by extensive work accomplished in the field of power grids. Some of these contributions are reviewed in the next Section.

## **1.4 Uses of synthetic grid models for energy network analyses**

In complex physical networks like large-scale energy grids, perturbations applied at some point may affect the state of other regions located even far away within the same system. The way and the extent to which these signals expand is strongly affected by the topology of the system (i.e., the connectivity relations

among the nodes constituting the network) and by the characteristics of the connections between its nodes.

Although it has been demonstrated that energy networks of a given class (e.g., power grids) may feature recurring topological and technical peculiarities – some of which have been described in [54] and [55] – each real-world network constitutes a unique case study and therefore features own behaviour and response to perturbations. Accordingly, the information that is commonly gathered in studies carried out over one or a limited set of networks is partly incomplete, and not generalizable.

Several testbeds (i.e., network models) would be needed to shift from the traditional case-specific approach to comprehensive statistical analyses of energy network infrastructures. The main factor hindering this practice is data availability, as publicly available energy network models are very limited due to privacy, security, and industrial secrecy issues. The scarcity of data is even more severe for gas grids, given that IEEE benchmarks and other real and surrogate power grid models are accessible from several sources [56–60].

A number of solutions have been proposed to produce synthetic energy network models to tackle data unavailability and enable statistical studies inspired, for instance, from Monte Carlo methods. Most of the published work in the field, if not all of it, focuses electrical grids. In the modelling of the synthetic networks, attention is devoted to the fair replication of the grid topological, technical (electrical) and, in some cases, spatial properties.

Some tools make use of geographic information system (GIS) data to estimate and plan the location and the topology of the power grid within a target geographical area [61–63]. Information employed by the models includes the location of roads, buildings and other barriers of the landscape, as well as remote sensing data like night-time lights. Other algorithms do not account for geographical information, but rather implement spatial and distance-based criteria to geographically distribute the network nodes and establish links among them [64–66]. Alternative approaches neglect the spatial embeddedness of the networks and establish grid topologies based on statistical observations of real case studies [67–69]. The topological properties are typically described and replicated by means of statistical tools like kernel density estimation. In other cases, network topologies are inspired by reference structures like small-world networks [70].

Most of the aforementioned contributions produce network models readily functional for simulation (electrical power flow) purposes, enabling the execution of studies over several networks (see, for instance, the generalized assessment of the effect of PV in distribution grids proposed in [67]) or compensating the lack of real data for a target geographical area.

Concerning gas grids, tools for the automated generation of synthetic network models are still lacking. Work accomplished in the field of gas and fluid networks has mostly regarded optimization problems applied to the grid topology [71,72] and the selection of network components [73–75]. Topological investigations on the networks have also partly been addressed, but mostly for system vulnerability and risk analyses, as well as for optimal network extensions [76–78]. Some benchmark models of gas networks have also been proposed [79], underlying the need for higher availability of network data for simulations in the gas networks field.

## **1.5 Motivations, objectives, and structure of the work**

While the simulation and analysis of gas networks in low-carbon scenarios witnessed increased momentum and gained several research contributions, knowledge gaps have been identified in terms of systematic and generalized assessments. As a further, but strictly related, limitation, the general difficulties in accessing real or representative models of gas networks for simulation purposes have also been evidenced. Following an intuition born in the field of power grid analysis, these gaps may be significantly bridged with dedicated tools for the generation of synthetic and realistic network models, providing large numbers of reliable case studies. To the best of the author’s knowledge, the implementation and application of such tools in the field of gas networks have not been investigated by any research contribution to date.

In this framework, the present work aims at delivering a tool for the synthetic generation of statistically similar gas networks to enable systematic and generalized gas grid studies in low-carbon and integrated energy systems. Specific attention is given to distribution-level grids which, in fact, have attracted particular interest in the existing literature, are serving as testbeds for several ongoing international projects and offer a higher compatibility to the deployment of alternative gases like hydrogen.

The subtasks addressed along the work address functional knowledge gaps and propose novel methodologies for the development of the synthetic network generator. These objectives include the following items.

- 1) Topological analysis of distribution gas networks: investigation and extraction of topological and structural properties from real world gas grids of medium and low pressure.
- 2) Topological modelling of distribution gas networks: development and implementation of methods for the creation of realistic and statistically similar synthetic network topologies.
- 3) Automated technical design of distribution gas networks: development and implementation of methods for the correct and efficient technical sizing of complex distribution systems, in compliance with target design parameters.
- 4) Creation of a large number of synthetic networks readily deployable for simulation purposes.
- 5) Application of the tool for the statistical assessment of gas networks in presence of distributed injection of hydrogen.

The above objectives are reflected in the structure of the thesis. The following diagram illustrates the outline of the work and describes the relations among its constitutive sections. It can be used by the reader to gather the overall rationale for the work and contextualize the subjects that will be treated starting from the next Chapter onwards.

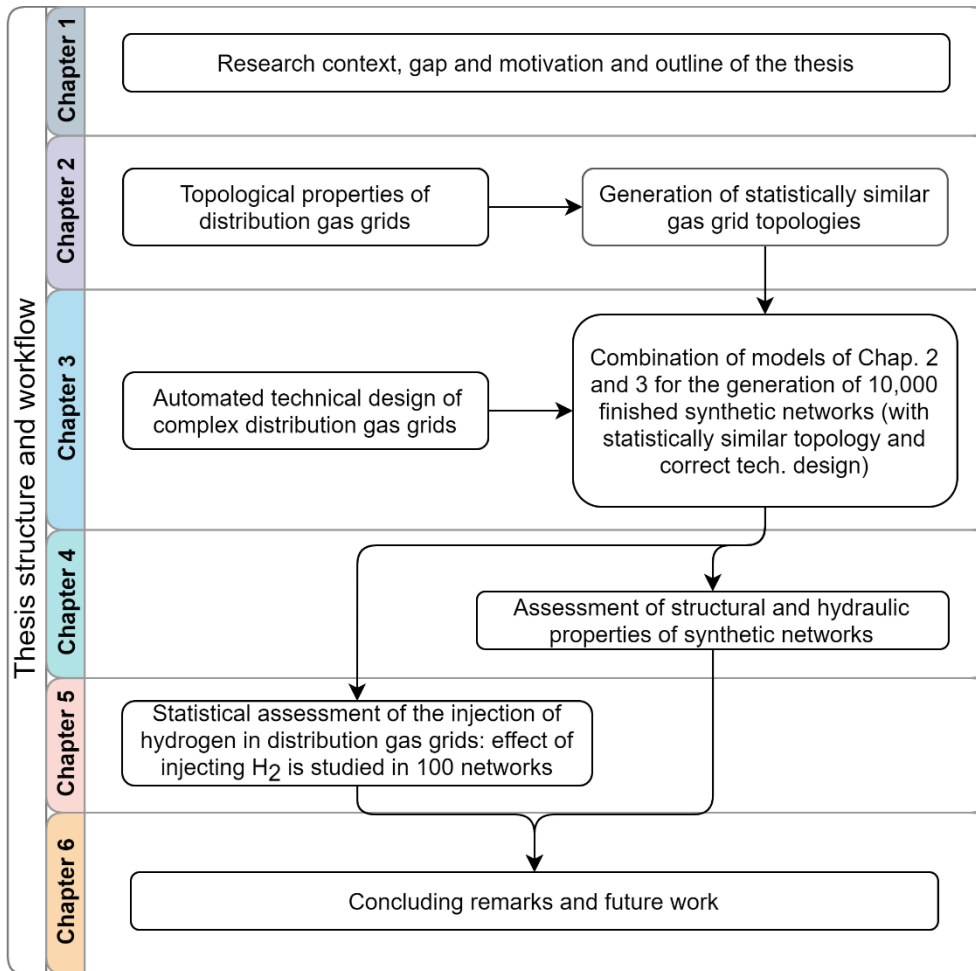


Figure 1. Structure and workflow of the thesis

# Chapter 2

## Topological modelling of distribution gas networks

### 2.1 Introduction

Several network systems, including energy network infrastructures, can be intuitively described by means of a graph-based representation. A graph is a mathematical model making use of nodes (or *vertices*) and links (or *edges*) to describe the elements of a system and the relations existing between them. The layout of the network system is closely related to its functionality. Therefore, providing an accurate description of the topology of a given class of networks is key to setting up studies around diverse applications, including – as a matter of example – system faults and vulnerabilities, as well as network evolution predictions. Additionally, as focused within this Chapter, an accurate topological analysis is essential to provide realistic and reliable models for simulation purposes.

Real-world systems commonly described by graph-based representation are of diverse nature and domains. Examples include the internet, food webs, citations of scientific papers and their authors, electronic circuits, roads networks and other infrastructures. Several topological models have been also developed around energy network infrastructures, most of which related to power transmission and distribution grids, as illustrated in the literature review provided by Chapter 1. According to these models, the nodes of the graph represent points of power generation (*sources*, according to network theory nomenclature [80]) and power

consumption (*sinks*), as well as intermediate substations and busbars. Edges of the graphs constitute power lines as well as other network components, like power transformers. This convention results suitable not only for purely topological applications, but also for the solution of network flow problems (*power flow*, in the case of electrical grids) adopting methods like, for instance, the modified nodal analysis [81], where specific equations are applied to the power grid components – i.e., the edges – to determine the state variables of the connected vertices.

Similarly to the approach described above for power grids, the following convention is used for the representation of gas network systems. The representation adopted within this thesis is consistent with several other contributions in the literature, including [46,50,82].

- Nodes of the gas network model represent:
  - *Points of gas supply*: sources of gas feeding the network, characterized by either fixed pressure or imposed gas injection rate, representing gas city gates and other main supply systems (e.g., pressure regulators in general) as well as LNG tanks for islanded systems. In networks featuring distributed injection of gas, these nodes include the connection points to biogas, biomethane, synthetic natural gas and hydrogen producers.
  - *Points of gas consumption*: location of grid customers, as well as network side interfaces with pressure reduction devices supplying gas to downstream distribution systems.
  - *Junctions between the pipelines*: intermediate nodes providing connections between two or more pipes.
- Edges of the gas network represent:
  - *Pipelines*: physical connections between network nodes.
  - *Pressure reduction stations and pressure regulators*: interfaces between sections of the system operated at different pressure levels.
  - *Compressor stations*: systems installed in series with the pipelines to ensure the motion of gas, mostly at high pressure and transmission levels.

For completeness, pressure reduction stations and compressor stations are included in the list of the components modelled as graph edges. These system elements are excluded from the topological analysis proposed later in this

Chapter, since the investigated networks are passive grids (no compressors are included) operated at single pressure level (no pressure reducers). Notwithstanding this, pressure regulators are included in the topological model of gas grids, i.e. the tool producing synthetic gas grid topologies, when it comes to link together grid sections belonging to different pressure tiers (see Section 2.3.5). Additionally, the definition of pressure regulators and compressor stations are still implemented as part of the formulation of the modified nodal analysis method in the fluid-dynamic gas network model that is subsequently used within this work (a full description is provided in [83]).

According to the above conventions, key topological properties are separately obtained for a set of medium and low-pressure distribution networks. Results of the topological analysis are subsequently used to calibrate a topological model whose function is generating large numbers of statistically correct network topologies. Details on the methodology behind the topological model and the outcomes of its deployment on a given case study are finally illustrated and discussed.

#### *2.1.1.1 Description of the case studies*

A topological investigation is carried out on a set of distribution networks. All the analysed grids are located in Italy and serve municipalities characterised by both urban clusters and surrounding agricultural areas with scattered industrial users. The distribution systems, described in Table 1, feature variable extensions in terms of total length and covered area (meant as the surface of the rectangle enclosing the network). Population densities of the served areas are conversely uniformly distributed around a mean of 225.4 inhabitants/km<sup>2</sup>. The grids can accordingly be classified as suburban distribution systems. All the network data were collected through a direct interaction with different Italian distribution system operators. The original information on these networks is protected by non-disclosure agreements.

Every network listed in Table 1 is a connected system – meaning that the infrastructure has no points of discontinuity – serving one or more municipalities and featuring one or more city gates (gas sources). All the networks are operated at multiple pressure levels, comprising both medium-pressure (MP) and low-pressure (LP) sections. The information on the pressure tiers included within each network is indicated accordingly to the Italian classification: 4<sup>th</sup> *species* operates

at 1.5 – 5 bar<sub>g</sub> (MP), 6<sup>th</sup> *species* operates at 0.04 – 0.5 bar<sub>g</sub> (MP), 7<sup>th</sup> *species* operates at 0.04 bar<sub>g</sub> or less (LP) [84]. Further details on the definition of the pressure tiers are given in Chapter 3.

Within the presented distribution systems, pipelines of 4<sup>th</sup> *species* (5 bar<sub>g</sub>) are deployed for long-range gas transportation from the city gates to the residential clusters, and to supply natural gas to intensive customers (e.g., industries). Additionally, they provide interconnections between different urban clusters. Network sections of 7<sup>th</sup> *species* (about 22 mbar<sub>g</sub>) are constituted by street-level pipelines deployed in denser urban clusters for residential and commercial customers. 6<sup>th</sup> *species* pipelines (0.5 bar<sub>g</sub>) are deployed for both medium-long range transportation and for delivery to final users.

The different locations and purposes of the pressure tiers lead to different design choices and layouts. In order to acknowledge and investigate these differences, the topological analysis has been carried out separately for every level of pressure. Accordingly, the distribution systems of Table 1 have been decomposed into *subnetworks* belonging to a same pressure tier. Since distribution systems may feature a multitude of independent clusters of users served by street-level pipes, many resulting lower-pressure subnetworks are disconnected structures with two or more standalone network components. Therefore, each subnetwork has been furtherly decomposed into its connected components, or *islands*. With these premises, the topological analysis illustrated below has been conducted on connected network *islands* operated at a single pressure level. Resulting islands with less than 30 nodes have been excluded from the study. The processing of data resulted into the definition of a total of 25 islanded networks to be analysed (5 islands of 4<sup>th</sup> *species*, 6 islands of 6<sup>th</sup> *species* and 14 islands of 7<sup>th</sup> *species*). A description of all the grids is provided by Table 2.

**Table 1. Description of the original set of distribution systems used for the study.**

ID	Network area [km <sup>2</sup> ]	Pop. density [km <sup>-2</sup> ]	Tot. length [km]	Nodes	Edges	<i>Species</i>		
						4 <sup>th</sup>	6 <sup>th</sup>	7 <sup>th</sup>
1	45.35	227.4	77.8	1238	1271	✓	✓	✓
2	22.78	227.0	74.9	1349	1386	✓	✗	✓
3	12.36	260.9	23.8	368	372	✓	✗	✓
4	118.56	166.0	117.6	2343	2385	✓	✗	✓
5	298.01	246.0	255	4628	4726	✓	✓	✓

**Table 2. Description of the system *islands* extracted and used for the topological analysis.**

<b>ID</b>	<i>Species</i>	<b>Class</b>	<b>Network area [km<sup>2</sup>]</b>	<b>Tot. length [km]</b>	<b>Nodes</b>	<b>Edges</b>
<b>1</b>	4	MP	28.48	34.4	373	375
<b>2</b>	4	MP	20.63	22.2	332	333
<b>3</b>	4	MP	6.36	6	74	73
<b>4</b>	4	MP	95.59	40.3	557	561
<b>5</b>	4	MP	169.63	94.5	1589	1595
<b>6</b>	6	MP	7.52	13.9	381	384
<b>7</b>	6	MP	6.83	10.5	159	160
<b>8</b>	6	MP	3.49	6.2	100	99
<b>9</b>	6	MP	1.04	3.4	38	37
<b>10</b>	6	MP	19.04	14.4	185	185
<b>11</b>	6	MP	3.44	5.4	45	44
<b>12</b>	7	LP	1.6	11.0	176	193
<b>13</b>	7	LP	16.13	50.6	982	1015
<b>14</b>	7	LP	0.39	2.0	31	30
<b>15</b>	7	LP	8.98	17.8	290	293
<b>16</b>	7	LP	9.16	52.9	1196	1216
<b>17</b>	7	LP	5.88	24.1	568	578
<b>18</b>	7	LP	2.72	14.7	351	356
<b>19</b>	7	LP	11.38	40.9	634	654
<b>20</b>	7	LP	0.96	3.1	55	54
<b>21</b>	7	LP	1.05	3.6	53	52
<b>22</b>	7	LP	0.74	5.9	153	153
<b>23</b>	7	LP	7.96	41.0	859	900
<b>24</b>	7	LP	6.86	16.0	284	287
<b>25</b>	7	LP	0.17	1.2	31	30

While the data processing led to 25 networks, all the data come from a total of five suburban network models. This constitutes indeed a limitation to the generalization of the outcomes of the topological analysis undertaken in the following Sections. Accordingly, the results are to be intended as valid for the analysed cluster of case studies, although similar infrastructures are likely to feature consistent properties. Despite the limited benchmark adopted for the study, the proposed methodology can be replicated for any other collection of reference networks, possibly with more available networks of diverse nature, including, for instance, urban and rural grids.

## 2.2 Topological properties of distribution gas grids

Suitable metrics have been selected for a comprehensive understanding of the typical topologies of distribution gas grids. Techniques generally adopted for analysing energy infrastructure networks are inspired from the fields of the complex network analysis and graph theory. A similar approach is adopted within this thesis. Additionally, further information is derived on the spatial characteristics of the networks. The adopted metrics and the results of the analysis are detailed in the following sections.

### 2.2.1 Degree related topological properties

In a given graph, the degree of a node represents the number of edges incident to that node. Information about the degrees is useful to assess the hierarchical relevance of the vertices, as well as the ease of interaction among vertices and regions within the network. The *degree distribution* of a network provides the probability  $P(k)$  that a vertex in the network interacts with  $k$  other vertices.  $P(k)$  is defined in Equation 2.1:

$$P(k) = \frac{n_k}{N} \quad (2.1)$$

where  $n_k$  is the number of nodes with degree  $k$  and  $N$  is the number of nodes in the network. Depending on the nature of the system, the nodes of a graph can be characterized by hundreds or thousands of connections (social networks, World Wide Web, genetic networks, neural networks, ...) down to a few units. Most of real-world physical networks, like energy networks and utilities infrastructures in general, are typically characterized by relatively low degrees, due to technical and economic limits of system installations.

This is also observable in distribution gas grids, as illustrated in Figure 2, where most of the nodes feature 3 or less connections. Significant changes can be observed among the topologies of the different pressure tiers, due to the different purposes and locations of the grids. 4<sup>th</sup> and 6<sup>th</sup> *species* networks feature a predominant number of degree-2 nodes, due to the abundant presence of linear paths – as needed for long-range connections. Conversely, low-pressure networks are characterized by a larger incidence of degree-1 and degree-3 nodes, respectively due to the denser presence of points of delivery to end-users, and to the overall higher spatial compactness of street-level distribution systems. The

latter, in fact, typically lay in denser residential areas and often overlap with the road network patterns, favouring the connectivity among close nodes and the establishment of cycles. As a final remark, the variability of the values of the degree distributions is higher in 6<sup>th</sup> *species* grids, due to the hybrid purpose of these networks, used both for medium-long range connections and for direct delivery to residential end-users.

The *maximum degree* of the networks amounts to 4 for all the pressure tiers. In most networks, however, the maximum number of connections amounts to 3. The *average degrees* of the networks feature limited variations around 2 and are listed in the summary Table 3.

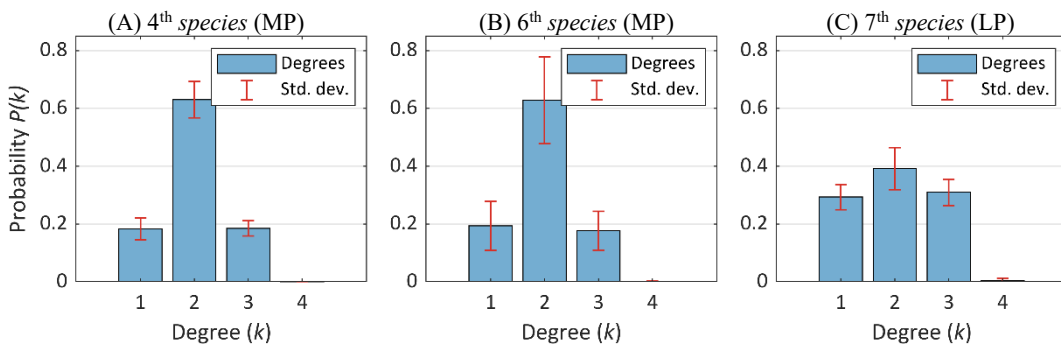


Figure 2. Degree distributions by pressure tiers of investigated real-world gas networks.

## 2.2.2 Length related topological properties

Within a distribution system, the lengths of the pipelines are critical to the hydraulic behaviour (pressure drops) of the network and to the system costs. Within this section, structural and topological metrics around the pipeline lengths are provided, according to models of distribution systems obtained by the respective distribution system operators (DSO). In the majority of cases, a pipeline is defined as a continuous line section featuring uniform properties (diameter and material). In some circumstances, according to the original network models, linear sequences of different pipelines may feature the same properties. These discontinuities have been consistently found in all the observed models and have been therefore kept in the analysis. Accordingly, the results of the topological and structural investigations carried out within this Chapter are referred to the original description of the networks, as received from the DSOs.

Pipelines may follow nonlinear routes, so that their length is higher than the Euclidean distance between their endpoints. However, due to comparison purposes against the synthetic topologies generated in later within this Chapter, point-to-point Euclidean distances are adopted instead.

### 2.2.2.1 Pipeline lengths

Pipeline lengths are extracted from the grid models and distributed into logarithmic classes, as illustrated in Figure 3. The obtained distributions are key for the assessment of the synthetic topologies generated in the following sections, as they will be adopted as terms of comparison.

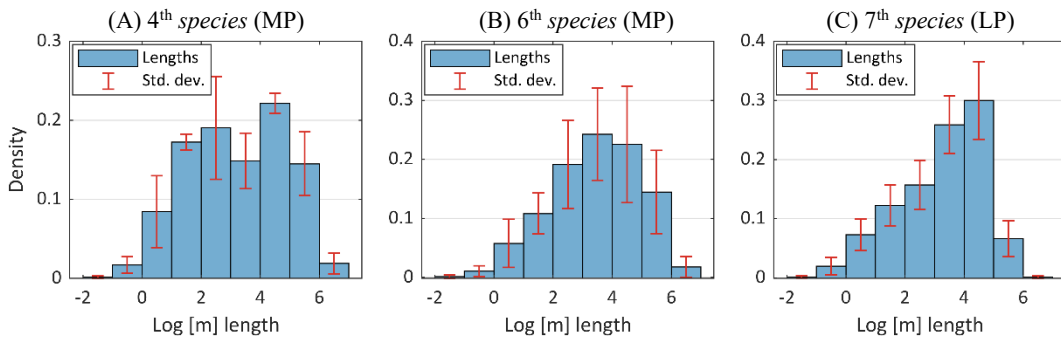


**Figure 3.** Length distributions of pipelines belonging to different pressure tiers of investigate networks. Lengths are computed as point-to-point Euclidean distances between the connected nodes. Lengths are in m and their logarithm is natural logarithm.

Intuitively, the average length of the pipes increases with the hierarchy of the in the pressure tier. Accordingly, the average pipe lengths amount to 67.2 m in 4<sup>th</sup> species MP sections, 59.1 m in 6<sup>th</sup> species, and 49.0 m in 7<sup>th</sup> species LP networks.

### 2.2.2.2 Average path length

In a connected graph with unweighted edges, the average path length is defined as the number of edges forming the shortest path between two vertices, averaged over all the possible couples of vertices. It provides a measure of the connectivity of the system. In unweighted graphs, distances are measured in *hops*, that is equivalent to the number of elements separating a couple of nodes. In many physical network systems like gas grids, however, the lengths of the edges can be used as weights, so that the average path length represents the average physical distance between every couple of nodes within the system. Calling  $D(v_i, v_j)$  the physical distance between the vertices  $v_i$  and  $v_j$  of the graph, and  $D_{hops}(v_1, v_2)$  the unweighted distance, the average path length is defined as follows.

$$L = \frac{1}{N(N-1)} \sum_{i \neq j} D(v_i, v_j) \quad (2.2)$$

$$L_{hops} = \frac{1}{N(N-1)} \sum_{i \neq j} D_{hops}(v_i, v_j) \quad (2.3)$$

According to the above definitions, the weighted and unweighted average path lengths have been evaluated for all the networks. Results are illustrated in Figure 4 where it is evidenced that the values scale with the network size (total network length and number of nodes, respectively).

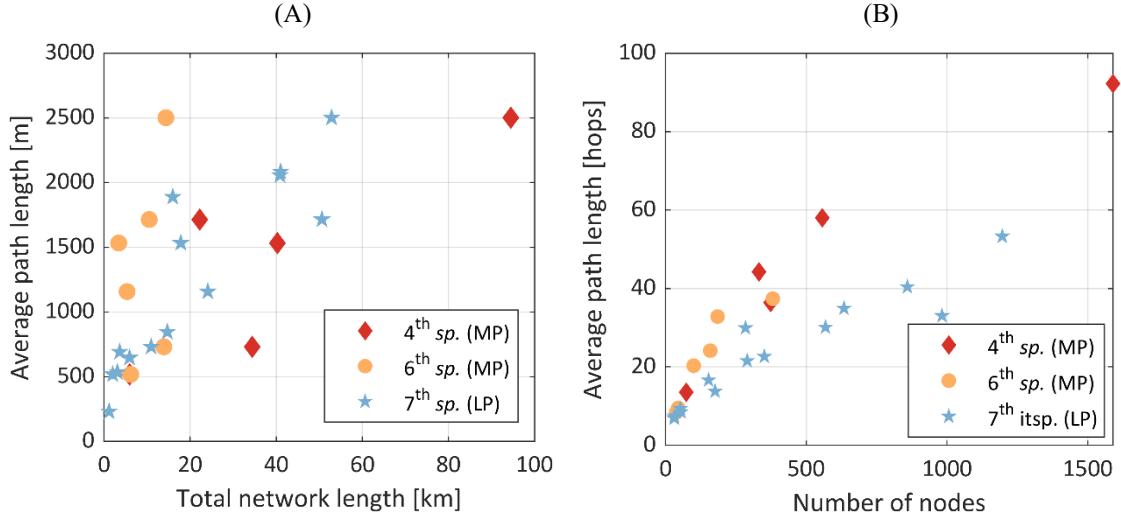


Figure 4. Variation of the average path length in *meters* (A) and *hops* (B) in the sampled networks, in function of the network size – total length (A) and number of nodes (B).

## 2.2.3 Clustering of nodes

### 2.2.3.1 Global clustering coefficient

The clustering coefficient  $C$  measures the likelihood for neighbouring nodes to have common neighbours. Local clustering coefficient refers to a single node and denotes the existing fraction of all the possible connections between the neighbours of the node. The global clustering coefficient (used in the present work) is the average of the local value over all the nodes of the network.

This metric is widely used for several complex network systems, including social network applications. Many real-world physical networks, however, feature zero or very low degrees of clustering. This is because it is often not feasible, nor beneficial, to design a highly interconnected system in networks which do not feature highly distributed sources like distribution gas grids. Accordingly, as indicated in the summary network properties of Table 3, clustering is completely absent in MP networks, while it is generally very low in street-level LP systems.

## 2.2.4 Loops related topological properties

Distribution gas grids are typically looped systems. Loops (or *cycles*, in graph theory terminology) provide the network with redundancies and ensure higher system resilience and more uniform hydraulic behaviour. The function and the extension of the loops in distribution gas grids change according to the pressure tier of the system, as they depend on the purpose and the spatial layout of the grid.

In tree-structured connected networks which, by definition, do not have any loop, the number of edges  $E$  is equal to the number of vertices  $V$  minus 1. Whenever a connected graph features a number of edges  $E$  such that  $E \geq V-1$ , it is characterized by one or more cycles. In particular, the number of linearly independent cycles  $C$  of a connected network is given by the following relation:

$$C = E - V + 1 \quad (2.4)$$

The *cycle matrix* of a graph is a matrix indicating what edges (columns) participate in each cycle (rows). In undirected graphs – which are suitable representations for gas grids –, the  $(i, j)$  element of the cycle matrix is 1 if the  $i$ th cycle includes the  $j$ th edge; otherwise, it is zero. A set of linearly independent rows of the matrix gives form to the *fundamental cycle matrix* of a graph  $B = [b_{ij}]_{C \times E}$ . The cycles described by the fundamental cycle matrix are called *fundamental cycles* and represent the minimum set of loops needed to fully describe the cyclicity of the graph. According to the above definitions, a formulation of the fundamental cycle matrix is provided below:

$$B = [b_{ij}]_{C \times E} \quad (2.5)$$

$$b_{ij} = \begin{cases} 1, & \text{ith cycle includes jth edge} \\ 0, & \text{otherwise} \end{cases}$$

There exist several algorithms for the detection of the fundamental cycles of a graph. In order to systematically identify the network cycles and derive their properties, the following procedure has been followed in the present work:

1. extract a spanning tree  $T$  from the looped graph  $G$ ;
2. identify the edges of  $G$  that have been excluded in  $T$ ;

*Repeating the following steps for each excluded edge:*

3. identify the end nodes  $n_1$  and  $n_2$  of the excluded edge;
4. determine the minimum path (sequence of edges) between  $n_1$  and  $n_2$  in  $T$ ;

5. add a new line in the fundamental cycle matrix and record the sequence of edges plus the excluded edge.

The loop-related properties of the analysed graphs are illustrated in the following sections.

#### 2.2.4.1 Number of cycles

The number of loops featured by the gas grids varies significantly with the type of network (pressure tier) and its size. Observing these relations in real-world grids is key to reproduce realistic network topologies. The total length of the grid is here adopted as a measure of the system size. As visible from Figure 5, the specific number of loops – intended as number of cycles over total network length – is much higher in low-pressure than in medium-pressure systems. This is due to the overall higher spatial compactness of the LP systems, which favours the establishment of redundant connections between neighbouring nodes. The lower and upper recorded bounds of the specific numbers of loops and their averages are listed below:

- 4<sup>th</sup> species (MP): 0 – 0.124 km<sup>-1</sup> (average: 0.075);
- 6<sup>th</sup> species (MP): 0 – 0.288 km<sup>-1</sup> (average: 0.091);
- 7<sup>th</sup> species (LP): 0 – 1.644 km<sup>-1</sup> (average: 0.411).

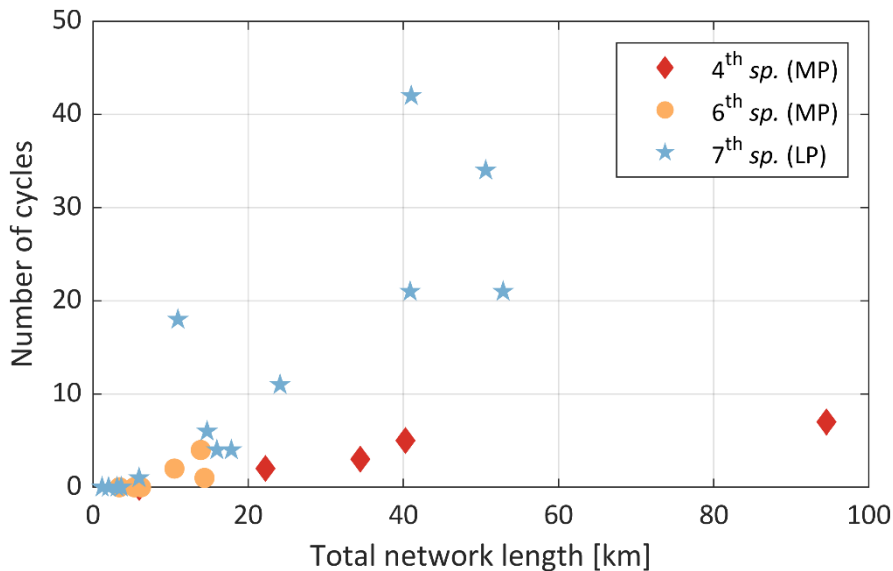
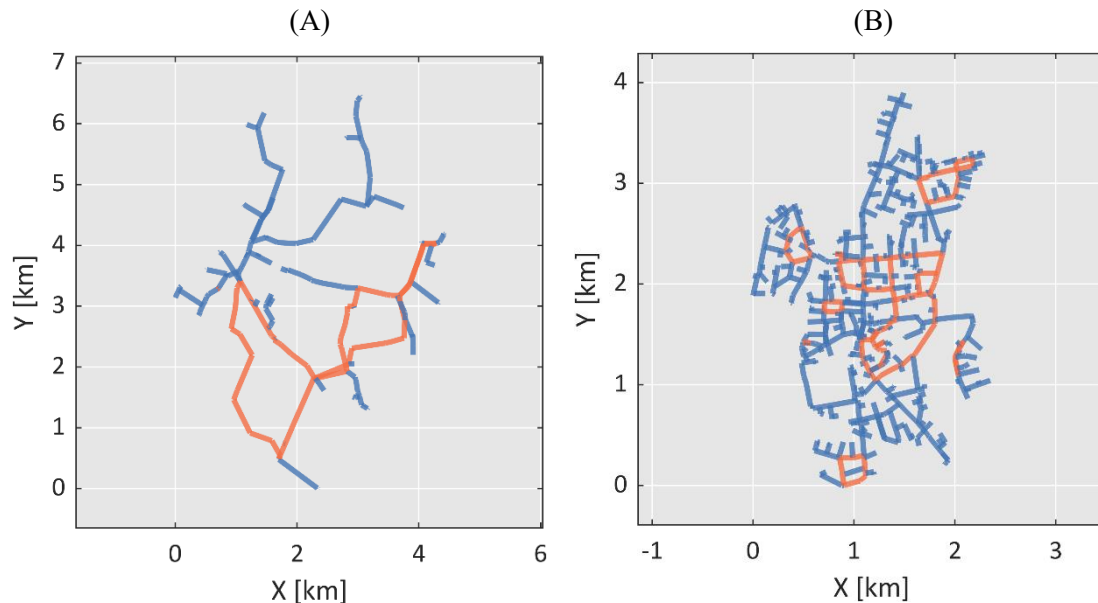


Figure 5. Number of cycles of gas distribution grids against total network length.

### 2.2.4.2 Length and location of cycles

Because of their different purposes, locations, and extensions, loops feature distinct characteristics in medium and low-pressure systems. These differences should be considered when it comes to building a topological model of these infrastructures. From a qualitative perspective, the typical layouts of the cycles in MP and LP systems are illustrated in Figure 6.



**Figure 6.** Comparison of network loops (highlighted in orange) in (A) MP system (4<sup>th</sup> species) and (B) LP system (7<sup>th</sup> species).

The main difference lies in the size (i.e., total length) of the loops, principally induced by the spatial extension of the systems. In MP networks, loops are key to provide shortcuts and alternative flow patterns between network regions that would otherwise be topologically distant, with considerable benefits in the system hydraulics (i.e., lower pressure drops) and reliability.

In LP networks and street-level grids in general, the establishment of loops is mostly linked to the overall spatial compactness of the system. Loops are found in dense areas and are typically of reduced extension with respect to MP. A comparison of cycle lengths is provided by the boxplots of Figure 7, where the data refer to all the 4<sup>th</sup> species and 7<sup>th</sup> species networks under analysis.<sup>3</sup>

<sup>3</sup> The boxes of Figure 7 cover the 25<sup>th</sup> and 75<sup>th</sup> percentiles of values, the whiskers the remaining observations. The horizontal line in the box indicates the median value. Blue points are detected as outliers.

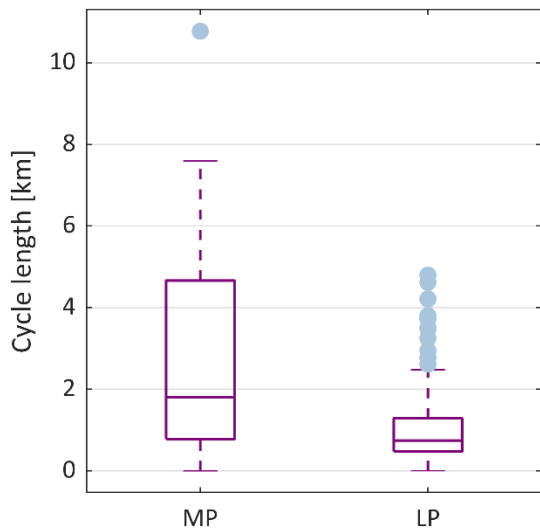


Figure 7. Comparison of cycle lengths in medium pressure (4<sup>th</sup> species) and low pressure (7<sup>th</sup> species) systems.

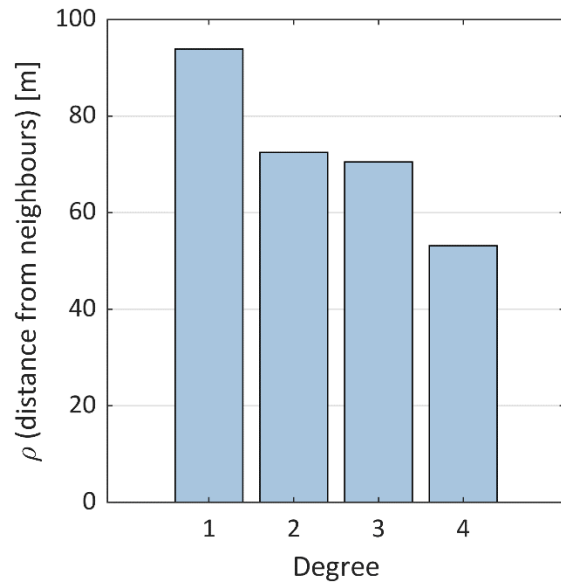


Figure 8. Relation between node degrees and average distance from 10 closest neighbours for nodes in LP (7<sup>th</sup> species) networks

The degree of the nodes in the networks and their participation in a loop are closely related, especially in street-level networks. 77% of the nodes with degree equal to 4 (maximum value) in LP networks participates in a loop. Network loops and nodes with a larger number of connections are more likely to be found in regions characterized by a high density of nodes. This behaviour is particularly evident in street-level low-pressure systems, as evidenced in Figure 8 through the average relation between the degree of a node and the spatial density of nodes in its surroundings. The latter information is provided through the variable  $\rho$ , which indicates the average Euclidean distance between each node in the network and its 10 closest neighbours.

Table 3. Summary of the structural properties of the investigated gas networks

<i>Species</i>		<i>4<sup>th</sup> species</i>	<i>6<sup>th</sup> species</i>	<i>7<sup>th</sup> species</i>
<b>Class</b>		<b>MP</b>	<b>MP</b>	<b>LP</b>
<b>Average degree</b>	Min	1.97	1.95	1.94
	<b>Average</b>	<b>2.00</b>	<b>1.99</b>	<b>2.03</b>
	Max	2.01	2.02	2.19
<b>Maximum degree</b>	-	<b>4</b>	<b>4</b>	<b>4</b>
<b>Normalized* average path length <math>L</math></b>	Min	0.074	0.123	0.034
	<b>Average</b>	<b>0.152</b>	<b>0.202</b>	<b>0.106</b>
	Max	0.287	0.288	0.257
<b>Normalized** average path length <math>L_{Hops}</math></b>	Min	0.058	0.098	0.034
	<b>Average</b>	<b>0.115</b>	<b>0.177</b>	<b>0.104</b>
	Max	0.183	0.221	0.241
<b>Clustering c.</b>	-	<b>0</b>	<b>0</b>	<b>0</b>
<b>Specific number of cycles [<math>km^{-1}</math>]</b>	Min	0	0	0
	<b>Average</b>	<b>0.075</b>	<b>0.091</b>	<b>0.411</b>
	Max	0.124	0.288	1.644

\* Normalized with respect to total network length

\*\* Normalized with respect to number of nodes

## 2.3 Generation of statistically similar topologies of distribution gas grids

The current section introduces a custom algorithm whose purpose is the creation of synthetic topologies replicating the properties of real-world gas networks. The model is suitably calibrated and validated based on the topological characterization of gas grids provided in the previous sections of this Chapter. The algorithm is developed and executed in MATLAB environment, making use of built-in and custom graph and network algorithms, as well as statistics and machine learning functions.

In principle, the algorithm receives in input a reference (real-world) network topology and returns a synthetic (fictitious) network which replicates the structural properties of the original grid. The tool is designed to handle complex

distribution systems with multiple pressure tiers. Its functioning is regulated by parameters that affect the resulting network layout. Distinct parameter values can be adopted to model the various pressure tiers, to acknowledge and suitably replicate their underlying structural differences (extensively discussed in Section 2.2). Most importantly, the whole functioning of the model relies on a probabilistic approach which ensures that each execution of the algorithm delivers a different and unique fictitious network.

The procedure unfolds in four stages:

- In a first stage, the algorithm determines the location ( $x, y$  coordinates) of the nodes of the synthetic network. The spatial scattering and density of the nodes mimics the distribution of the original network nodes.
- In a second stage, a minimum number of connections is established by growing a spanning tree among the nodes.
- The network connectivity is subsequently reinforced in a third stage, where loops are created through the integration of additional connections between the nodes.
- The previous stages are separately carried out for every pressure tier of the network. The final stage determines the location of the pressure regulators needed to link together the different pressure levels, thus ensuring the connectivity across the whole fictitious infrastructure.

While a high-level schematic of the procedure is provided below in Figure 9, a detailed description of the above stages is provided in the next sections, which also offer an application to a multi-level distribution gas grid.

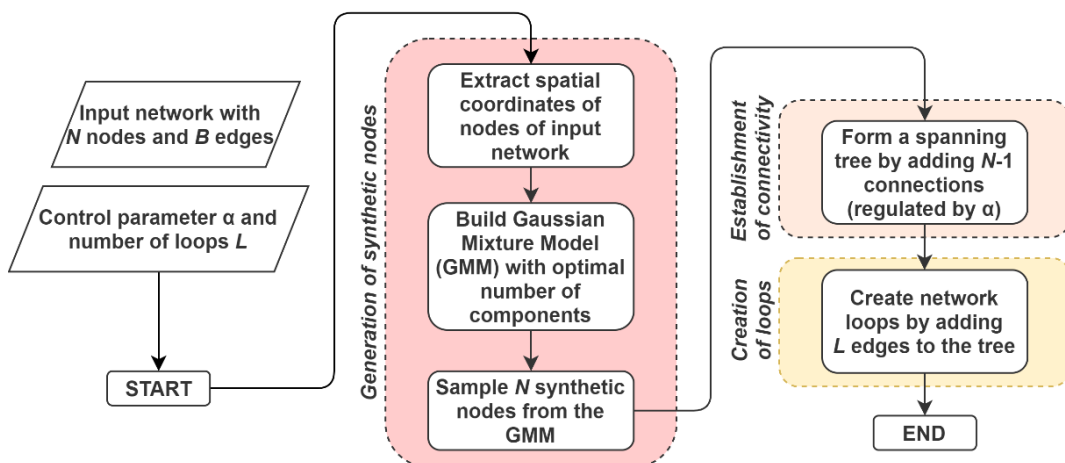


Figure 9. High-level diagram of the algorithm designed for the generation of synthetic network topologies.

### 2.3.1 Description of case study: multi-level distribution gas grid

The reference network is a MP and LP gas distribution grid of a small town of approximately 7000 inhabitants, located in Central Italy. The case study corresponds to the network with ID 1 in Table 1. The infrastructure can be organized into three *subnetworks*: the first grid layer (*Level 1*) has a nominal pressure of 5 bar<sub>g</sub> (*4<sup>th</sup> species*) and is directly fed by a HP/MP pressure reduction station; the lower layers are operated at 0.5 bar<sub>g</sub> (*Level 2, 6<sup>th</sup> species*) and 0.022 bar<sub>g</sub> (*Level 3, 7<sup>th</sup> species*) and are fed by Level 1 through a set of internal pressure reduction stations. The model of the infrastructure is displayed in Figure 10.

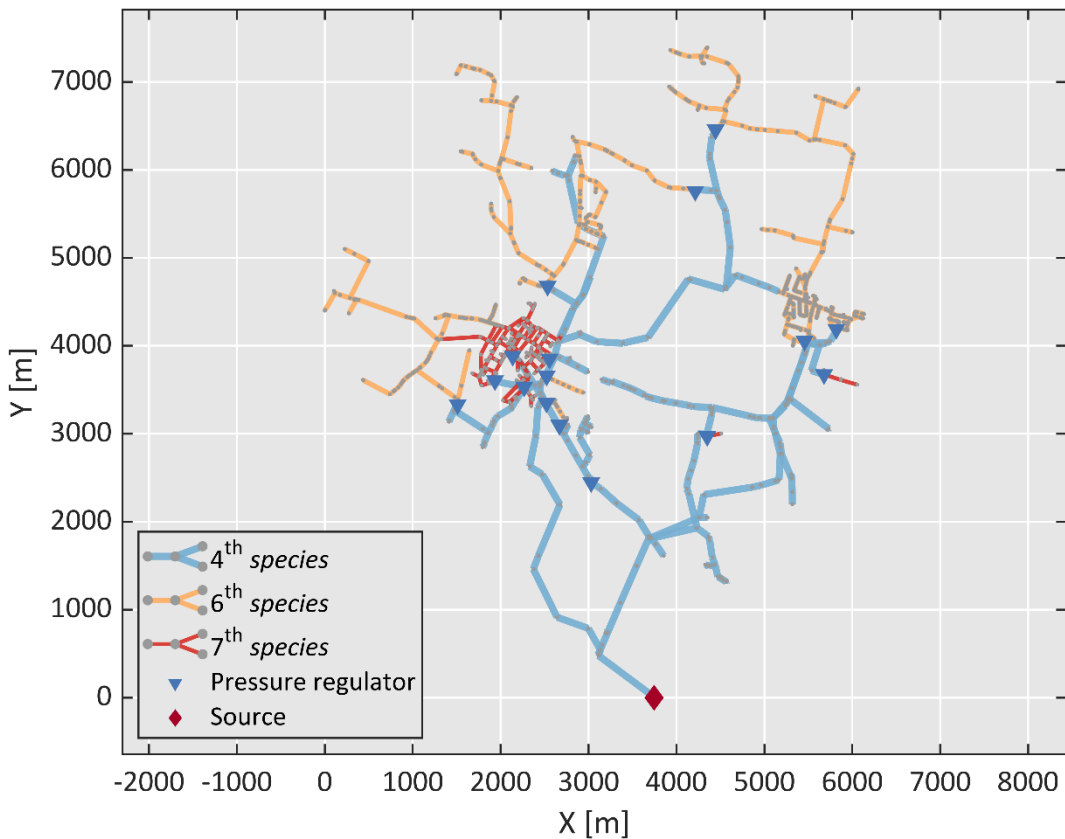


Figure 10. Real-world distribution gas grid adopted as reference case study.

### 2.3.2 Spatial distribution of nodes in the synthetic network

Synthetic nodes are created in such a way to replicate the spatial density of reference network nodes. For this purpose, a probabilistic model based on Gaussian mixtures is fitted to the geographical coordinates of the nodes in the original network. Afterwards, the location of the synthetic nodes is determined by sampling random points in accordance with the obtained probability distribution.

In multi-level networks, the above procedure is separately applied to each pressure tier. For these cases, a clustering technique is also deployed to define the groups of nodes belonging to the same cluster in lower distribution levels. Both the above methods are described in the following sections.

### 2.3.2.1 Spatial distribution of the synthetic nodes

For each network level, bivariate Gaussian Mixture Models (GMM) are deployed to inspect the spatial (geographical) distribution of the real nodes. GMM are probabilistic models constituted by the weighted sum of individual Gaussian distributions, that are called *components* of the mixture.

$$p(\mathbf{x}|\boldsymbol{\theta}) = \sum_{i=1}^M \omega_i G(\mathbf{x}|\boldsymbol{\mu}_i, \boldsymbol{\Sigma}_i), \quad (2.6)$$

$$\boldsymbol{\theta} = \{\omega_i, \boldsymbol{\mu}_i, \boldsymbol{\Sigma}_i\} \quad i = 1, \dots, M$$

In the above expression,  $G$  is a Gaussian function, parameters  $\boldsymbol{\mu}_i$  and  $\boldsymbol{\Sigma}_i$  are the mean and the covariance matrix of the  $i$ th Gaussian component,  $\omega_i$  is its weight and  $M$  is the number of components of the mixture. Vector  $\mathbf{x}$  is for the planar coordinates of the network nodes.

The parameters  $\{\omega_i, \boldsymbol{\mu}_i, \boldsymbol{\Sigma}_i\}$  fitted to data (i.e., coordinates of nodes) and optimized using the Expectation Maximization (EM) algorithm to increase the maximum likelihood (ML) of the GMM via off-the-shelf functions. Additionally, GMM are iteratively fitted to the node populations increasing the number of components in the model. The optimal number of components is hence selected based on the Bayesian Information Criterion (BIC), to ensure a fair likelihood while avoiding overfitting.

The obtained probability distribution function is deployed to resample as many random points as the number of real nodes in the respective subnetwork, thus generating the nodes of the synthetic grid. This procedure is similar to and inspired by the methodology illustrated in [64] and extends its applications to multi-level network infrastructures. Randomly generated sets of synthetic nodes with realistic spatial distributions are illustrated in Figure 11 for each pressure level of the gas grid. It is showed that generated nodes replicate the spatial distribution of real nodes while hiding their actual position.

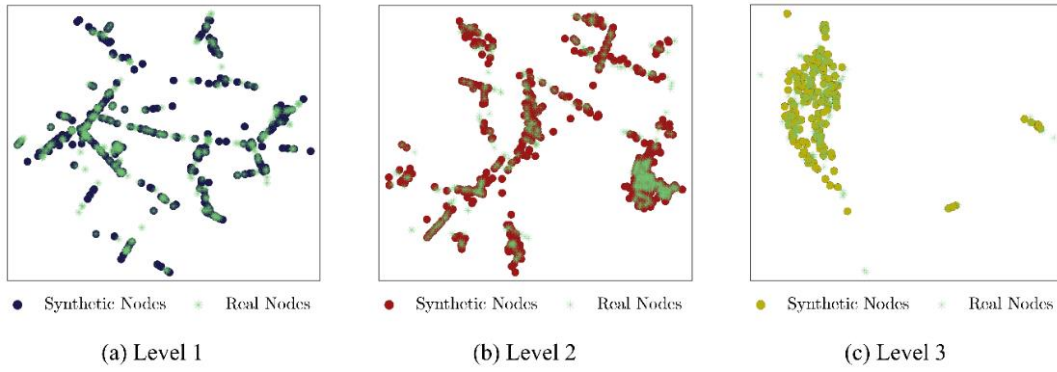


**Figure 11.** Real nodes of the gas network and synthetic nodes generated using GMM for each pressure level. Numbers of GMM components are 50, 36 and 11 in Levels 1, 2 and 3.

### 2.3.2.2 Identification of subnetwork islands

An important structural difference between Level 1 of the real network and the lower Levels (2 and 3) is that the first features a self-connected structure, whereas the latter are made up of several network islands. While these clusters of nodes form links with the upper pressure level (Level 1), they are completely disconnected one with another. This implies that, for a given synthetic subnetwork level, connections should be generated exclusively between nodes belonging to a common cluster.

In order to identify clusters in the generated datapoints, the Density-Based Spatial Clustering of Applications with Noise (DBSCAN) algorithm is applied separately for the synthetic nodes of Level 2 and Level 3. DBSCAN can detect clusters of arbitrary shapes and is resistant to noise, which turns it very suitable for this application. Additionally, like all the density-based clustering methods, DBSCAN groups datapoints forming contiguous regions of high point density. This latter property is particularly useful for identifying clusters of nodes belonging to lower network levels. These network portions should, in fact, be sufficiently distant to justify the absence of pipelines connecting them. These particular needs could hardly be met by other clustering methods, like K-means and its variants, which may encounter difficulties in handling clusters with highly different sizes, shapes and densities.

The DBSCAN algorithm is fully described in the paper from Ester et al. [85] and governed by the parameters *MinPts* and *Eps*. The latter represents the maximum distance between observations belonging to the same cluster, while *MinPts* is the minimum admitted number of points in each cluster. DBSCAN is executed for a fixed value of *MinPts* equal to 3 (based on observations on the real

networks) and for varying values of  $Eps$ . Being  $Eps$  an arbitrary parameter, its optimal value is determined by maximizing a custom performance metric, namely the Average Between-Cluster Minimum Distance (ABCMD). ABCMD returns the average of the minimum inter-cluster distances, that is the distances of the closest couples of points belonging to different clusters, for each couple of clusters. In this manner, the procedure favours the creation of well separated subnetwork islands. Nodes detected as outliers by the DBSCAN algorithm are excluded from the synthetic subnetworks.

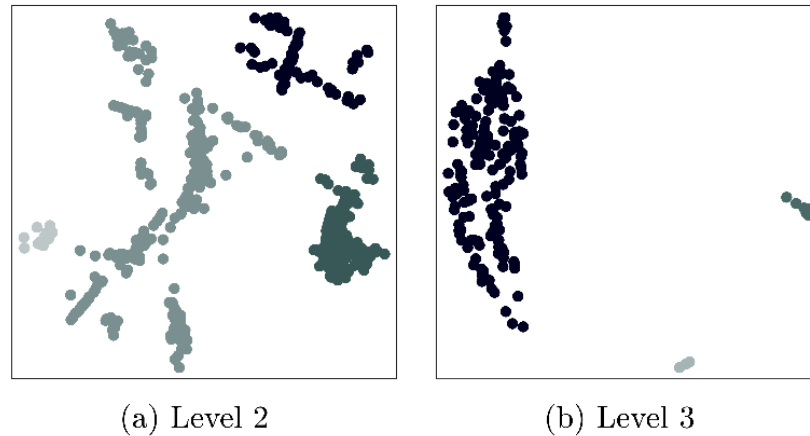


Figure 12. Clusters of synthetic nodes detected for (a) Level 2 and (b) Level 3, displayed with different colours. The nodes of Level 2 and 3 are the same as displayed in Figure 11.

In the last stage, clusters of nodes in the same pressure level are merged if their minimum distance is less than a fixed threshold, assumed to be 500 m for Level 2 and 350 m for Level 3. This is needed to reduce the number of subnetwork islands determined by the DBSCAN and achieve a better conformity with respect to the real network. This step represents the only tailored user intervention in the whole procedure. Yet, the choice of the above values could be generalized and/or automatized having access to a sufficiently high number of real networks.

The above procedure is applied to the set of synthetic nodes generated as from Figure 11. The results of the clustering procedure are displayed in Figure 12. Excluding the nodes detected as outliers, the procedure led to the establishment of 4 and 3 clusters of nodes (or network islands) in Level 2 and Level 3, respectively. Values of  $Eps$  for DBSCAN algorithm are 296 (in  $m$ , for Level 2) and 134 (for Level 3), while  $MinPts$  is 3.

### 2.3.3 Establishment of basic connectivity: formation of tree

For each pressure level, connections are generated between the synthetic nodes in a way that replicates the spatial evolution of network infrastructures in the real world. In this stage, the basic connectivity is provided to the network by growing a spanning tree between its nodes. In order to ensure the formation of islands within each subnetwork, links are drawn exclusively between nodes belonging to the same cluster.

The construction of spanning trees relies on a custom algorithm inspired by the work of reference [64]. The procedure connects the synthetic nodes imitating the spatial evolution of infrastructure networks and is carried out in a probabilistic fashion, which favours the creation of connections among near pairs of nodes. The procedure iteratively selects one of the synthetic nodes and adds it to a growing structure of the tree. The probability for a node to be sampled increases with its closeness to  $\bar{\mathbf{p}} = (\bar{x}, \bar{y})$ , that is the average position of nodes in the given cluster. In particular, for a  $i$ -th node with position  $\mathbf{p}_i = (x_i, y_i)$ , its probability to be sampled and added to the spanning tree is proportional to  $\exp\left(-\frac{\|\mathbf{p}_i - \bar{\mathbf{p}}\|^2}{2\alpha^2}\right)$ , where  $\alpha$  is a parameter which can be suitably controlled. Once sampled, the new node is connected to the closest node already incorporated in the spanning tree.

It has been observed that nodes of gas networks never feature a degree higher than 4. Therefore, the procedure also exerts a control action over the number of connections of the nodes, that are kept minor or equal to 4.

### 2.3.4 Network reinforcement: creation of cycles

Typically, distribution gas networks are meshed grids. Starting from the synthetic spanning trees created in the prior step of the procedure, cycles are therefore created by adding an extra number of pipelines. For each  $k$ th pressure level, a total of  $m_k - n_k + 1$  new pipelines are included, where  $m_k$  and  $n_k$  are the number of edges and nodes of real network, belonging to the  $k$ th pressure level. The new pipelines are distributed among the various synthetic subnetwork islands proportionally to their size (i.e., number of nodes).

The properties of the loop resulting from the addition of one edge strongly depends on the selection of the nodes to be connected. According to the findings

on the loop-related topological properties of real-world grids (see Section 2.2.4 of this thesis), different approaches are adopted for street-level and higher-level networks.

#### 2.3.4.1 Street-level networks

In street-level networks (typically LP systems, although some sections of MP grids like 6<sup>th</sup> species may be included in the definition) the creation of loops is favoured in areas characterized by high nodal densities, and it is realized by linking preferentially close pairs of nodes. Recalling from Section 2.2.4 the definition of  $\rho$  (average Euclidean distance between a node in the network and its 10 closest neighbours), the procedure is executed for each pressure level, and for network island, as follows.

Initially, a node is sampled from the spanning tree with a probability that increases with the surrounding node density. More precisely, the probability for a node  $i$  to be sampled is proportional to  $\exp\left(-\frac{\rho_i^2}{2\beta^2}\right)$ , and  $\beta$  is a parameter. In a second stage, the sampled  $i$ th node with position  $\mathbf{p}_i = (x_i, y_i)$  is preferably linked to a nearby  $j$ th node with position  $\mathbf{p}_j = (x_j, y_j)$ . Accordingly, the probability for a  $j$ th node to be selected and linked to node  $i$  is proportional to  $\exp\left(-\frac{\|\mathbf{p}_i - \mathbf{p}_j\|^2}{2\gamma^2}\right)$ , being  $\gamma$  another parameter. The procedure precludes self-connections and multiple connections. Additionally, similarly as in the formation of the spanning trees, the procedure prevents the assignment of more than 4 connections to a node.

It should be noted that  $\beta$  and  $\gamma$  are parameters that affect the width of the respective Gaussian-shaped functions. A large value of  $\beta$  allows for the generation of pipelines even in sparse (low-density) areas while a small  $\beta$  favours the creation of new pipelines in high-density regions of the network.  $\gamma$  affects the physical length of the pipelines to be generated: low  $\gamma$  values facilitate the creation of short connections, while high  $\gamma$  allow establishing connections among nodes far from one another.

#### 2.3.4.2 Long-range distribution networks

A different approach is adopted for modelling loops in longer-range distribution infrastructures, such as most of the medium-pressure grids illustrated in the previous sections. The extra edges must contribute to an efficient

improvement of the connectivity of the growing network, providing shortcuts among regions that are topologically distant and spatially close. For this purpose, couples of nodes  $i$  and  $j$  are described in terms of mutual physical (Euclidean) distances  $\|\mathbf{p}_i - \mathbf{p}_j\|$  and mutual topological distances  $D_{ij}$  (node-to-node path length). Accordingly, at each iteration the network structure is integrated with a new edge among the couple of nodes featuring the highest  $\frac{D_{ij}}{\|\mathbf{p}_i - \mathbf{p}_j\|}$  ratio.

### 2.3.5 Links among the pressure levels

The procedures described above generate connections between nodes belonging to the same pressure level and to a common subnetwork island. The resulting network is made up of several components that do not communicate between each other. In this last stage, the connectivity of the whole network is guaranteed by including pressure reduction stations between Level 1 and the lower network levels. The model assigns to Level 2 and Level 3 as many reduction stations as in the real network. These are distributed among the network islands proportionally to their size, which can lead to the creation of a slightly different number of reduction stations than the real one, due to rounding operations. Synthetic pressure reduction stations of a given island are placed in correspondence of the closest end-node (node with degree = 1) of Level 1 and connected to a neighbouring node of the island. The result is showed in Figure 13.b for a synthetic network island of pressure level 2.

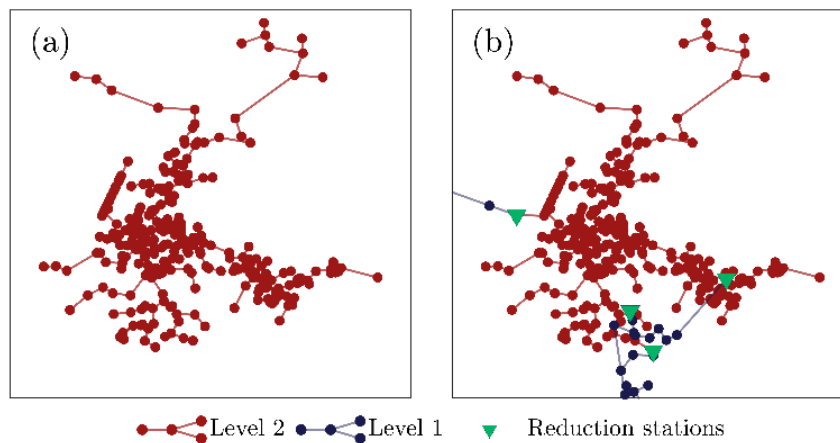


Figure 13. (a) Close-up of a stand-alone synthetic island of Level 2; (b) connection of the island to the upper network level by means of reduction stations (b). Connections within the island were generated with parameters  $\alpha = 28 (m)$ ,  $\beta = 326 (m)$  and  $\gamma = 116 (m)$ .

## 2.4 Model evaluation

The algorithm is applied to the reference distribution network of Figure 10. The realism of the synthesized network is assessed by means of suitable metrics, that are described later within this section. Since the spatial and topological properties of the gas grid substantially depend on the network pressure level, separate analyses are performed for each level of the generated synthetic grid.

The control parameters of the algorithm ( $\alpha$ ,  $\beta$  and  $\gamma$ ) have been tuned for every pressure level, measuring the similarity of the synthetic networks against the reference grid. Tests have been carried out with around 5000 permutations of the parameter values. While the choice of  $\beta$  and  $\gamma$  affects the location and size of the loops in street-level networks, the connectivity of the grids, and especially their average path length, is mostly affected by the calibration of  $\alpha$ .

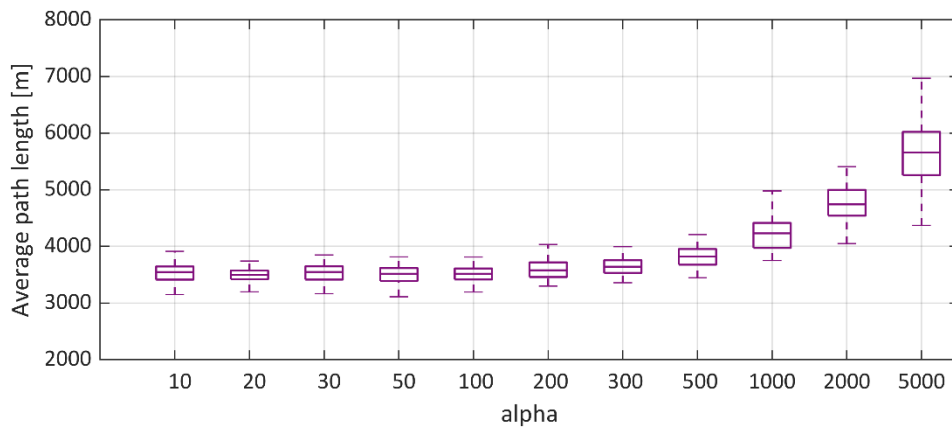


Figure 14. Sensitivity of level-1 network topologies to the choice of parameter  $\alpha$ .

The sensitivity of level-1 networks to the choice of  $\alpha$  is showed in Figure 14. The average path length of the networks diverges for  $\alpha$  values higher than 100, while it is rather constant around realistic values of about 3700 m for lower  $\alpha$ . Based on similar observations, the resulting selection of values for  $\alpha$ ,  $\beta$  and  $\gamma$  is showed in Table 4.

Table 4. Selected values of  $\alpha$ ,  $\beta$  and  $\gamma$  for the reference distribution network.

	$\alpha$	$\beta$	$\gamma$
Level 1 (4 <sup>th</sup> species)	93	.	.
Level 2 (6 <sup>th</sup> species)	28	.	.
Level 3 (7 <sup>th</sup> species)	140	559	5

The parameter selection of Table 4 can produce a virtually infinite number of different networks with similar spatial and topological properties. This is due to the probabilistic nature of the algorithm, which ensures that each execution leads to a different spatial disposition of the nodes and of their connections.

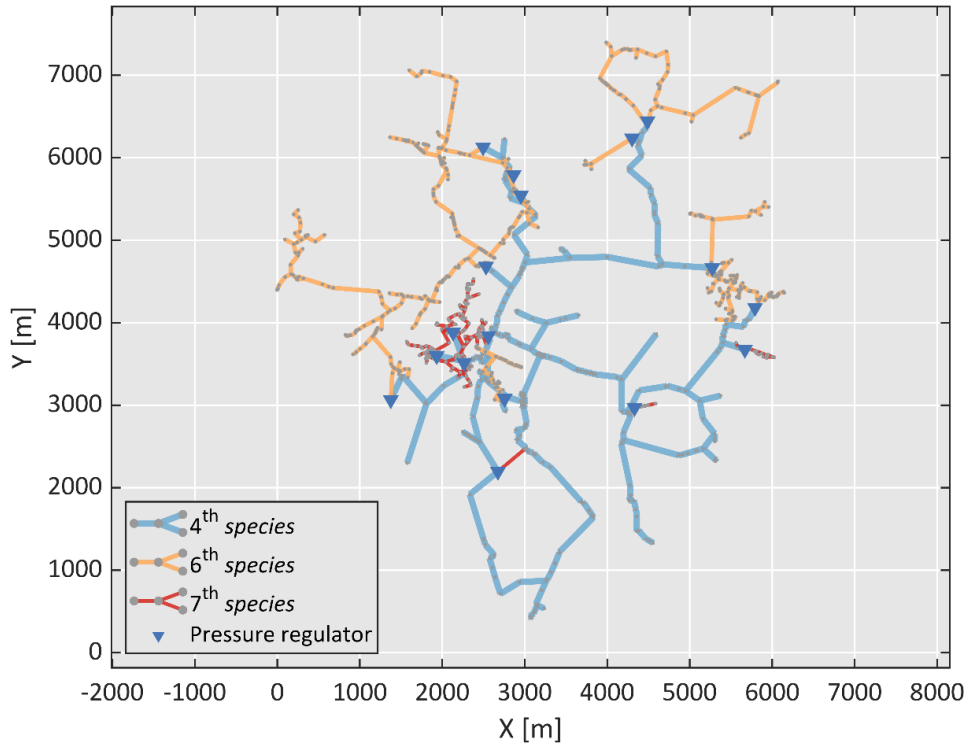


Figure 15. Sample of one out of 100 multi-level synthetic gas networks generated by the algorithm with the parameter selection of Table 4.

Accordingly, the generator of synthetic topologies is executed 100 times, producing as many fictitious networks. Figure 15 shows one of the obtained multi-level synthetic gas grids. The networks feature a visually similar spatial distribution of nodes and edges with respect to the real case. Pressure reduction stations are drawn in correspondence of the terminals of Level 1 that are closest to the other subnetworks. Their modelled position is appreciably consistent with the reference distribution grid (for comparison, see Figure 10).

#### 2.4.1 Methods for assessing the structural similarity

To assess the consistency of the structural properties of the synthetic and real gas networks, the following sections propose a comparison between the degree distributions, pipeline lengths, average path lengths and clustering coefficients of

the real-world and fictitious grids, together with other basic network information. Each pressure level of the synthetic network is separately analysed.

The comparison between the real and synthetic distributions of properties (i.e., degrees and pipe lengths) is carried out by means of suitable statistical tools. The adopted metrics, i.e., the two-sample Kolmogorov-Smirnoff statistic and the Kullback-Leibler divergence, are described below.

#### 2.4.1.1 Comparison of degree distributions

The two-sample Kolmogorov-Smirnoff (KS) statistic ( $D_{KS}$ ) is deployed to test the degree distributions generated by the model against the real distributions. This is done consistently with the work in reference [64].

The two-sample KS statistic measures the fit between two empirical distributions. It is defined as the maximum absolute difference between the cumulative distributions of the two empirical distributions in question. Its value can span between 0 (high correlation) and 1 (low correlation).

Defining the cumulative of the discrete distributions to be compared as:

$$P = \{p_1, \dots, p_n\} \quad (2.7)$$

$$Q = \{q_1, \dots, q_n\} \quad (2.8)$$

the KS statistic is given by:

$$D_{KS} = \max |p_i - q_i| \quad \text{for } i = 1, \dots, n \quad (2.9)$$

#### 2.4.1.2 Comparison of line length distributions

In agreement with the methodology in [64], the length distributions of the pipelines in the real and synthetic networks are compared using the Kullback-Leibler (KL) divergence  $D_{KL}$ . If  $P = \{p_1, \dots, p_n\}$  and  $Q = \{q_1, \dots, q_n\}$  are discrete distributions, the KL divergence is a measure of their statistical distance and it is given by:

$$D_{KL}(P\|Q) = \sum_{i=1}^n p_i \log \frac{p_i}{q_i}, \quad i = 1, \dots, n \quad (2.10)$$

. The KL divergence is a non-symmetric measure, hence  $D_{KL}(P\|Q) \neq D_{KL}(Q\|P)$ . In all its following utilizations, the KL divergence is computed as  $D_{KL}(\{\text{Real distribution}\} \| \{\text{Synthetic distribution}\})$  using natural logarithms.

## 2.4.2 Topological properties of synthetic networks

The statistical tools illustrated above and the topological metrics already introduced in the characterization of real-world grids (section 2.2) are deployed for a description of the synthesized networks and an assessment of their similarity to the adopted reference grid. Results are illustrated and discussed separately for each pressure level. A summary of the resulting properties – and of the similarity assessment – is provided in Figure 16 (degree distributions), Figure 17 (line length distributions) and Table 5 (summary of structural properties).

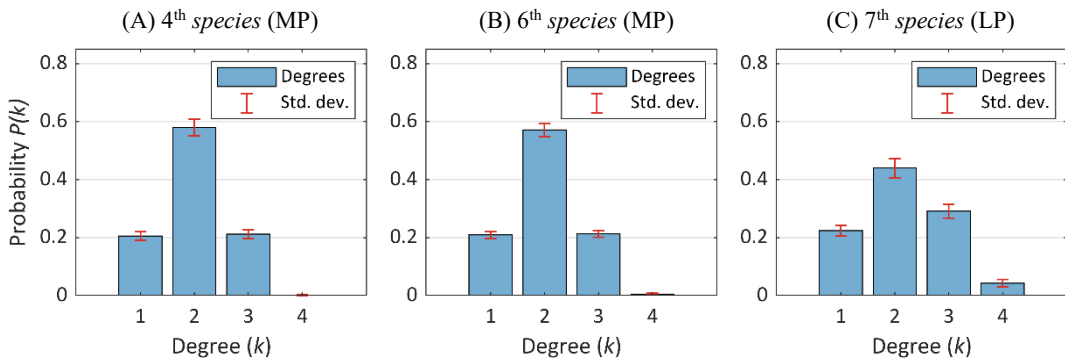


Figure 16. Degree distributions by pressure tiers of synthesized gas networks.

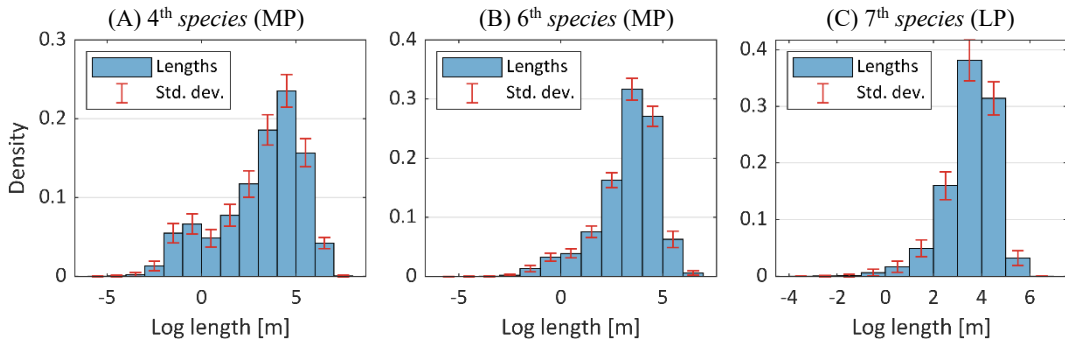


Figure 17. Length distributions of pipelines belonging to different pressure tiers in synthesized networks. Lengths are computed as point-to-point Euclidean distances between the connected nodes. Lengths are in m and their logarithm is natural logarithm.

### 2.4.2.1 Level 1 (4<sup>th</sup> species)

The generated synthetic subnetworks of Level 1 exhibit a fair agreement with the corresponding level in the reference network. The networks feature on average a very low clustering coefficient ( $C = 7 \times 10^{-4}$ ), which is satisfactorily representative of the zero-clustering coefficient of the real subnetwork ( $C = 0$ ).

Table 5. Summary of the structural properties of the synthetic and the reference gas networks, for each pressure level of the network.

		Level 1		Level 2		Level 3	
		Synth.	Real	Synth.	Real	Synth.	Real
<b>Number of independent components</b>	Min	1	<b>1</b>	1	<b>5</b>	1	<b>5</b>
	<b>Average</b>	<b>1</b>		<b>3.6</b>		<b>3.0</b>	
	Max	1		5		4	
<b><math>L</math> [m]</b>	Min	2824	<b>3751</b>	1424	<b>1627</b>	508	<b>686</b>
	<b>Average</b>	<b>3235</b>		<b>2179</b>		<b>625</b>	
	Max	3601		4887		736	
<b><math>L_{HOPS}</math></b>	Min	24.8	<b>36.4</b>	23.8	<b>30.1</b>	8.5	<b>12.9</b>
	<b>Average</b>	<b>30.1</b>		<b>31.9</b>		<b>10.7</b>	
	Max	35.8		69.2		12.8	
<b><math>C</math></b>	Min	0	<b>0</b>	0	<b>0</b>	0	<b>0</b>
	<b>Average</b>	<b>0.0007</b>		<b>0.0013</b>		<b>0.0125</b>	
	Max	0.0080		0.0057		0.0468	
<b><math>D_{KS}</math></b>	Min	0.038		0.066		0.090	
	<b>Average</b>	<b>0.069</b>		<b>0.094</b>		<b>0.128</b>	
	Max	0.099		0.122		0.165	
<b><math>D_{KL}</math></b>	Min	0.078		0.036		0.007	
	<b>Average</b>	<b>0.147</b>		<b>0.070</b>		<b>0.059</b>	
	Max	0.255		0.102		0.168	

The average path lengths oscillate around a mean value of 3235 m, that is close to the reference ( $L = 3751$  m). A good agreement is also obtained when using unweighted edges lengths (30.1 hops vs. 36.4 hops).

The synthetic subnetworks of level 1 feature a maximum nodal degree equal to 4, while maintaining a real-like predominant presence of degree-2 nodes (see Figure 16). On an average basis, the KS statistic  $D_{KS}$  between the real and modelled cumulative degree distributions is 0.069, which is accepted as a satisfactory value and is comparable to results obtained by [64].

The comparison between the pipeline length distributions of  $R_1$  and  $S_1$  generates a KL divergence  $D_{KL}$  equal to 0.123, evidencing a fine agreement between the two networks.

#### 2.4.2.2 Level 2 (6<sup>th</sup> species)

The level-2 synthetic subnetworks are disconnected graphs made up of multiple system islands (3.6 on average). As visible from the sample provided by Figure 15, the level-2 islands (in yellow) are independent one from another and are instead connected to the upper subnetwork of level 1. The interface between the subnetworks of Levels 1 and 2 is given by a set of pressure reduction stations, whose number varies among the synthesized networks.

The mean clustering coefficient  $C$  in the generated subnetwork amounts to 0.0013. In a fraction of modelled subnetworks, clustering is zero as in the real-world reference. On average, the unweighted average path length is 28.5 *hops*, which is very close to the respective real value ( $L = 30.1$  *hops*).

Pipeline lengths of the level-2 subnetworks are illustrated in Figure 17. The average KL divergence  $D_{KL}$  between the real and synthetic networks is equal to 0.070, indicating a fine agreement, in line with results from [64].

The two-sample KS statistic between the real and synthetic degree distribution amounts to 0.094 and reflects a relatively poorer correspondence, compared to the upper network level. This result is mainly driven by the twofold function of the Level 2 section of the real grid, which causes parts of it to acquire structural properties similar to Level 1 while other portions exhibit analogous properties to Level 3. This phenomenon is quite visible in the representation of the real network (Figure 10) and turns it more challenging to correctly calibrate the parameters  $\alpha$ ,  $\beta$  and  $\gamma$ .

#### 2.4.2.3 Level 3 (7<sup>th</sup> species)

The generated low-pressure subnetwork topologies of Level 3 are constituted by several islanded systems – 3 on average –, similarly to Level 2. The subnetworks are characterized by an overall higher spatial compactness. As a consequence, the clustering coefficient  $C$  results higher than in the other subnetworks and amounts to 0.0125 on average (still low, however, in absolute terms). On an average basis, the modelled average path length  $L$  is 625 m (10.7 *hops*), considerably lower than in the previous cases due to the smaller structures of level-3 subnetworks and reduced spatial extensions. The KS statistic  $D_{KS}$  amounts to 0.128 on average, which, with respect to the other network levels, represents a poorer performance in the modelling of the degree distributions. Despite a low similarity with the reference gas grid, a comparison between panels

(C) of Figure 2 and Figure 16 shows that the modelled degree distribution for the low-pressure grid is realistic, when compared against other real-world benchmarks. It can be inferred that the model is fairly well calibrated for low-pressure network tiers and the poorer accuracy mainly derives from the peculiar degree distribution of the LP sections of the reference grid. A fine agreement is finally obtained between the real and modelled length distribution of the pipelines, which return an average KL divergence  $D_{KL}$  equal to 0.059.

## 2.5 Concluding remarks

The Chapter has proposed a systematic topological characterization of real-world distribution gas grids, followed by the description and the application of a tool for the establishment of synthetic realistic network topologies.

The topological analysis of the grids has been carried out separately for the different pressure tiers that typically compose distribution systems. The different network levels have demonstrated to feature different characteristics (in terms of degree distributions, pipeline lengths and average path lengths), highlighting the importance of adopting differentiated approaches to build correct network models. At the same time, all the pressure tiers are in general characterized by degree values limited to 4 and by the absence of clustering among the nodes.

The model for the construction of synthetic network topologies follows a parameter-based probabilistic approach (each execution produces a different and unique network) and is capable of generating multi-level networks interfaced by pressure reduction stations, accounting for their underlying structural differences. This latter aspect constitutes the major novelty of the tool with respect to previously published research works.

The proposed application adopts a real-world multi-pressure grid as a reference and performs the synthetic generation of 100 statistically similar network topologies. The resulting properties of the networks provide evidence on the substantial similarity between the reference real-world gas grid and the networks generated by the proposed algorithm. The correspondence of the spatial distributions of the respective nodes, pipelines and pressure regulators can be verified by comparing Figure 10 with the sample synthetic network in Figure 15. In addition, numerical data illustrated and compared in Table 5 prove that the structure and the topology of the networks are also very similar.

The distribution of the number of connections in the synthetic networks is fairly representative of the real case study ( $D_{KS}$  lower than 0.1 in Levels 1 and 2). A poorer agreement is obtained for the LP topologies of Level 3. However, it has been pointed out that the obtained level-3 degree distributions are consistent with the other LP real-world networks investigated.

Length distributions of synthetic pipelines are consistent with the real grid in all the pressure levels. The resulting KL divergences do not substantially vary with the levels, being the worst average  $D_{KL}$  equal to 0.147 (Level 1). As a result of the fair modelling of the degree and line length distributions, a satisfactory agreement is also achieved between the modelled and actual average path lengths  $L$ .

These results imply that the algorithm can generate realistic network structures that, if assigned with proper technical specifications (i.e., pipeline diameters, nominal operating pressures, etc.) can offer a large number of reliable fictitious case studies for carrying out fluid-dynamic simulations and techno-economic analyses on gas grids. The missing building-blocks for achieving this objective, i.e., the assignment of technical specifications to the synthetic grids, are addressed in the following Chapters of this thesis.

# Chapter 3

## Technical design of distribution gas grids

### 3.1 Design criteria for gas distribution systems: standards and best practices

Distribution gas networks constitute the final ring of the supply chain of natural gas to end-users. Their purpose is delivering gas to residential, industrial and commercial consumers guaranteeing safety conditions and continuity of supply. Distribution systems are typically operated at intermediate, medium and low-pressure tiers (IP, MP, LP), whose classification varies with national standards and legislations. Pressure levels under the competence of distribution grids span from a few tenths of millibars gauge (street level, LP networks) to a few bars (MP and IP). Table 6 lists pressure tiers of gas networks for different countries, as defined by local legislation and standards. Infrastructures are frequently operated at multiple pressures, disposed in decreasing order from the points of supply down to the final users, and interfaced by pressure regulators. The gas supply occurs in correspondence of one or more sources of pressure, which can be served by either liquefied natural gas (LNG) storage tanks or, most frequently, by pressure reduction and metering stations (*city gates*) connected to the upstream high-pressure network. In the vast majority of cases, these sources of pressure induce the whole functioning of the distribution grids, which in fact do not make use of compressors (largely deployed in transmission systems) to actively sustain the motion of gas. The technical sizing of the system must

therefore ensure that the grid complies with specific technical constraints (e.g., minimum pressure, maximum velocity) in a passive operational mode. There may exist several viable configurations for the correct design of distribution grids, comprising diverse system layouts and pressure tiers. The dimensioning of the grid also needs to account for uncertainties in immediate and projected gas demand, as well as for possible system extensions. For these reasons, the design of distribution systems consists of an iterative process, making use of heuristic methods and producing technical solutions that, in most real-world applications, are not optimal but rather provide sufficient degrees of confidence and flexibility against planning uncertainties.

**Table 6: Definition of pressure tiers of gas distribution systems for several European Countries. High-pressures are included when specific definitions within the distribution system are applied. Source: adapted from [86].**

Country	High pressure (bar)	Medium pressure (bar)	Low pressure (bar)
<b>Austria</b>	-	> 6	≤ 6
<b>Croatia</b>	> 5	0.1 – 5	≤ 0.1
<b>Czech Republic</b>	-	0.05 – 4	≤ 0.05
<b>France</b>	-	MPC: 4 – 25 MPB: 0.4 – 4 MPA: 0.05 – 0.4	≤ 0.05
<b>Germany</b>	-	0.1 – 1	≤ 0.1
<b>Hungary</b>	-	0.1 – 4	≤ 0.1
<b>Italy</b>	-	4 <sup>th</sup> species: 1.5 – 5 5 <sup>th</sup> species: 0.5 – 1.5 6 <sup>th</sup> species: 0.04 – 0.5	≤ 0.04
<b>Latvia</b>	4 – 16	0.05 – 4	≤ 0.05
<b>Lithuania</b>	5 – 16	Cat. 1: 2 – 5 Cat. 2: 0.1 – 2	≤ 0.1
<b>The Netherlands</b>	-	Four MP tiers: 0.2 – 1; 1 – 2; 2 – 4; 4 – 8	≤ 0.2 (0.1 and 0.03 bar)
<b>Poland</b>	-	0.1 – 5	≤ 0.1 bar
<b>Portugal</b>	-	4 – 20	≤ 4
<b>Spain</b>	4 – 16	MPB: 0.4 – 4 MPA: 0.05 – 0.4	≤ 0.05
<b>UK</b>	-	IP: 2 – 7 (*) MP: 0.075 – 2	≤ 0.075

(\*) Intermediate pressure

### **3.1.1 Estimation of gas demand**

The estimation of the gas demand to be satisfied by the gas grid is a critical stage for the design of the distribution system. The gas network should be designed to guarantee reliable operations at conditions of maximum gas demand. These conditions are firstly assessed by identifying the number and the categories of the supplied customers, that can be either residential, commercial, industrial or electrical power generation plants (mostly connected to high-pressure and transmission level gas networks). Determining maximum values of instantaneous gas consumption can be a challenging and partially inconvenient practice to approach the problem. Often, average consumption rates over a period of time are adopted instead. In addition, diversity factors are applied to the aggregated maximum loads of individual users to account for the unlikelihood of simultaneous gas consumption. Statistics on historical data and/or reference consumption values are usually deployed to identify the maximum gas demand that the system should be able to cope with. According to the UK standards, for instance, this is represented by the maximum load, averaged over any period of 6 minutes, that occurs in a single day, in not more than 1 winter in 20 years. Other methodologies make use of load duration curves and hourly, daily, weekly or seasonal load profiles.

### **3.1.2 System layout and pipeline locations**

The network must be able to supply all the identified customers and its layout should be drawn with considerations on cost minimization, system looping and uniformity of pressures, planned grid extensions, and geographical restrictions. The routing of the pipelines is constrained by safety standards and physical impediments. It is generally recommended that distribution system lines should never be installed below buildings, nor along heavy-traffic roads, when practically feasible. When crossing or running along other utilities, gas pipes should always be installed above, and possibly distanced from, the other lines. Other buffer zones should usually be respected according to local, regional and national environmental constraints. Whenever feasible, the network should feature structural sources of redundancy for a higher reliability and hydraulic uniformity. System loops and multiple sources of pressure (city gates and MP/LP pressure

regulators) are among the options. In large distribution systems supplied by multiple sources of pressure, consideration should be given to a redundant design of the pipework, to ensure that each point of delivery can be correctly supplied by more than one source – two regulation stations in most cases –, thus guaranteeing continuity of supply in case of failure or maintenance of a regulator or in-the-middle network sections.

### **3.1.3 Hydraulic design**

The hydraulic design of gas grids must ensure that the distribution system complies with safety and service quality constraints, that are normally defined by national standards and legislation. The selection of the pressure tiers of each network section is derived by the typology, the entity and the location of the supplied customers. Medium-pressure systems offer a higher capacity, smaller pipe diameters (with, however, higher thicknesses), wider admissible pressure ranges, and higher flexibility in case of potential system expansions. On the other hand, distributing gas in MP involves tighter safety constraints, and requires installing pressure regulators for most of the connections to residential and commercial customers. Low-pressure grids are widely deployed for street-level gas delivery, given that their pressures (few dozens of millibars) are typically compatible with customers' equipment, net of pressure drops along the service lines. No pressure regulators are therefore needed in LP systems (with benefits in capital and O&M costs) and softer restrictions are generally applied, in the face of less distribution capacity and limited potential for system expansions.

In real-world applications, gas networks are dimensioned to constrain their working conditions within target boundaries of operational states. The operational bounds, namely admissible gas pressure and velocity ranges, can be specified by the system designer considering best practices and case specificities. However, pressure and velocities must normally comply with national legislation and standards. Accordingly, the hydraulic design of distribution gas grids needs to satisfy a maximum allowable operating pressure (MAOP), a design minimum pressure (DMP) and a maximum flow velocity. The MAOP is the maximum pressure at which the pipework can be continuously operated at ordinary working conditions. The DMP is the minimum pressure level to be guaranteed across the whole infrastructure to ensure the safe and correct operation of customer

appliances, service regulators and intermediate pressure reduction stations. The maximum gas flow velocity constitutes a further constraint to prevent excessive mechanical stress, noise, dragging of impurities and corrosion of pipelines. The above design parameters can differ among grid pressure tiers and national standards. As a matter of example, in Italy, MAOPs and DMPs must obey to the pressure bounds indicated by the classification specified by the national legislation for each pressure tier. According to D.M. 16<sup>th</sup> April 2008 [84], gas grids are classified in *species* with decreasing pressure ranges. At distribution level, the most extensively deployed classes are represented by 4<sup>th</sup> and 6<sup>th</sup> *species* (MP) and 7<sup>th</sup> *species* (LP). Recommended maximum velocities for each pressure level are indicated in the standard UNI 9165:2020 [87]. Accordingly, gas velocities up to 5 m/s are recommended for 7<sup>th</sup> *species* LP networks, operated – by definition – at not more than  $40 \times 10^{-3}$  bar<sub>g</sub>, and not less than a minimum pressure for the correct functioning of end-users’ appliances (usually values down to  $20 \times 10^{-3}$  bar<sub>g</sub> are admitted). Velocities up to 15 m/s are recommended for MP grids belonging to 6<sup>th</sup> *species* (operated between  $40 \times 10^{-3}$  bar<sub>g</sub> and 0.5 bar<sub>g</sub>), while 25 m/s is the limit indicated for MP grids of 4<sup>th</sup> *species* (operated between 1.5 bar<sub>g</sub> and 5 bar<sub>g</sub>). Table 7 provides a summary of the network classes and their respective operational restrictions.

**Table 7: Classification and operational bounds of medium and low-pressure networks according to Italian legislation and standards.**

Pressure level	Network class	MAOP (bar <sub>g</sub> )	DMP (bar <sub>g</sub> )	Maximum velocity (m/s)
LP	7 <sup>th</sup> <i>species</i>	$40 \times 10^{-3}$	$20 \times 10^{-3}$	5
MP	6 <sup>th</sup> <i>species</i>	0.5	$40 \times 10^{-3}$	15
MP	4 <sup>th</sup> <i>species</i>	5	1.5	25

The minimum sizing of the system is provided by the solution ensuring a minimum pressure equal to the DMP at design (maximum design load) conditions. In real-world applications, however, oversizing the capacity of pipelines and regulators within the distribution grid is a common practice, especially at MP level, mainly due to the following reasons:

- Readiness for possible future system extensions and increase in downstream gas demand;

- Larger linepack of the infrastructure, with a consequent higher flexibility and resilience in cases of fast transients or upstream supply failures;
- Limited additional investments compared to the minimum design solution, since materials constitute a minor share of the total capital costs;
- Determined pipe diameters and regulator capacities must be adapted (rounded up) to discrete commercially available component sizes;
- Pressure at specific consumption points or regulation devices is required to be higher than DMP;
- Pressure level at the source may be subject to fluctuations, and in certain moments it may be lower than the nominal supply pressure.

It is therefore common for distribution grids to feature significant tolerances to minimum admissible pressures. Grid oversizing practices do not imply particular operational adjustments in MP networks, in which gas is delivered to intermediate, final and service pressure regulators. In network sections operated in LP, where the gas delivery to final users must occur at compatible pressure levels, a suitable compensation of the pressure at the source outlet must be foreseen.

Additional devices must be however included in the complete design of a distribution system to ensure safety conditions and correct fluid-dynamic behaviour. Typical components may comprise overpressure protections, relief valves, isolation valves, check valves, monitor regulators, drips, gas heaters and others. Despite their absolute relevance for the distribution system safety and proper functioning, the above devices and their design and installation are not furtherly treated in the present dissertation. This is primarily done for sake of simplicity and to focus on the scope of the intended applications.

The correctness of the hydraulic design is commonly verified with the support of network analysis tools. In the computer-aided design process, the criticalities of the distribution system are identified by the fluid-dynamic simulations carried out within a commercial software. The operational issues are subsequently addressed by the system designer, which corrects the size of some network sections, like the diameter of the pipelines and the capacities of the regulator stations. In the next section, an automated procedure for the realization of an efficient and accurate hydraulic design of a gas network is proposed.

## 3.2 Gas network technical designer

### 3.2.1 Purpose of the algorithm

Based on the previous design principles, a custom tool for the technical sizing of gas distribution grids has been developed. The tool offers the capability of providing a given input network with correct and realistic technical properties, in a completely automated fashion. The algorithm is developed in MATLAB environment and it can handle complex infrastructure topologies and custom design parameters in a computationally efficient way. The tool addresses design problems in which suitable diameters need to be assigned to the pipelines of a distribution system, when the following information is known:

- Network topology, system layout and route of the pipelines (i.e., known lengths);
- Pipeline materials (i.e., known roughness);
- Location of the supply points (city gates or, in general, sources of pressure);
- Pressure of gas supply at sources at design or test conditions;
- Location and thermal demand of gas loads at design conditions;
- Target operational restrictions: MAOP, DMP and maximum velocity.

On the one hand, the proposed algorithm potentially represents a *per-se* solution to address part of the computer-aided design process for real-world infrastructures. It could not however be intended as a complete and exhaustive library for the dimensioning of distribution systems: dedicated commercial computer programs (see for instance [88,89]) offer a wider set of functions that include transient analyses as well as safety and regulation devices that are not here contemplated. On the other hand, the tool constitutes a flexible, fully integrated and high-efficiency package for the assignment of accurate and realistic dimensions to the network structures produced as from Chapter 2. In this way, the generated networks assume the form of finished and fully synthetic gas grid models, readily deployable for simulation purposes. The present dissertation focuses this latter application. Accordingly, the technical designer of gas grids here presented constitutes a module in the framework of the generation of

synthetic network models, which follows and complements the package for the generation of statistically similar gas grid topologies (Chapter 2).

The technical sizing performed by the proposed tool replicates the design criteria typically adopted in the hydraulic design of a distribution system, discussed in the previous sections of this Chapter. Although the model has been designed to offer a wider flexibility, its description and application is here restricted to infrastructures operated at a single pressure tier and supplied by a single source node. For sake of completeness, details on how the tool has been designed to handle more complex cases are given later. The tool accomplishes the technical design of input network structures according to a set of custom parameters. Its major purpose is assigning the pipelines of the input network with suitable diameter sizes picked from a discrete set of off-the-shelf commercial sizes<sup>4</sup>. The diameter sizes are taken from a set of six real-world Italian distribution grids, operated at multiple pressure levels. The sizes of the diameters and their distributions across *species* 4<sup>th</sup>, 6<sup>th</sup> and 7<sup>th</sup> are illustrated in Table 8 and Figure 18.

Diameters (m)	
0.02	0.11
0.025	0.125
0.032	0.15
0.04	0.16
0.05	0.18
0.06	0.2
0.063	0.225
0.065	0.25
0.075	0.3
0.08	0.315
0.09	0.35
0.1	0.4

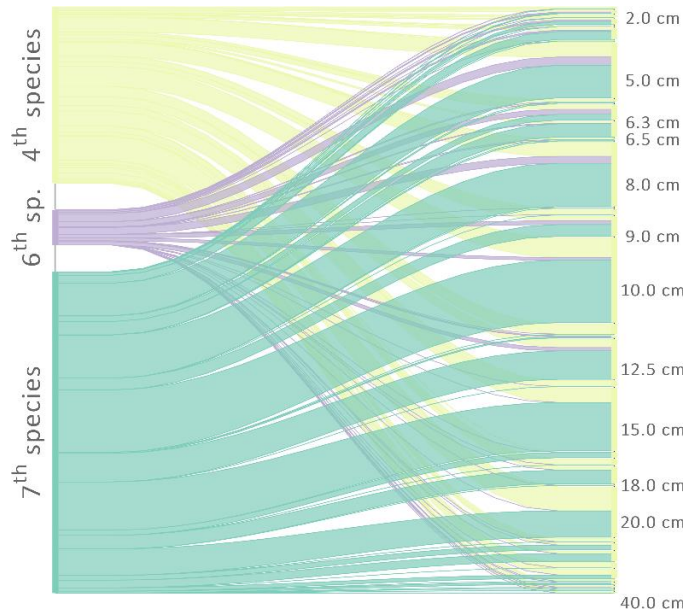


Figure 18: Distribution of diameter sizes by pressure tier, as from the sample of real-world Italian distribution grids.

Table 8: Diameter sizes from real-world Italian distribution systems.

The procedure ensures that, at design conditions, all the nodes are characterised by acceptable pressure values ( $p \geq p_{min}$ ) and all the pipelines feature admitted velocities ( $v \leq v_{max}$ ), when the gas supply at the source node occurs at the

<sup>4</sup> Mostly taken from real-world networks analysed in Chapter 2.

nominal pressure  $p_{nom}$ . The operational constraints  $p_{min}$ ,  $p_{nom}$  and  $v_{max}$  and other design parameters can be arbitrarily changed, so that the tool can be adapted to different types of networks and target design and/or test conditions. Other parameters and input information include the composition of the natural gas delivered by the system (needed to compute thermo-chemical and fluid-dynamic properties of the gas), the temperature of the ground (assumed in thermal equilibrium with the gas, i.e., isothermal conditions), and the roughness coefficient of the pipelines (i.e., varying with assumed materials). Complementary information is constituted by the location of the gas supply point, and the location and thermal demand of gas loads at design conditions. The list of inputs required by the model and their descriptions are provided by Table 9.

Design considerations that lie outside the merely hydraulic dimensioning of the network, and which are of central relevance in real-world gas distribution systems, are not addressed by the model as out of scope for the current applications. These aspects include safety and regulation devices and installation practices, and have been partly discussed and presented in earlier sections of the present Chapter.

**Table 9: Inputs required by the tool for the technical design of distribution gas networks.**

<b>Inputs</b>	<b>Unit</b>	<b>Description</b>
<b>Nominal source pressure, <math>p_{nom}</math></b>	bar <sub>g</sub>	Gas pressure at the supply node at design conditions
<b>Design minimum pressure, <math>p_{min}</math></b>	bar <sub>g</sub>	Minimum pressure to be guaranteed at all the nodes of the network
<b>Maximum flow velocity, <math>v_{max}</math></b>	m/s	Maximum admitted velocity of gas flow in the pipelines
<b>Location of gas supply point</b>	-	Index of the network node which withdraws gas from a source and supplies it to the grid at the nominal source pressure $p_{nom}$
<b>Nodal gas consumptions at design conditions</b>	MW	Design gas loads (in thermal power) at the consumption nodes – convertible into Sm <sup>3</sup> /h with known NG composition
<b>NG composition</b>	-	Molar composition of NG, needed to compute gas properties (i.e., higher heating value, density, viscosity, compressibility factor, etc.)
<b>Ground temperature</b>	K	Temperature of the ground – assumed in thermal equilibrium with the temperature of the gas across the network
<b>Roughness coefficient</b>	μm	Internal roughness of the pipelines – based on the material

### 3.2.2 Structure of the algorithm

The procedure, as detailed in Figure 19, consists in an iterative process in which, at each iteration, pipelines serving directly or indirectly one or more critical nodes (i.e., nodes for which  $p < p_{min}$ ) are enlarged. The process stops when all the nodes have acceptable pressure levels, and the network has therefore been correctly sized. The procedure pays particular attention to the achievement of realistic patterns of diameters, and it is designed to avoid oversizing with respect to the target minimum pressure  $p_{min}$ . Accordingly, the algorithm for the technical sizing of distribution gas grids is articulated in the following stages:

- 1) Acquisition of inputs: the tool receives input data, complying to standard formats, which need to include:
  - network (*Net*) topology,
  - design parameters: nominal operating/supply pressure  $p_{nom}$ , design minimum pressure  $p_{min}$ , maximum velocity  $v_{max}$ ,
  - location of load nodes and the respective thermal powers required at design conditions,
  - composition of natural gas.
- 2) Extraction of a spanning tree from the whole network structure: gas networks, also as produced by the algorithm of Chapter 2, are typically looped systems. For several reasons, however, it is desirable to refer to a tree network structure along the sizing process. A minimum spanning tree is therefore extracted from the looped structure of the original network making use of available MATLAB libraries. In particular, the Prim's algorithm for weighted undirected graphs is here deployed [90]. The weight of the edges, used to find the minimum tree structure, coincides with their length expressed in meters.
- 3) Initialization of pipeline diameters: the diameters of the pipelines in the *Tree* structure are initialized proportionally to the respective amount of transported fuel, calculated as the sum of the downstream gas loads. Downstream gas demands – originally expressed as thermal powers – are converted to volume flow rates estimating a uniform pressure drop across the network, and therefore used to compute diameter required for each pipeline. Diameters are dimensioned to obtain, in each pipeline, a flow velocity equal to 90% (conservative approach) of the maximum allowed velocity  $v_{max}$ . In this way,

all the subsequent enlargement of the pipes will ensure acceptable gas velocities. Afterwards the initialization of diameters in *Tree*, the remaining pipelines (i.e., belonging to the whole network but excluded from the spanning tree *Tree*) are sized as from bullet 6). All the obtained diameters are subsequently rounded to the closest available commercial diameter size.

- 4) Steady-state hydraulic analysis: a custom isothermal steady-state fluid-dynamic model of gas networks fully illustrated in [83] is deployed for a hydraulic test of the gas grid, to check for unfeasible physical solutions (i.e., pressures in the complex domain) or violations of the minimum pressure constraint (i.e., pressures lower than  $p_{min}$ ). The indices of the critical nodes – nodes featuring complex or unadmitted pressures – are collected in vector  $C$ . The fluid-dynamic test of the grid is set up at design conditions, therefore the pressure at the supply node is  $p_{nom}$  and the rates of gas demand of consumption node are as specified in the inputs. In order to reduce computational times, the GERG-88 equation of state and an explicit approximation of the friction factor equation (Vatankhah [91]) are adopted as options for the gas network simulator (the latter is used only for partially and fully turbulent flows). In the last stages of the procedure, when no more critical nodes are detected, a further check on the pressures and velocities is carried out using the more accurate implicit Colebrook-White equation [92].
- 5) Resizing of the pipeline diameters of *Tree*: if critical nodes are detected (i.e., vector  $C$  is not empty), the algorithm proceeds with the enlargement of a suitably identified set of pipelines. The enlargement is realized picking the next available size from the list of the commercially available diameters. In a first stage, the procedure is applied to the network spanning tree; afterwards, involved loops are resized as well. In principle, pipelines of *Tree* serving one or more critical nodes are identified as target pipes to be resized. The identification of the pipelines of *Tree* needs to comply with two main conditions, highlighted in the diagram of Figure 19:
  - *Condition n. 1*: A pipeline cannot be assigned with a diameter size that is larger than the diameter of its predecessor pipeline (i.e., the diameters of the pipes decrease from the supply node down to the terminals of the network). The algorithm verifies whether the targeted pipelines feature smaller diameters than their predecessors. Target

pipelines which do not satisfy the condition are therefore iteratively replaced with their upstream predecessor, until no violations are detected. This rule is inspired from observations from real-world distribution gas systems<sup>5</sup>, where most of the source-sink network patterns feature decreasing diameter values.

- *Condition n. 2*: No more than the strictly necessary number of pipelines is resized at one iteration: if enlarging two or more pipelines causes multiple beneficial effects on some downstream nodes, then only one of the pipelines is resized. This is done to avoid overlapping of effects which may incur risks of system oversizing. In particular, the algorithm ensures that the targeted pipelines belong to independent source-sink patterns. If overlapping paths are found, then only the pipeline closest to the root is resized.
- 6) Computation of diameters in loops: afterwards the resizing or the initialization of the pipelines in the spanning tree, loops in the whole network *Net* are assigned with an average diameter, as computed from the *Tree* pipelines participating in the same loop.
  - 7) Returning the finished network model: actions described in bullets 4 to 6 are repeated until all the nodes feature admitted pressure values. Afterwards, the correctly sized network model is returned in a standard format comprising all the technical specifications and the operational variables at design conditions.

### 3.2.3 Oversizing the networks

It has been discussed that real-world distribution grids are frequently oversized with respect to their actual demand. As a result, the minimum pressures occurring across the networks, at design conditions, may be higher than the design minimum pressure prescribed by the standards. The reasons behind these design choices have already been listed. The gas network technical designer illustrated above can be deployed to account for these design practices in a straightforward way, through a suitable adaptation of the input design parameters. Some options are here proposed:

---

<sup>5</sup> Real-world networks described in Chapter 2.

- Increasing  $p_{min}$ : the target minimum pressure can be changed to a higher value than the DMP, granting that network pressures are always higher than another custom lower pressure bound. Diversified values of target minimum pressure can also be specified for every node, for those cases where particular service requirements apply to specific nodes.
- Increasing the gas demand: thermal loads at design conditions can be increased with respect to the maximum expected gas consumption rates. A uniform oversizing coefficient can be deployed for all the load values. Alternatively, oversize degrees can be specified for each consumption node.
- Decreasing  $p_{nom}$ : the pressure at the source can be assumed lower than the nominal supply pressure to account for fluctuations.

### 3.2.4 Design of multi-source and multi-pressure systems

For sake of clarity and conciseness, the description of the tool provided in the previous sections assumed that the designed system should feature only one source of pressure and one pressure level. This is not the case for many real-world distribution grids. For this reason, the tool has been prepared to handle complex cases involving an arbitrary number of pressure sources, as well as multiple pressure tiers interfaced by pressure reduction devices. This has been done consistently with the approach adopted for the generation of synthetic network topologies (Chapter 2).

In multi-pressure systems, the algorithm proceeds with the identification of system *islands*, that are portions of the grid operated at a single pressure tier. When each island is supplied by a single source of pressure – regardless of whether the source is a city gate or an intermediate pressure regulator – the technical design of the grid is carried out separately for every island, following the procedure illustrated in the previous sections.

In cases where one or more islands are supplied by multiple sources of pressure, a slightly different approach is undertaken. Every island featuring multiple sources is internally partitioned into as many subnetworks, whose pipelines and nodes lay closest to a given source. Afterwards, each of the subnetworks undergoes the same dimensioning procedure as before.

In previous sections it has been said that in large systems with more than one source of pressure it may be worth implementing a redundant design, which ensures that every point of consumption can be correctly supplied by more than one source of pressure. This may be useful for contingencies when one of the points of supply offers a limited capacity or is out of service. Based on these considerations, the tool offers the capability to prepare the system against the failure of one supply point. If this option is activated, the sizing of a network island is repeated assuming each time the unavailability of a source of pressure. Afterwards, the algorithm updates the diameter values of all the pipelines for which the unavailable source constitutes the first or second closest source of gas. Diameter values are updated only when the new diameter is larger than the one previously assigned to the pipeline.

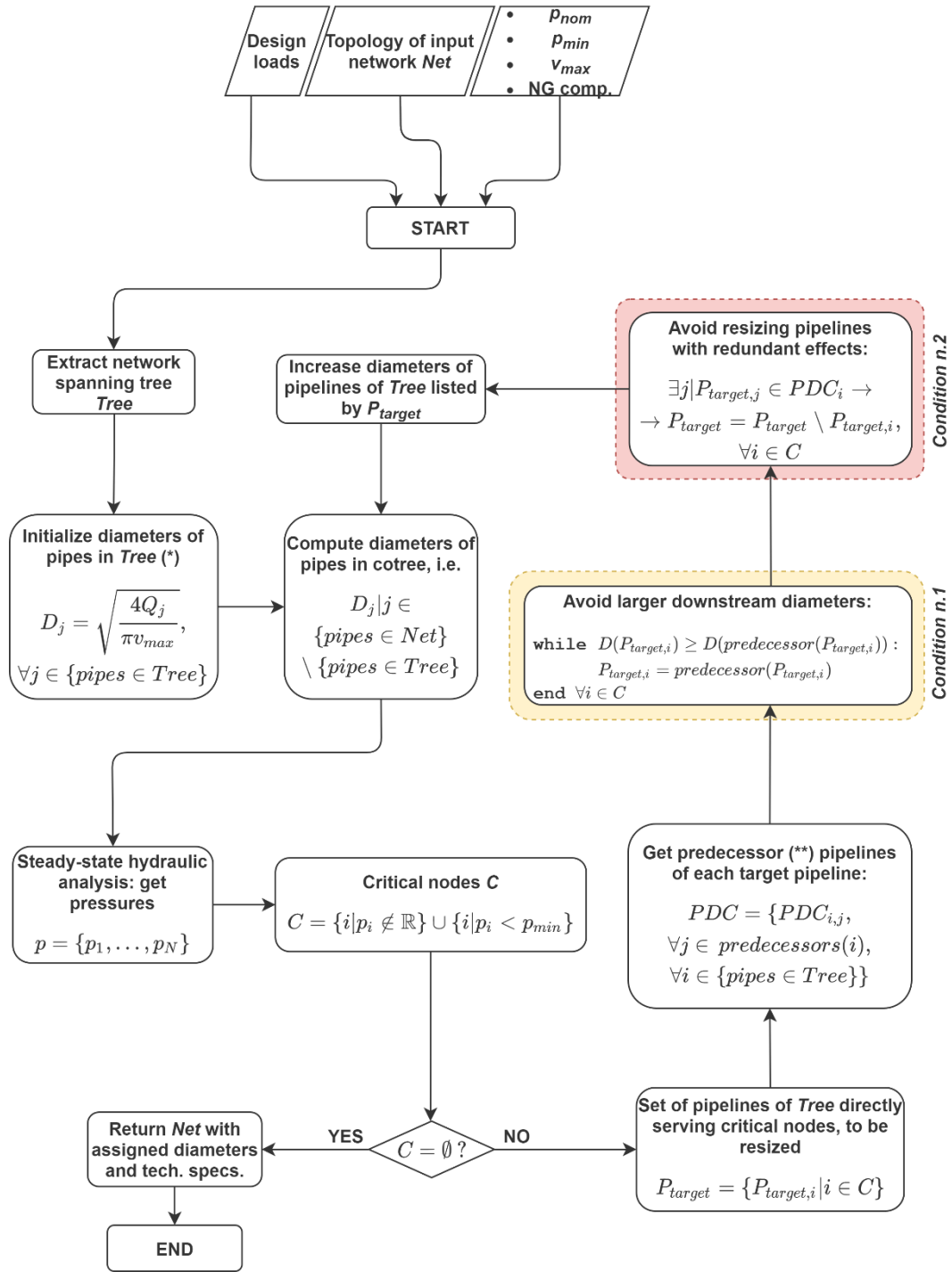


Figure 19: Diagram of the algorithm accomplishing the technical design of distribution gas networks with given topology and target operational restrictions. Conditions imposed for the identification of the pipelines are highlighted.

(\*)  $Q_j$  represents the volume flow rate of gas [m<sup>3</sup>/s] streaming in the  $j$ -th pipe of *Tree*.

(\*\*) The term *predecessors* of a pipeline is here used in a non-rigorous way to indicate the set of pipes that precede the given pipeline along the source-sink paths of the spanning tree. The *predecessor* (singular) of a pipeline is here intended as the pipeline directly preceding the given pipe.

# Chapter 4

## Structural and hydraulic properties of synthetic gas network models

### 4.1 Generation of synthetic case studies

Within this Section, the technical designer presented in the previous Chapter and the topology generator introduced in Chapter 2 are sequentially combined in a MATLAB implementation to produce finished synthetic models of gas distribution grids. Taking advantage of the probabilistic nature of the presented tools, unique synthetic networks are generated at each execution of the algorithm. Additionally, numerous networks can be produced within reasonable times, thanks to the computational efficiency of the tool. The chart of Figure 20 illustrates the time required to produce a finished network model, comprising both the establishment of the grid topology and the technical sizing, with increasing network complexity (i.e., number of nodes). It can be noticed that less than 1 minute is required to produce a full network with up to 500 nodes. Up to 7 minutes are instead needed to generate a network model of 1000 nodes (less than 3 min on a median basis).

Accordingly, a large number (i.e., 10,000) of network models is produced to evaluate the performance of the synthetic gas network generator and to analyse the properties of the obtained case studies from a statistical perspective.

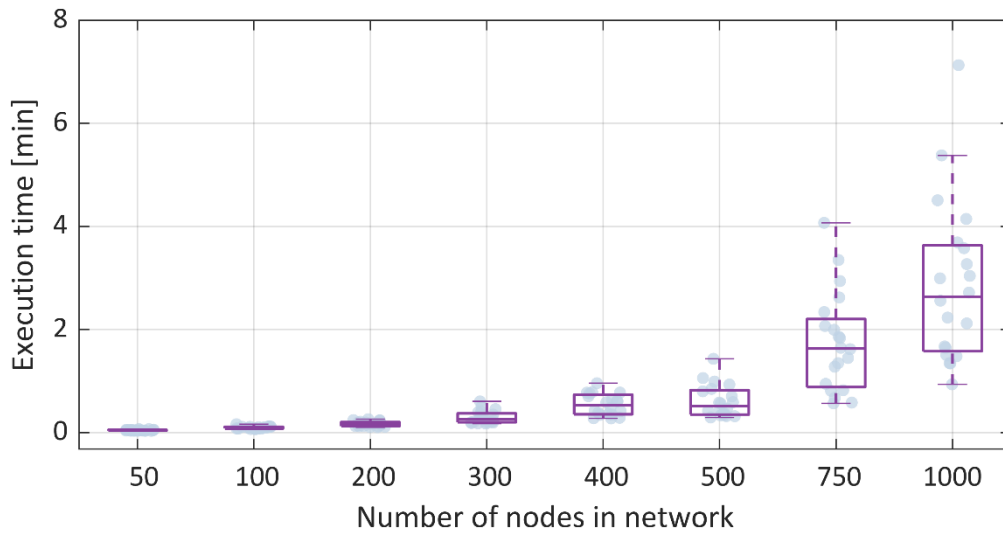


Figure 20. Time required for the creation of finished network models with increasing number of network nodes. Results refer to 20 different executions for each network size.

Attention is given to medium-pressure infrastructures with maximum allowable operating pressure (MAOP) equal to 5 bar<sub>g</sub> (Italian 4<sup>th</sup> species), with consistent operational constraints applied to the synthetization process. The generated networks are inspired from a reference real-world grid located in Italy, serving approximately 3400 customers, connected to both medium and downstream low-pressure tiers. The total network extension is 34 km, and its maximum total capacity is estimated at 47 MW. The actual peak gas demand may however be lower due to oversizing.

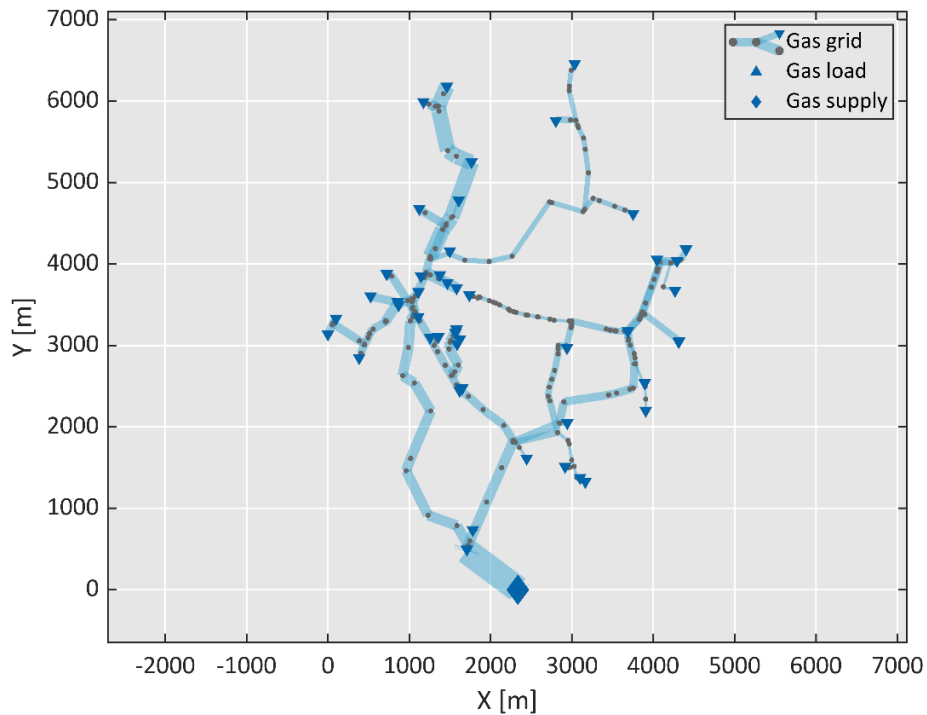


Figure 21. Real-world MP distribution grid used as reference. The width of the edges (pipelines) of the graph is proportional to the diameter values. For comparison: the largest pipeline (connected to the source node) has a diameter of 0.25 m.

The model of the infrastructure, represented in Figure 21, comprises 373 nodes and 375 pipelines (edges), and it therefore features 3 loops. In the last sections of this Chapter, synthetic networks are produced adopting also other reference grids, to evidence the straightforward applicability of the tool to different cases.

Three different objectives are pursued through the experiments that are carried out and illustrated within this Chapter. Accordingly, results are organized in three cases:

- *CASE A*: 10,000 unique network models are generated with several degrees of freedom to consider, replicate, and finally observe the multitude and variability of cases that may be found in real-world distribution systems.
- *CASE B*: a set of topological, spatial and technical constraints is applied to the synthetization process of other 10,000 grids, to gain a higher control over the obtained networks and, consequently, test the consistency of the tool.
- *CASE C*: an a-posteriori enforcement is applied to the large and heterogeneous set of synthetized grids to demonstrate the possibility of selecting a reduced number of case studies with specific target properties.

The rationale for the synthetization process is the same in all the proposed cases, which in fact only differ in the constraints applied to the procedure. Accordingly, the process for the creation of a single network is articulated in the following stages, which are replicated for each of the 10,000 generated grids:

1. Establishment of the spatial distribution and topology of the grid: the synthetic nodes are randomly positioned on a two-dimensional plane, replicating the spatial distribution of the nodes in the reference grid; afterwards, the topology of the network is established by connecting the nodes. The procedure provides the output grid with correct topological and spatial properties. This step is carried out according to the methodology proposed and fully described in Chapter 2.
2. Identification of the source node: one source node is selected among all the nodes in the network having degree equal to 1 (i.e., nodes having only

one connection). This is done to avoid unrealistic locations for the supply of gas, such as in correspondence of junctions between the pipelines.

3. Identification of consumption nodes: loads are identified in correspondence of all the nodes with degree equal to 1, excluding the source node. This choice is consistent with observations on models of Italian real-world networks operated at MP (*4<sup>th</sup> species*), in which most of the customers and the MP/LP pressure regulators lay at endpoints of the grid.
4. Assignment of load values to consumption nodes: a total load equal to 47 MW (equal to the estimated reference network capacity) is distributed among the consumption nodes. Different allocation schemes (deterministic and stochastic) are proposed in the next sections.
5. Technical design of the grid: network pipelines are sized and assigned with suitable technical properties, as extensively described in Chapter 3. In this stage, the nominal source pressure is assumed to be equal to 5 bar<sub>g</sub> (upper bound of the admitted range of pressures for the network class), while the design minimum pressure is taken to be 1.5 bar<sub>g</sub> (lower bound). A conservative value of 20 m/s is adopted as maximum admitted velocity in the pipelines [87]. A complete list of the inputs adopted in this stage is given in Table 10.

**Table 10. Design parameters used for the technical sizing of the synthetic networks.**

<b>Inputs</b>	
<b>Nominal source pressure, <math>p_{nom}</math></b>	5 bar <sub>g</sub>
<b>Minimum design pressure, <math>p_{min}</math></b>	1.5 bar <sub>g</sub>
<b>Maximum flow velocity, <math>v_{max}</math></b>	20 m/s
<b>Ground temperature</b>	283.15 K
<b>Roughness coefficient</b>	140 μm
<b>NG properties</b>	
▪ <b>Higher heating value</b>	51.3 MJ/kg
▪ <b>Specific gravity</b>	0.64

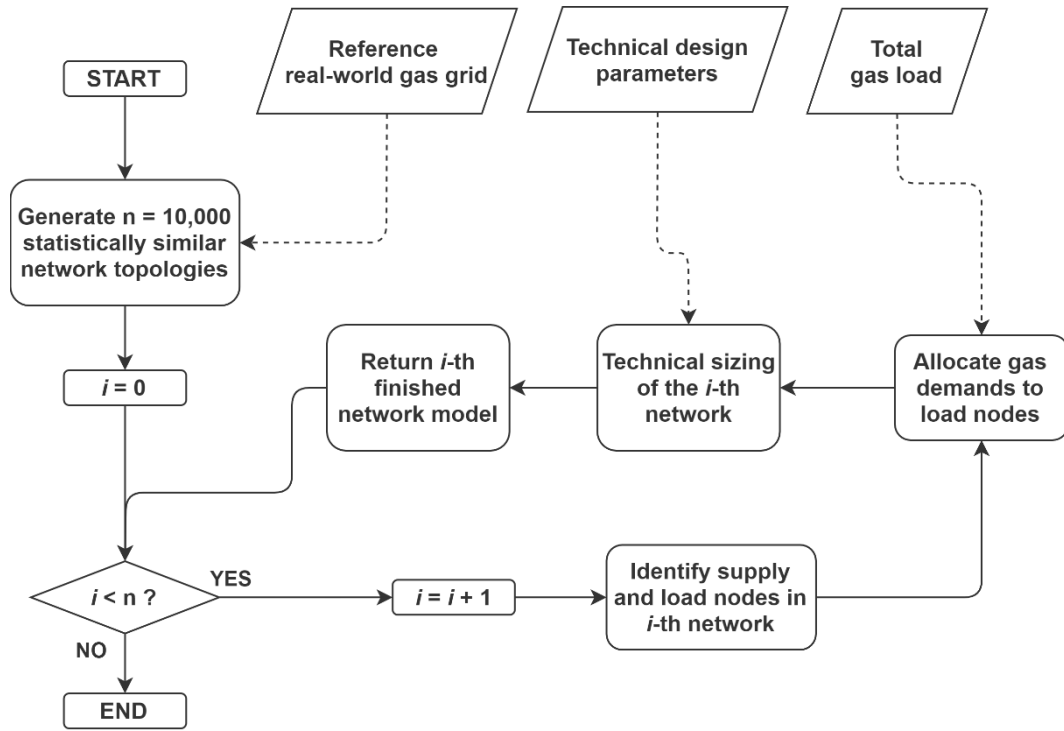


Figure 22. Process for the creation of ten thousand finished gas network model

## 4.2 Case A: constraint-free generation of synthetic networks

Ten thousand networks are generated in a constraint-free fashion. The procedure acknowledges the differences that may exist among distribution networks in real-world applications. The characteristics and the response of the distribution systems can be highly affected by the location of the supply node, the magnitude of the loads and their distance from the supply, and the presence of loops in the system. Accordingly, the following assumptions are formulated:

1. The number of loops in the grids varies randomly according to ranges of network cyclicity (here meant as ratio of number of loops over total network length) observed in real MP systems, which span between 0 and  $0.29 \text{ km}^{-1}$  (see Chapter 2).
2. The supply node can be located in any region of the network, and it is randomly identified in one node out of all the nodes with degree equal to 1 (i.e., nodes with only 1 connection).

3. Nodal gas loads are randomly established by distributing the total design load (47 MW) according to a suitable statistical model (Weibull distribution appears to fairly reproduce load magnitude distributions in real networks – as observed from networks of Chapter 2 -- and is here adopted).

A sample of 10 networks generated in this way is illustrated in Figure 23. As expected, the grids feature a spatial extension and density similar to the reference network of Figure 21. It can be observed how the location of the source node (largest marker) changes in each case study, as well as the number of loops.

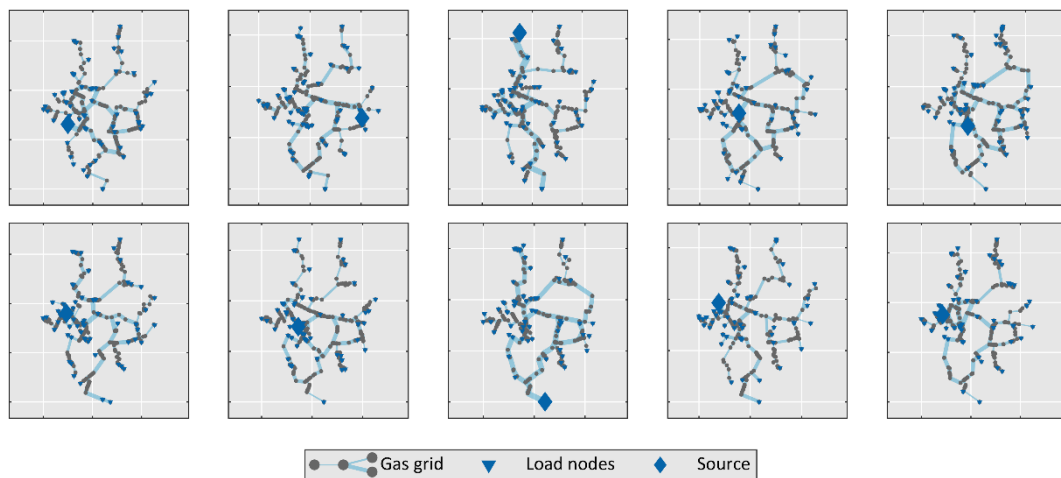


Figure 23. Ten random samples out of the 10,000 networks generated in the constraint-free synthetization process.

The random allocation of load value among the consumption points in each network determines significant variabilities in the magnitudes of the gas demands and their distances from the point of supply. For every case study, the total *momentum* of the gas loads with respect to the supply point, as defined by equation 1, has indeed a substantial impact on the technical design of the system.

$$Total\ momentum\ of\ gas\ loads = \sum Gas\ load \times Distance\ from\ supply \quad (1)$$

In cases with low load momentum (i.e., loads located close to the supply) most of the gas volumes are delivered within short distances, reducing the need to deploy large-diameter pipes with high distribution capacity. On the contrary, the technical solutions for cases with high load momentum involve a higher number of pipes with large diameters. As a direct consequence, such differences determine different network volumes, *linepacks*, and dynamic behaviours, even among

systems with similar spatial extensions and equivalent gas consumptions. The variability of the load momentum in the generated networks can be observed in Figure 24, which compares the patterns of the gas loads against their distances from the supply point. While in some networks nearly all the load is within 4 km from the source, in other cases it is concentrated in remote regions of the grid. For comparison, the chart includes the same curve obtained for the reference real-world distribution network.

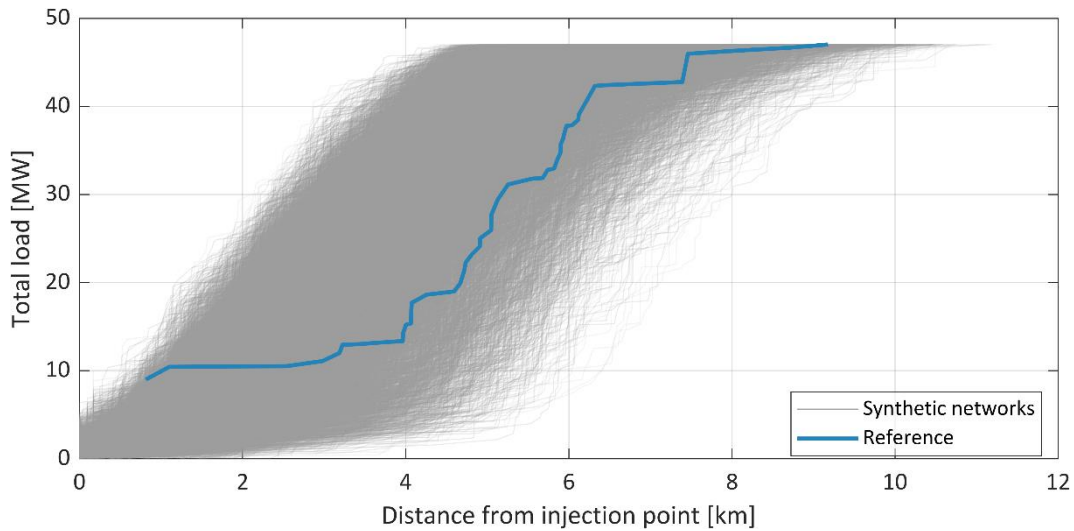


**Figure 24.** Cumulative gas loads against their distance from the supply node. The chart includes the information for the real-world network used as reference, for comparison.

Due to the many degrees of freedom discussed above, the characteristics of the networks feature a substantial variability. A statistical approach is therefore adopted in their representations in Figure 25, where attention is given to diameter sizes (A), network volumes (B), nodal pressures (C) and gas flow velocities in pipes (D) at steady-state design conditions. In charts A, C and D the network properties are described by cumulative distribution functions (CDF) displayed in grey. Each grey CDF refers to a single network, so that the resulting grey area indicates the band of values covered by the different networks. Blue boxplots are also included to highlight the variability of the CDF values at discrete intervals of the observed property. Thick blue rectangles of the boxplots cover the 2nd and 3rd percentiles of records, while white and black dots indicate the median values. Whiskers reach the minimum and maximum values of the observations. For graphical reasons, the bins used for the boxplots are different (wider) than the bins used for the CDF.

The synthetisation process produced networks with realistic structural properties and compliant hydraulic behaviours. Pipeline diameters are within a

sensible range of sizes, varying between 2.5 and 16.0 cm (chart A in Figure 25). The band of their distributions is significantly wide, being the maximum recorded two-sample Kolmogorov-Smirnov (KS) statistic (KSstat2) equal to 0.97<sup>6</sup>. This aspect influences the distribution of the volumes as well – see chart B – whose standard deviation amounts to 49.6 m<sup>3</sup> against a mean value of 154.9 m<sup>3</sup>.

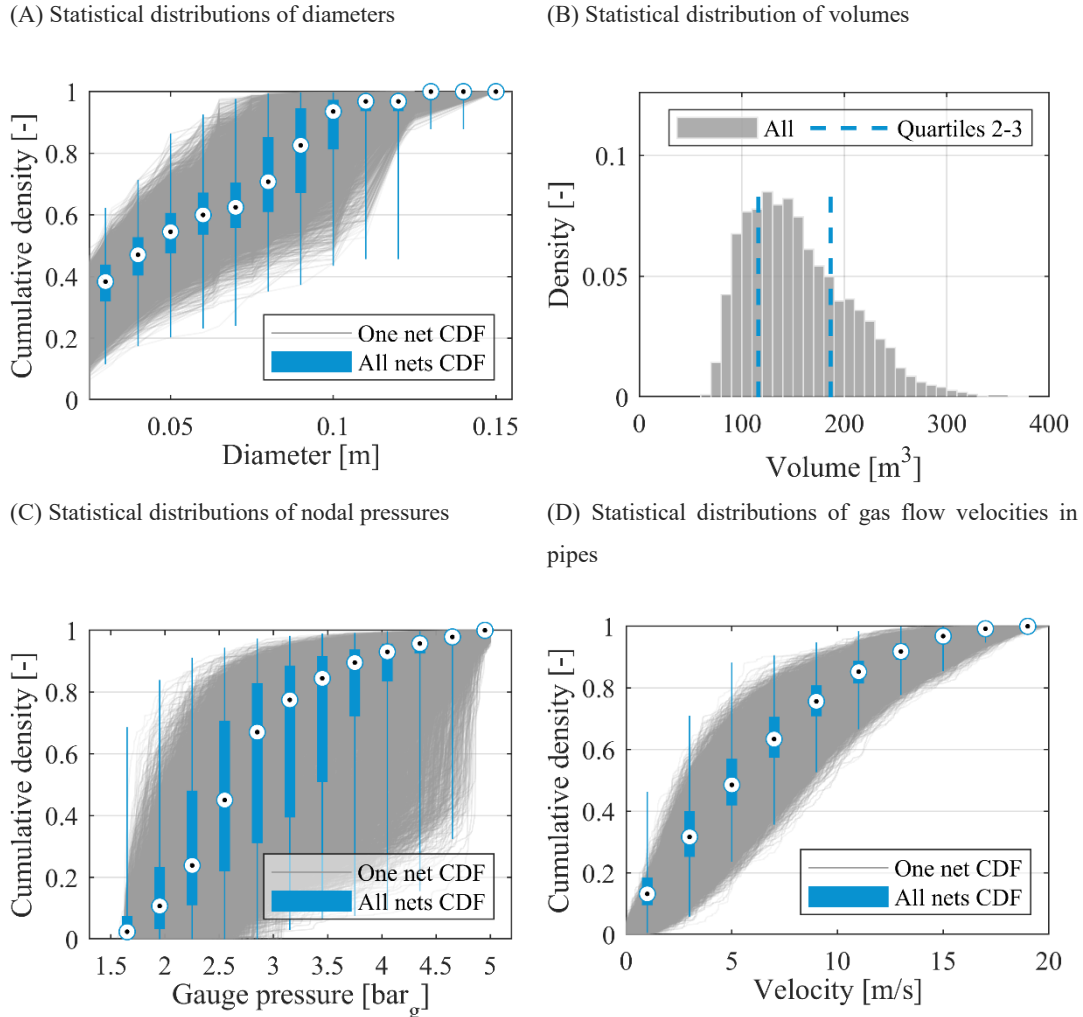


**Figure 25. Structural properties and fluid-dynamic response of synthetic networks generated by the algorithm in the constraint-free process. Cumulative distribution functions (CDF) of diameters, pressures and velocities are illustrated as overlaid histograms. Boxplots are added for a complete description of the CDF values.**

The charts C and D of Figure 25 evidence that the algorithm has correctly sized all the 10,000 networks. Complying with the imposed design criteria, pressures are never lower than 1.5 bar<sub>g</sub> and velocities never exceed 20 m/s. The average pressure of the networks is 3.01 bar<sub>g</sub>. In 60% of the cases, most of the

<sup>6</sup> Recalled from Chapter 2: the two-sample KS statistic measures the fit between two empirical distributions. It is defined as the maximum absolute difference between the cumulative distributions of the two empirical distributions in question. Its value can span between 0 (high correlation) and 1 (low correlation).

nodal pressures are comprised within 1.5 and 3 bar<sub>g</sub>. As evidenced by the grey band of CDF and the blue boxplots of chart C, pressure distributions are remarkably variable, being the maximum recorded KS statistic equal to 0.97. The mean gas flow velocity in pipes amounts to 6.8 m/s and, on average, 50.1% of values are lower than 6 m/s. Only 6.1% of the velocities is higher than 15 m/s, indicating that most of the pipelines operate well below the imposed limits (20 m/s).

Results highlight that distribution systems designed with identical sizing criteria can be characterised by substantially dissimilar structures and hydraulic behaviours. Different responses of these systems are to be expected also in alternative simulation scenarios (e.g., distributed injection of fuels). Accordingly, statistical-based approaches may offer a more suitable solution to capture this information, that would be otherwise lost in case-specific studies.

### **4.3 Case B: generation of synthetic networks with technical and topological constraints**

In a second stage, a set of constraints has been exerted to the synthetisation process to gain a higher control over the configuration of the output networks. The main purpose is assessing the consistency of the tool by observing the properties of the networks when the degrees of freedom of the grids are sensibly reduced a-priori. The system layouts are induced to feature reduced variations around a common reference, which is found in the real-world grid of Figure 21. The technical and structural properties of the obtained networks are not meant, however, to reproduce the characteristics of the reference grid, because of the several variables influencing the design of real-world systems, which in general cannot be known and replicated.

Overall, the steps leading to the synthetisation of the networks are unvaried from the previous case. Given that the overall gas demand and the design parameters are unchanged, the restrictions are applied over those remaining factors that mostly affect the properties of distribution grids. In particular, attention has been given to the location of the supply node, the allocation of gas consumptions and the number of network loops. Accordingly, the following input constraints are included:

1. The number of loops is the same in all the generated networks and it is equal to 3, as in the reference grid.
2. The location of the supply point of the synthesised networks is fixed and it is found in correspondence of the closest node to given reference coordinates (the position of the source in the reference grid is used – see large “diamond” marker in Figure 21).
3. The sum of the loads weighted by their distance from the supply node is similar in all the networks, and it is inspired from the reference real-world grid.

The configurations of the networks generated in this way exhibit limited variations. This behaviour can be qualitatively observed from Figure 26, which illustrates ten random samples extracted from the 10,000 synthetic networks. What emerges from the illustration is that the networks feature similar topology, spatial extension, and point of supply. Also the diameter sizes (widths of the lines in the plot) follow comparable spatial patterns in all the grids. The effect of the constraint imposed over the allocation of gas loads is noticeable in Figure 27: load patterns are considerably more uniform with respect to the previous case (see Figure 24), and consistently replicate the adopted reference. Consequently, the load *momentum* of the modelled grids features reduced fluctuations around the adopted reference, for which it amounts to 205.2 MW-km.

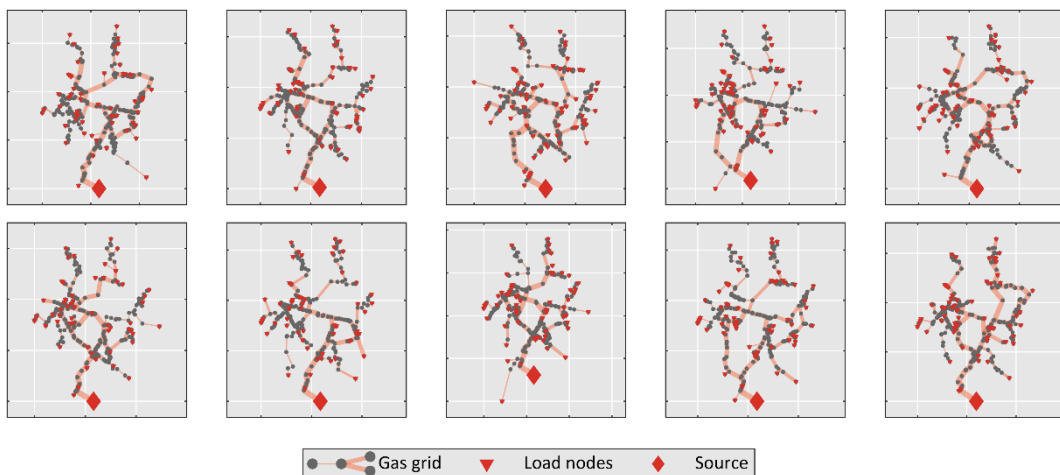
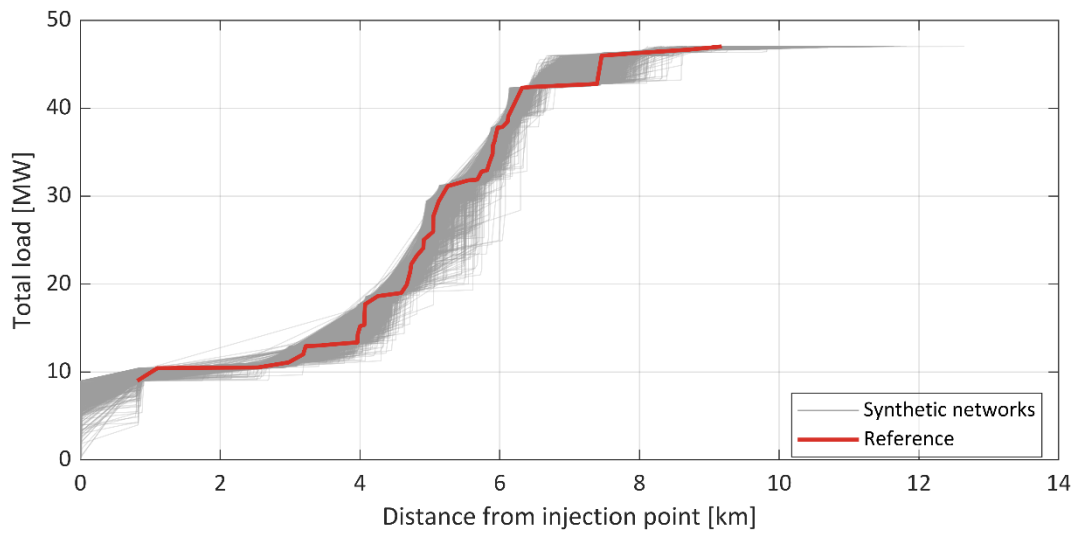
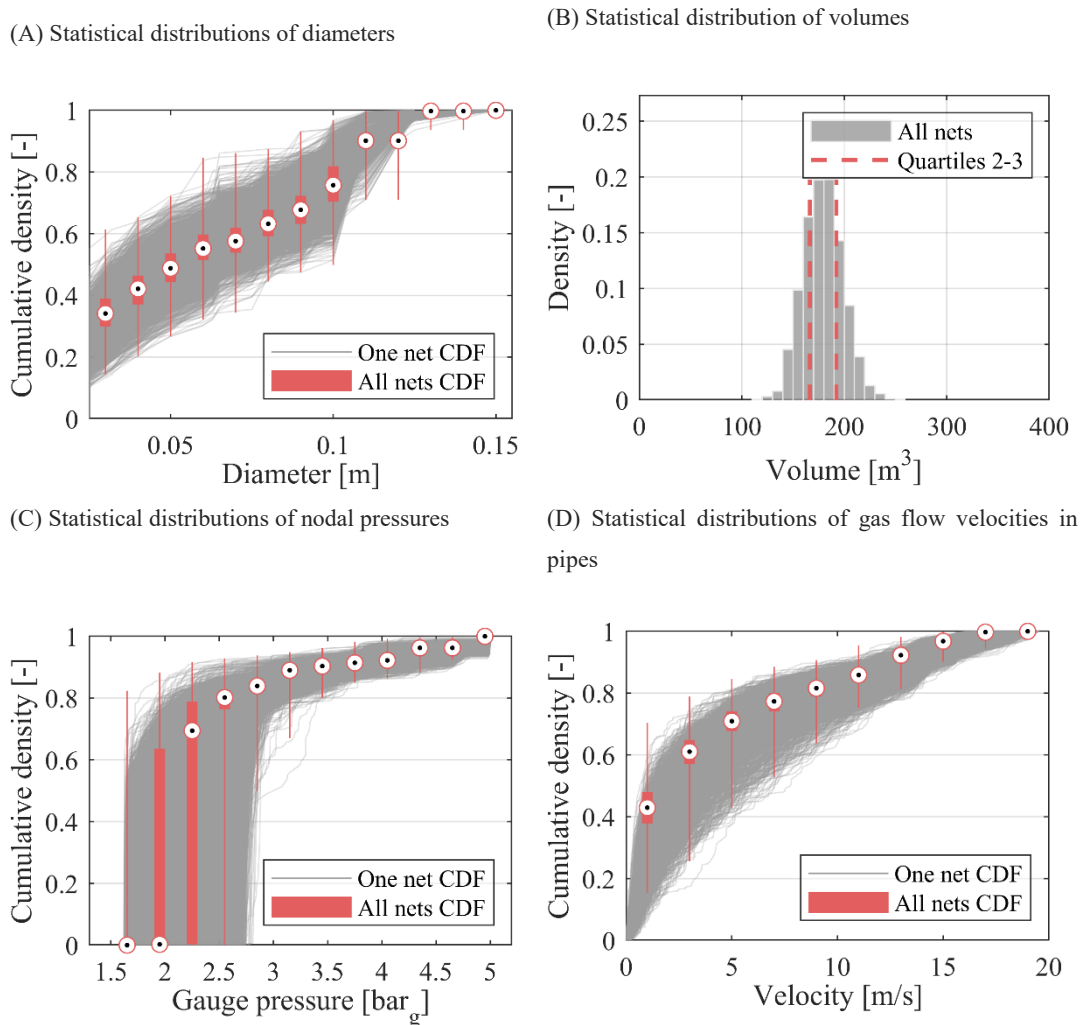


Figure 26. Ten random samples out of the 10,000 networks generated in the constrained synthetization process.



**Figure 27. Cumulative gas loads against their distance from the supply node. The patterns of gas consumption within the synthetic networks are constrained to follow the behaviour of the reference real-world gas grid, as visible from the fine agreement of the grey curves and the reference red line.**



**Figure 28. Structural properties and fluid-dynamic response of synthetic networks generated by the algorithm in the constrained process. Cumulative distributions functions (CDF) of diameters, pressures and velocities are illustrated as overlaid histograms. Boxplots are added for a complete description of the CDF values.**

As an effect of the application of the constraints, the properties of the networks – displayed in Figure 28 – feature a substantially reduced variability, providing evidence on the consistency of the tool. The maximum KS statistic recorded among the diameter distributions decreased from 0.97 to 0.52, while the standard deviation of network volumes was reduced from 49.6 m<sup>3</sup> to 19.0 m<sup>3</sup> (see charts A and B). The average volume amounts to 179.5 m<sup>3</sup>, being higher than in Case A. In fact, because of the imposed peripheral location of the supply node, the algorithm deploys more frequently large pipelines with higher capacity and lower resistance to flow.

Average values of nodal pressures and gas flow velocities respectively decreased to 2.55 bar<sub>g</sub> and 4.8 m/s. In virtually all the cases, most of the values are comprised between 1.5 and 3 bar<sub>g</sub>. An appreciably higher uniformity characterises the pressure distributions of chart C, indicating that the applied constraints have proven effective. Nevertheless, non-negligible variations are still found for pressures lower than 3 bar<sub>g</sub>, indicating that partially diverse hydraulic responses may be obtained even among very similar distribution systems. This aspect emphasises the value of statistical-based approaches in the study of gas grids.

Despite a significantly wide grey band, red boxplots in chart D indicate that most of gas flow velocities feature limited variations from their median values. Overall, the average gas velocity in pipelines is 4.8 m/s and in virtually all the networks most of the velocities are below 6 m/s. Velocities higher than 15 m/s represent only 5.5% of cases on average.

The tool demonstrates again to generate networks with consistent structures and correct technical designs. Under the applied constraints, the structural and hydraulic variations of the grids occur within significantly reduced, but in part non-negligible, ranges of values.

#### **4.4 Case C: a-posteriori selection of the synthetic networks**

It has been observed that the proposed tool can produce large quantities of unique ready-made models of distribution gas grids. The synthetic networks can be characterised by many degrees of freedom (see Case A); alternatively, suitable a-priori constraints can be applied for a higher control over their properties (see Case B). As already argued, having a large set of networks with diverse properties

is particularly suitable for statistical-based studies. However, in other specific applications it may be required that the generated grids feature peculiar structural and/or hydraulic properties. For these cases it is possible to perform an a-posteriori selection of the networks based on the target properties of interest. The selection can be carried out excluding all those networks whose features are too different from a target reference. A graphical example is provided in Figure 29 and Figure 30, where it is assumed that the networks generated according to the procedure of Case A require featuring pressure distributions similar to the real-world reference grid (previously depicted in Figure 21). The correlation of the 10,000 synthetic networks and the reference real-world grid is assessed via the two-sample KS statistic (see Figure 29). Subsequently, only those 468 grids featuring KSstat2 values lower than 0.2 are kept to meet the similarity requirement (see Figure 30).

Since real-world infrastructure models are often protected by non-disclosure agreements, we add that the capability of the tool illustrated above can be furtherly exploited to produce anonymised twins of the real-world network. Depending on the targeted property, the anonymised twin can ensure equivalent structural characteristics or hydraulic performances (or a combination of them) and can be disclosed without incurring in industrial secrecy, privacy and security issues.

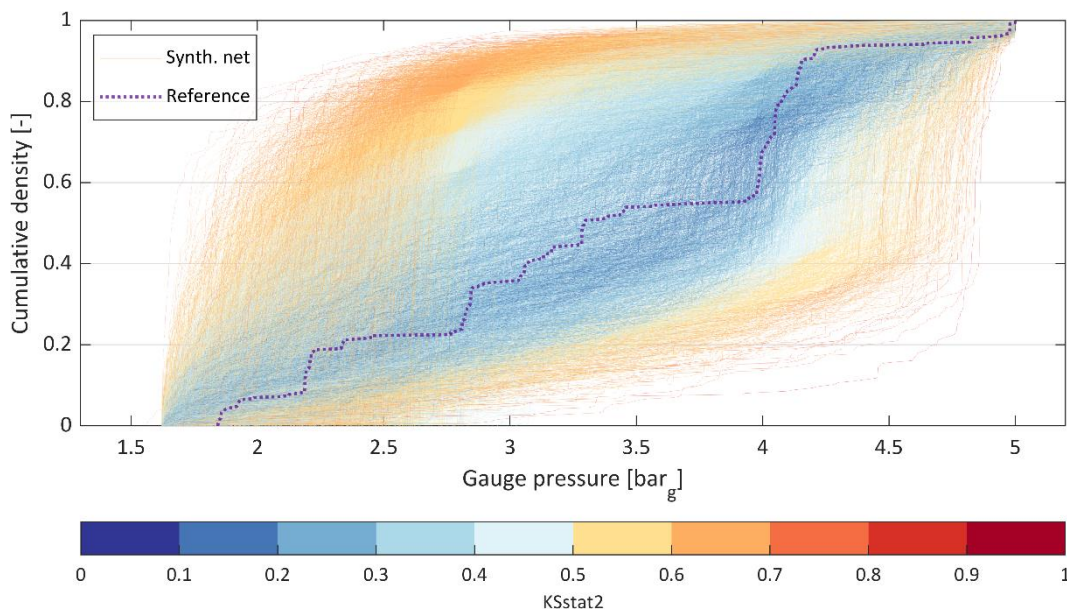


**Figure 29.** Statistical distribution (CDF) of pressures in the 10,000 synthetic networks generated in Case A (see panel C in Figure 25). Colours indicate the fit between the curves and the target reference, expressed by the two-sample KS statistic (KSstat2).

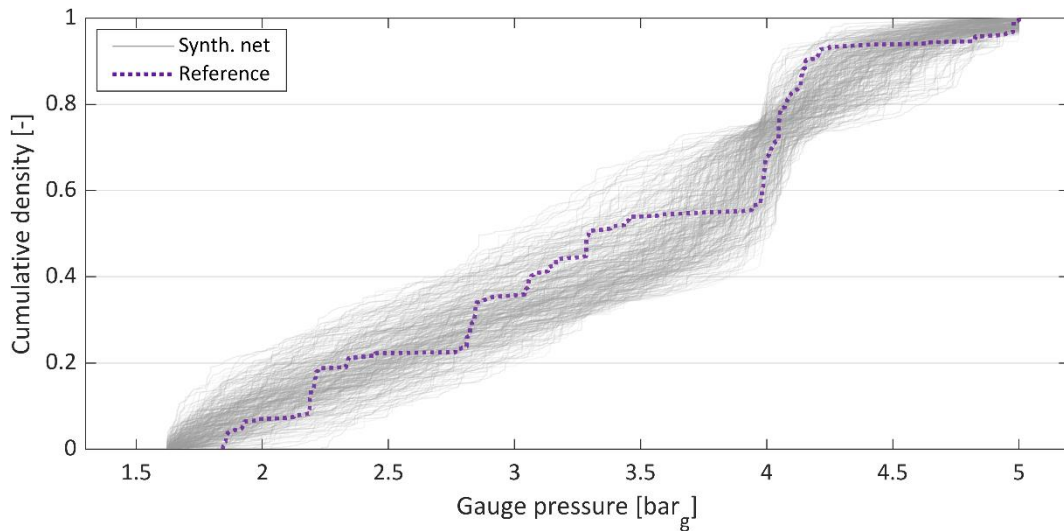


Figure 30. Resulting selection of the networks featuring the most similar pressure distributions to the target reference ( $KSstat2 \leq 0.2$ ). See Figure 29 for comparison.

The anonymized twin can be identified in the synthetic network featuring the closest structural or hydraulic properties to the target reference. In the example case of above, the lowest  $KSstat2$  recorded between the synthetic pressure profiles and the reference curve is 0.086, which indicates an almost equivalent hydraulic behaviour with respect to the reference case. Accordingly, the corresponding anonymized twin of the real-world sensible infrastructure is depicted in Figure 31.

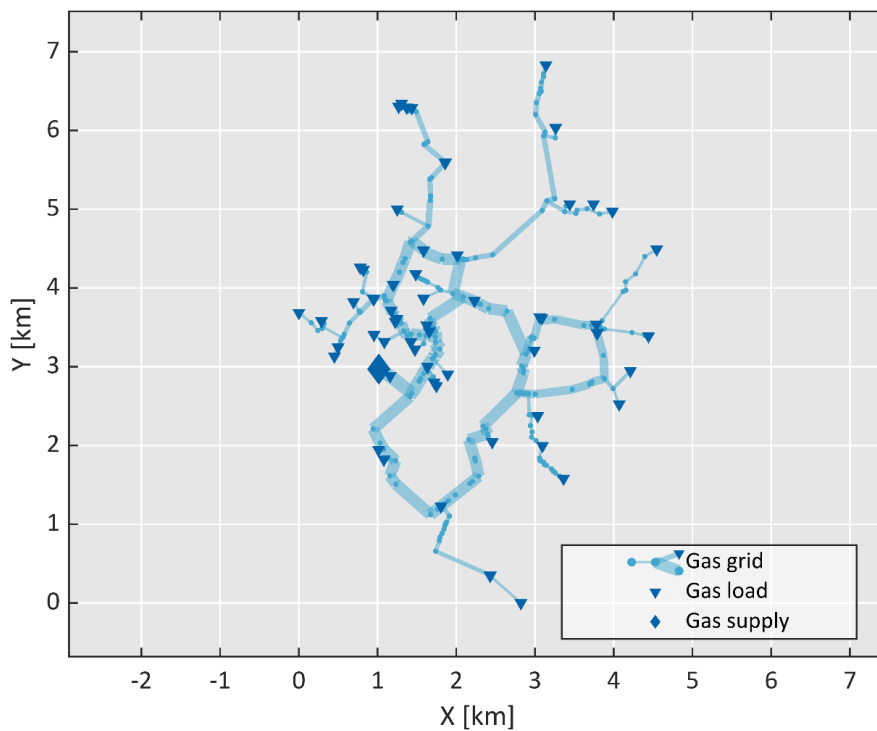


Figure 31. Anonymized twin of the reference network of Figure 21, featuring similar hydraulic behaviour (pressure profile).

## 4.5 Application to other reference case studies

Despite its proven capability of producing virtually infinite models of realistic networks, the current implementation of the tool requires an input reference gas grid from which inspiring the subsequent production of synthetic network models. It follows that, to a non-negligible extent, the properties of the generated grids may present a high dependency on the adopted reference. This aspect may partially prevent the generalization of the results obtained in statistical studies carried out over several networks, which constitutes the main purpose of the tool instead. On the one hand, this limitation is acknowledged and should be addressed in future extensions of the tool. On the other hand, the range of hydraulic behaviours (pressure and velocity profiles) obtained by using a single reference is so wide that the information gained by adopting other reference real-world grids is almost negligible. This is demonstrated within this section by observing the results of the application of the tool to two other real-world distribution systems.

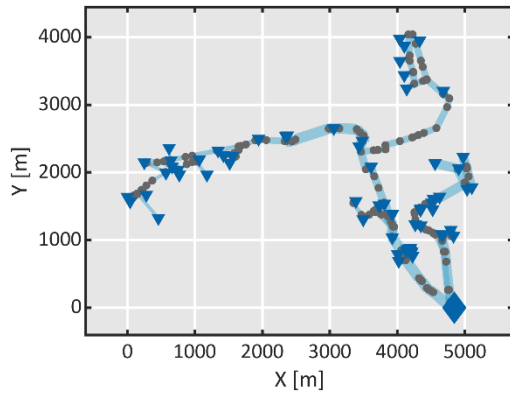
The purpose of adopting two new reference grids is two-fold: on the one hand, it provides a further validation of the tool and verification that it can successfully produce correct and realistic synthetic network models based on any target reference. On the other hand, as already mentioned above, it helps assessing how much information is being lost when the tool is deployed adopting only one real-world network as a reference. With these premises, 100 networks have been synthesized for each of the new case studies adopted as a reference. The synthesis process has been carried out with the same input parameters as the ones illustrated in previous sections and summarized in Table 10. Design parameters used for the technical sizing of the synthetic networks.

The first alternative reference case study is constituted by a MP distribution network operated at 5 bar<sub>g</sub>, serving an Italian municipality of 17,400 inhabitants. The estimated total capacity of the distribution system amounts to 102.5 MW, being the total length of the network equal to 22.2 km. The model of the network comprises 332 nodes and 333 edges. The second reference case study is another MP grid operated at 5 bar<sub>g</sub>, supplying two towns with a total of 27,000 inhabitants. The total network length is 40.3 km and the estimated total capacity amounts to 82.7 MW. The network model features 557 nodes and 561 edges.

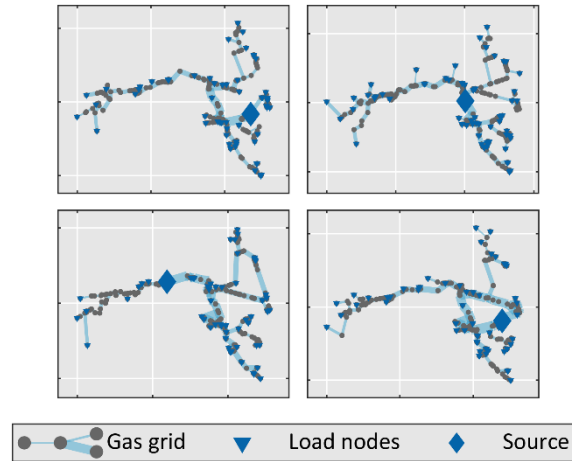
The representations of the networks, as well as the results of the synthesis processes adopting them as a reference, are provided by Figure 32

and Figure 33. It can be observed that the networks synthesized in both the applications comply again with the target design parameters, as they never violate the minimum pressure of 1.5 bar<sub>g</sub> and the maximum velocity of 20 m/s. The structural properties of the networks (diameters and volumes) feature different distributions and ranges of values. This is evidently due to the different extensions of the systems, as verifiable by comparing panels A of Figure 32 and Figure 33. Accordingly, attention should be paid when deploying the proposed tools in applications where the statistical variation in the network structural properties is of crucial importance, as it may be significantly affected by the adopted reference. On the other hand, it can be noticed that the hydraulic behaviours (pressure and velocity distributions) of the synthetic networks generated with the first (ref. previous sections) and the latter two references cover similar ranges of values. This result suggests that the fluid-dynamic response of the synthesized networks is not significantly affected by the adopted reference. Accordingly, the fact that the generated grids are inspired by a common single reference does not substantially mine the generalization of the hydraulic behaviour of the observed systems.

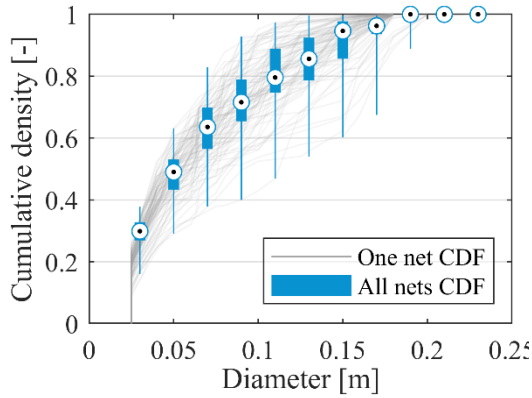
(A) Reference real-world network



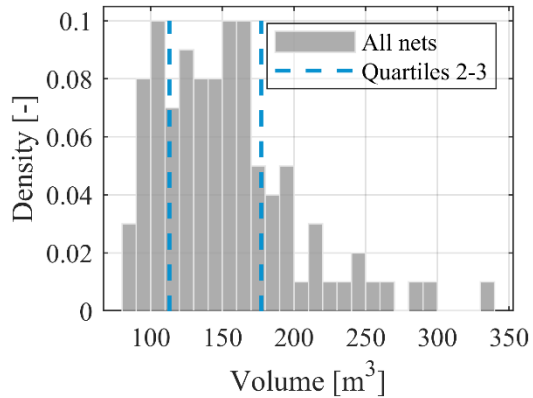
(B) Sample of 4 synthetic networks



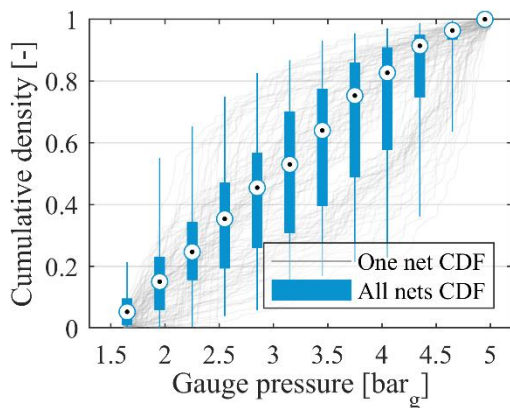
(C) Statistical distributions of diameters



(D) Statistical distribution of volumes



(E) Statistical distributions of nodal pressures



(F) Statistical distributions of gas flow velocities in pipes

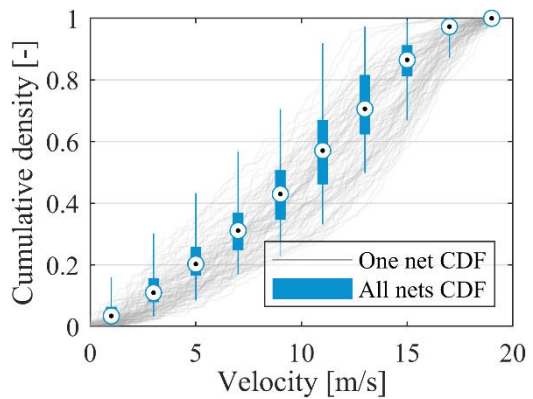
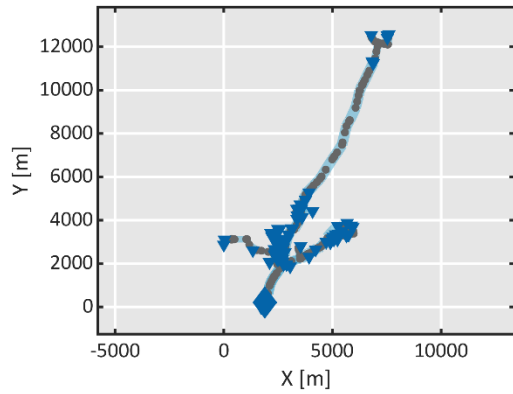
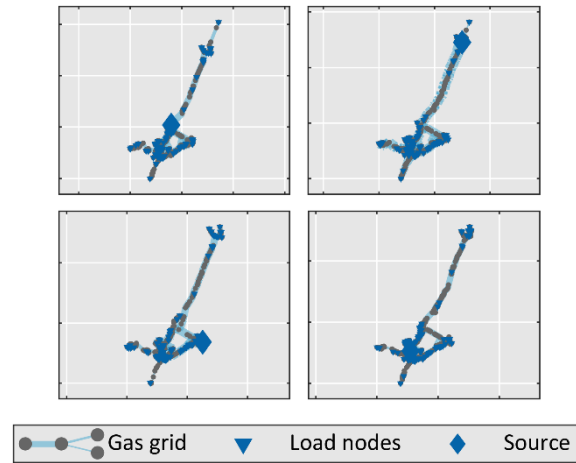


**Figure 32. Results obtained with the application of the tool to first alternative network. Panel A illustrates the reference real-world grid; panel B illustrates a sample of 4 synthetic networks; panels C, D, E, F provide the statistical structural and hydraulic properties of the synthetic grids.**

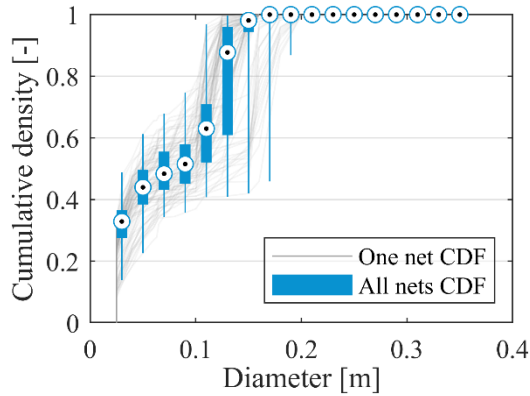
(A) Reference real-world network



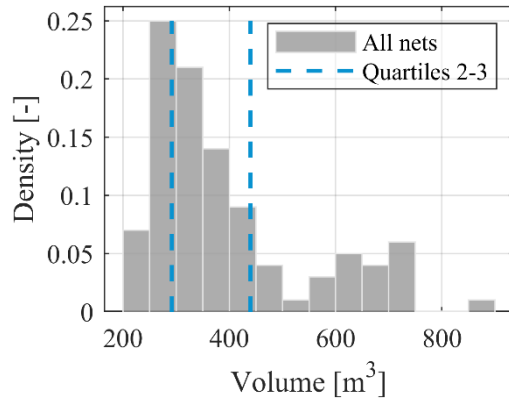
(B) Sample of 4 synthetic networks



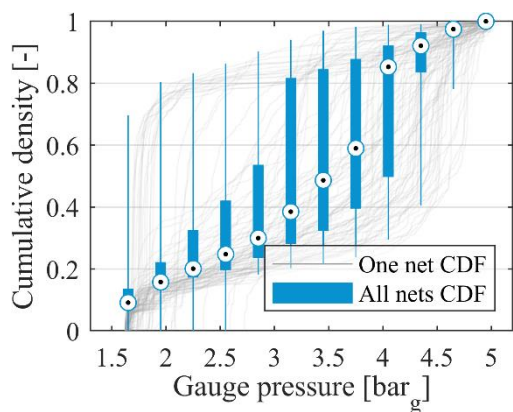
(C) Statistical distributions of diameters



(D) Statistical distribution of volumes



(E) Statistical distributions of nodal pressures



(F) Statistical distributions of gas flow velocities in pipes

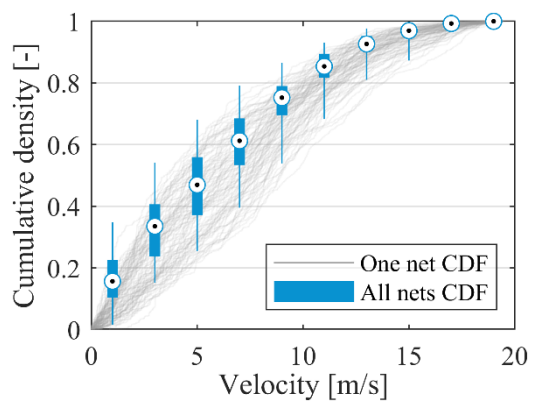


**Figure 33. Results obtained with the application of the tool to second alternative network. Panel A illustrates the reference real-world grid; panel B illustrates a sample of 4 synthetic networks; panels C, D, E, F provide the statistical structural and hydraulic properties of the synthetic grids.**

# Chapter 5

## Statistical assessment of the injection of hydrogen in distribution gas grids

### 5.1 Introduction

The introductory section of Chapter 1 delivered an overview of the current and perspective role of gas and its related transmission and distribution infrastructures towards the establishment of a low-carbon energy scenario. While particular importance is given to the gas sector in a transitional phase that envisions the decommissioning of power and heat generation plants based on more polluting sources, like coal, many opportunities are foreseen in a gradual decarbonization of the gas system itself. Although further research is being carried out and, in some cases, economies of scale still need to be fully established, technological options for the decarbonization of gas sector are already in place and are being increasingly deployed in pilot plants, full-scale demonstrators and commercial facilities. Integrating the technologies into the existing gas supply chain comes with challenges that are of technical and regulatory nature. This is mostly due to the fact that renewable and low-carbon gaseous fuels produced by the available technologies are not, unless further refinements, of the same nature as natural gas, thus raising compatibility issues both on transmission and distribution operations, and at the final users' equipment. Research works in the field have therefore provided experimental and simulation results related to the

deployment of alternative gaseous fuels, like hydrogen and biogas, in conventional end-use equipment (e.g., gas boilers), as well as in transmission and distribution infrastructures. Concerning the latter aspect, attention has been devoted to the suitability of the materials employed within the infrastructures to handle unconventional gases (in particular H<sub>2</sub>), as well as to system-level dynamics that occur when networks are operated with multiple, distributed and diversified sources of gas. In particular, issues related to the system hydraulics and to the quality of the gas delivered to the users in presence of NG-H<sub>2</sub> or NG-biogas blends have been investigated. Gas network operators are in fact subject to technical requirements that constrain the fluid-dynamic operations and the quality of gas delivered to the end-users. These prescriptions are likely to be conserved along a transitional phase which, despite envisioning a gradual integration of alternative fuels in blended forms, is predominantly characterized by a business-as-usual operation of the networks.

Concerning the quality of gas, some Countries not only prescribe limitations to its thermophysical properties, but impose explicit limits to the admixtures with unconventional fuels, like hydrogen, in quantities that are illustrated in Table 11. For some of these cases (especially UK), a number of studies has evidenced how the injection of hydrogen beyond the legislative limits actually ensures that the quality of the distributed blend is still compliant with the remainder of the thermophysical requirements [32,45].

**Table 11. Limits to volume concentrations of hydrogen in natural gas according to international legislations [93].**

<b>Country</b>	<b>%vol H<sub>2</sub> limit</b>	
<b>Germany</b>	10%	2% in presence of CNG stations
<b>France</b>	6%	
<b>Spain</b>	5%	
<b>Austria</b>	4%	
<b>Switzerland</b>	2%	
<b>UK</b>	0.1%	

The Italian legislation does not explicitly indicate limits for the presence of hydrogen and other fuels in natural gas. Limits are instead indicated for the thermophysical properties of the gas, including the higher heating value (HHV,

[MJ/Sm<sup>3</sup>]), the specific gravity [-] and the Wobbe index (WI, [MJ/Sm<sup>3</sup>]) [94]. The properties of gas can vary within the limits indicated in Table 12, where values are referred to standard conditions of 101325 Pa and 283.15 K.

Table 12. NG quality constraints as from Italian legislation [94].

Parameter	Admitted interval
Specific gravity	0.555 – 0.700
Higher heating value	34.95 – 45.28 MJ/Sm <sup>3</sup>
Wobbe index	47.31 – 52.33 MJ/Sm <sup>3</sup>

The specific gravity (or relative density)  $\rho_s$  is a dimensionless property providing the ratio between the densities of the gas mixture and a reference (air with molar mass equal to 28.965 kg/kmol, according to ISO 6976:2016 [95]), computed at reference conditions. The Wobbe index provides a measure of the interchangeability of different gases for combustion applications, as it is proportional to the heat input to a burner at constant pressure [96]. It is calculated according to the following relation.

$$WI = \frac{HHV}{\sqrt{\rho_s}} \quad (5.1)$$

Hydrogen ( $\rho_{H_2} = 0.125 \text{ kg/Sm}^3$ ,  $HHV_{H_2} = 12.08 \text{ MJ/ Sm}^3$ ) is about 8 times lighter than methane and its volume-based HHV is about 3 times lower. Accordingly, blending hydrogen with natural gas alters the thermophysical properties of the gas mixture and raises risks of violating quality requirements indicated by law. With reference to H<sub>2</sub>-CH<sub>4</sub> mixtures, the variation of the thermophysical properties of blends with increasing fractions of hydrogen is illustrated in Figure 34, below. In the same figure, the minimum bounds for the thermophysical properties prescribed by the Italian legislation are included. It is worth pointing out that violations of the minimum HHV and specific gravity typically occur at higher concentrations of hydrogen in blends with natural gas, which, depending on its composition, is typically characterized by a higher calorific value and density than pure methane.

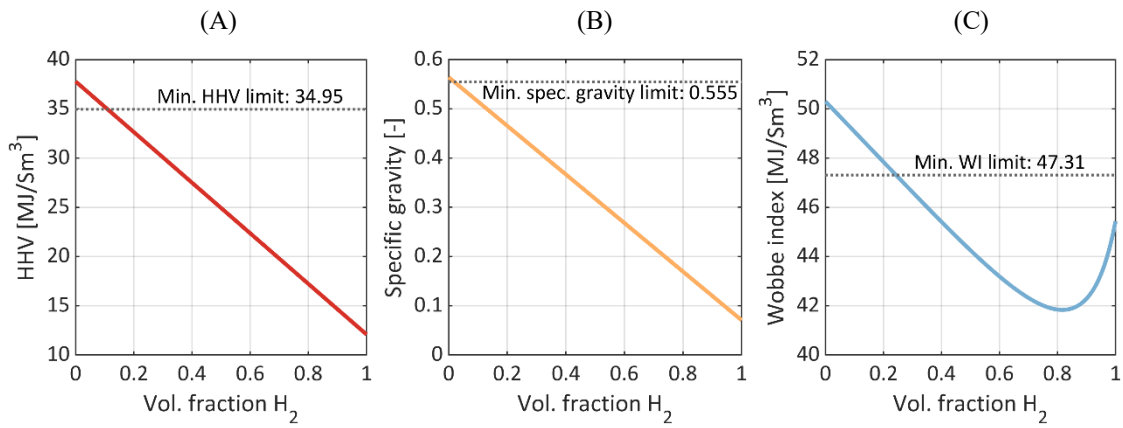


Figure 34. Variation of thermophysical properties of hydrogen-methane blends with volume concentrations of H<sub>2</sub>: (A) HHV, (B) specific gravity, (C) Wobbe index.<sup>7</sup>

The introduction of hydrogen in gas networks also alters the hydraulics of the system. Firstly, fluid-dynamic changes are driven by the lower HHV of H<sub>2</sub>-NG blends, which require higher volume flow rates compared to traditional operations, to supply equivalent thermal powers to the end-users. Another change is driven by a distributed nature of the H<sub>2</sub> injection, which has the effect of converting part of the network to an active infrastructure with internal generation of fuel. Both the aspects have a direct effect on the gas velocities and on the pressure profiles across the system, undermining its correct functioning as under- and over-pressure and maximum velocity violations may arise.

The analysis of gas network operations at distribution level in presence of hydrogen and other alternative fuels has been proposed in numerous works, under both steady-state and transient simulation scenarios, some of which have been discussed in the literature review of Chapter 1 [45–51]. Attention has been devoted to the hydraulic and gas quality implications deriving from the injection of hydrogen, biogas and biomethane in pure and blended forms. While there is a general acknowledgement that limited concentrations of alternative fuels in NG do not cause operational criticalities on the grid, what emerges is also that the available results are sensible to specificities of the studies, like the topology of the networks adopted as testbed, and the location of the injection point of the alternative or blended gas.

Accordingly, a gap exists in the attempt to provide a comprehensive analysis of gas networks in presence of diversified supplies of renewable fuels. In this framework, the present Chapter aims at providing a novel contribution to the

<sup>7</sup> Maximum allowable H<sub>2</sub> concentrations depend on the composition of natural gas. In the chart, the extreme case of pure methane has been considered.

existing research in the field, adopting an alternative and generalized approach. The study proposes the steady-state analysis of gas networks at distribution level in presence of increasing levels of hydrogen injection. To overcome the case specificities that are typical of traditional studies, simulations are carried out over a large number of grids. The networks used are synthetic and realistic models generated by means of the tool presented in the previous chapters of this dissertation. Variations on other factors are also considered in the study including, for instance, the location of the hydrogen injection point within the infrastructure. The hydraulic response of the grids and issues related to the quality of the distributed blend are analysed in a statistical fashion, highlighting the principal trends and the variability of the observations. While a steady-state scenario is here investigated, the methodology can be replicated for transient analyses accounting, for instance, for unmatching daily and seasonal patterns of gas demand and H<sub>2</sub> injection (e.g., solar-driven), as well as for temporal fluctuations of gas quality and pressures delivered to users, and aiming at finding optimal strategies to operate the grids under these conditions.

The following sections illustrate the methodology of the study and present the statistical results. Conclusions are derived in the final section of the Chapter.

## **5.2 Rationale for the study and methodology**

The study proposes a generalized approach to investigate the behavior of gas grids when increasing amounts of hydrogen are injected in the network. The extent to which H<sub>2</sub>-NG blends impact on the infrastructure is assessed in terms of hydraulic response of the system and composition of gas delivered to the points of consumption. Obtained results are compared against operational and gas quality limits imposed by the Italian national legislation to keep track of possible violations. Simulations are performed in steady-state conditions, making use of a suitable fluid-dynamic model of gas grids that has been explained in [46], that offers the capability of tracking the composition of gas across the network, as well as its fluid-dynamic and thermophysical properties, in presence of distributed injections of gases of different qualities.

Unlike existing research works in the field, the present application relies on a large basis of networks, that are generated by means of the tool described across Chapter 2 and Chapter 3 of this thesis. Accordingly, results on the effects of the

injection of hydrogen are derived with a statistical-based approach, in which the response of gas networks is broadly observed for variable boundary conditions and testbeds. In particular, one hundred statistically similar networks are generated and deployed for the analysis. Several blending levels are considered, spanning from 0 to 75% in volume, and different locations for the hydrogen injection are modelled. All the inputs that are subject to variations within the study are listed and discussed below. Furthermore, a complete diagram of the study is provided in Figure 35.

- Networks.

Fluid dynamic simulations are executed on 100 statistically similar networks, following the procedure detailed in the previous chapters. In accordance with the methodology, the topologies and the technical features of the generated networks are consistent with a reference real-world grid. The reference is identified in the network model previously deployed for validating the synthetic network generator, which is depicted in Figure 21 (Chapter 4). The networks are medium-pressure infrastructures operated at 5 bar<sub>g</sub>. A complete list of the properties of the networks and of the technical parameters used for their technical sizing is provided in the table below.

**Table 13. Properties of the statistically similar networks used in the study and input parameters deployed for their technical sizing.**

<b>Network parameters and properties</b>	
<b>Total design load</b>	47.0 MW
<b>Number of nodes</b>	373
<b>Nominal source pressure, <math>p_{nom}</math></b>	5 bar <sub>g</sub>
<b>Minimum design pressure, <math>p_{min}</math></b>	1.5 bar <sub>g</sub>
<b>Maximum flow velocity, <math>v_{max}</math></b>	20 m/s
<b>Ground temperature</b>	283.15 K
<b>Roughness coefficient</b>	140 μm
<b>NG properties</b>	
▪ <b>Higher heating value</b>	51.3 MJ/kg
▪ <b>Specific gravity</b>	0.64

- Hydrogen penetration.

Increasing levels of hydrogen penetration are considered in the analysis. With the term *penetration* it is here meant the fraction of the total volume flow rate of blend (Nm<sup>3</sup>/s) demanded by the users that is met by hydrogen. This quantity is denoted in the following relations as  $x_{H_2}$ , where it is deployed to evaluate the volume flow rate of hydrogen  $\dot{Q}_{H_2}$  injected into the grid, when the sum of the loads (thermal powers)  $\sum_i P_i^{th}$  is a known input:

$$\dot{Q}_{H_2} = x_{H_2} \dot{Q}_{Blend} \quad (5.2)$$

where

$$\dot{Q}_{Blend} = \frac{\sum_i P_i^{th}}{HHV_{Blend}} \quad (5.3)$$

and

$$HHV_{Blend} = x_{H_2} HHV_{H_2} + (1 - x_{H_2}) HHV_{NG} \quad (5.4)$$

$\dot{Q}_{Blend}$  is the volume flow rate of the H<sub>2</sub>-NG blend consumed by the network, and *HHV* represents the volume-based higher heating value at standard conditions.

With these premises, the analysis is carried out with the following values of hydrogen penetration: 0%, 1%, 3%, 5%, 10%, 20%, 30%, 40%, 50%, 75%. Penetration levels span from initial exploratory admixture levels, up to systems that are predominantly run on H<sub>2</sub>.

- Location of hydrogen injection.

Two different scenarios are examined, which foresee the application and the removal of a constraint over the location of the hydrogen injection within the grid. Additionally, in both the cases, the selection of the H<sub>2</sub> injection node must comply with the following criteria:

- 1) The node must be served by a pipeline of at least 6 cm of diameters, to avoid hydrogen injections in too weak network regions (which would lead to trivial cases of operational violations).
- 2) The node must not represent a point of gas consumption.
- 3) The maximum allowed number of connections (degree) for the node must be 2, to avoid unrealistic H<sub>2</sub> injections into junctions of several pipelines.

In addition to the above conditions, in the first (constrained) case, the node of H<sub>2</sub> injection is forced to be nearby the source of NG. The closest available node is selected. There exist a number of reasons why it is convenient to foresee the injection of H<sub>2</sub> nearby the NG city-gate. In a first place, it is useful for maximizing the uniformity gas quality delivered to the points of consumption across the grid. This strategy is particularly effective in networks with single NG source to reduce the occurrence of local H<sub>2</sub> concentration levels beyond the targeted threshold. Additionally, pipelines located close to the city-gate typically offer a higher distribution capacity, which can more suitably accommodate the distributed injection of fuels, with lower impacts on the system fluid-dynamics (with particular attention to pressure drops and maximum flow velocities).

Despite the discussed advantages, the injection of hydrogen may occur in regions of the grid dislocated from the main source. Not always, in fact, it is possible to foresee the installation of power-to-gas facilities and/or pressurized hydrogen storage tanks nearby the natural gas city-gate. A first reason relies in the geographical and safety constraints that typically are applied to these systems. Another aspect is that, in the case of power-to-gas (PtG) facilities, the location of the plant may be determined with priority on the effectiveness of the system on the electrical side. PtG plants, and the annexed connection to the gas grid, may therefore be installed nearby renewable power generation plants and in saturated regions of the electrical network, in view of providing grid services. In the above cases, the gas grid accepts the location of the injection of hydrogen as is. For these reasons, in a second stage, simulations are carried out assuming a random location of the hydrogen injection, as long as the injection node complies with the same basic constraints listed above (not too small adjacent diameters, degree lower or equal to two, not in correspondence of gas load nodes).

As already mentioned, simulations are carried out at steady-state conditions. It is assumed that the distribution systems operate at maximum load conditions. These conditions deliver the most critical operational scenario, typically characterized by the highest pressure drops and flow velocities in pipelines. It has been pointed out that the networks are sized in such a way to sustain a total design load of 47 MW. In these load conditions, the guaranteed pressure at the most

disadvantaged node is equal to 1.5 bar<sub>g</sub>, representing the lower bound of the pressures admitted by the National legislation for the class of the networks (4<sup>th</sup> species, MP). Nevertheless, it is often unrealistic for real-world networks to reach very low-pressure levels, even at maximum load conditions. For this reason, as a further assumption, an utilization coefficient is introduced, which provides a relation between the total *design load* – i.e., the gas demand that can be sustained by the system – and the actual total *maximum load* – i.e., the gas load actually demanded by the system in the most critical conditions. The utilization coefficient  $u$  is taken to be equal to 0.6 (such value has been observed in at least one real case study) and it is used in the relation below to compute the total maximum load of the system, which results equal to 28.2 MW.

$$\sum_i L_i^{Max} = u \cdot \sum_i L_i^{Design} = 0.6 \cdot 47 \text{ MW} = 28.2 \text{ MW} \quad (5.5)$$

In this framework, the penetration of hydrogen constitutes an input and provides a measure of the fraction of the volume consumed in the network that is covered by hydrogen at peak demand conditions.

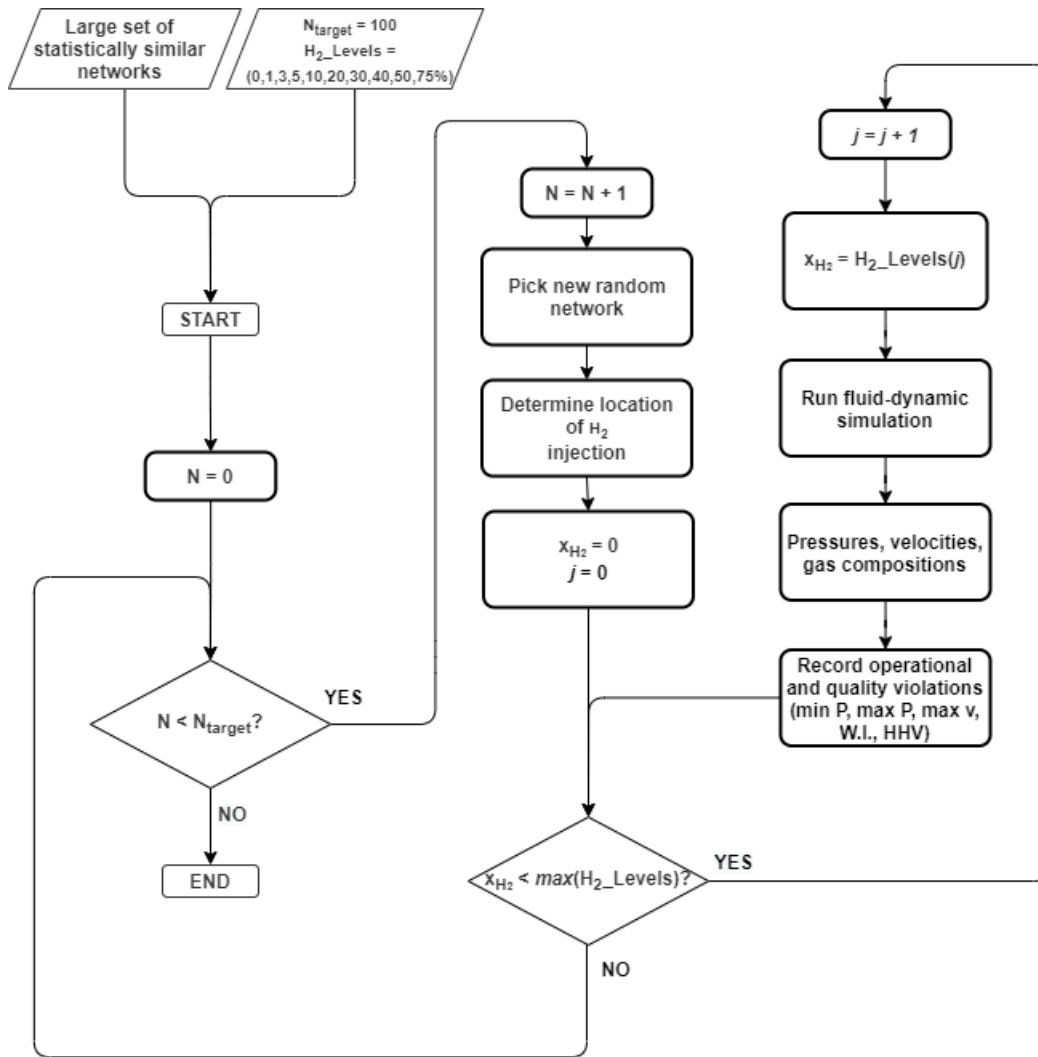


Figure 35. Diagram of the statistical study on H<sub>2</sub> injection in distribution gas grids.

### 5.3 Effect of blending hydrogen in distribution gas grids

The effect of blending hydrogen in gas networks is assessed by observing the fluid-dynamic response of the networks and the quality of gas delivered to the consumption points in the distribution system.

As long as the system hydraulics are concerned, it is here assessed the extent to which the blending of hydrogen with NG affects the pressures at the network nodes, as well as the velocities of gas in the pipelines, at steady-state conditions. Regarding the gas quality aspects, changes of the physical properties of the distributed blend are evaluated at increasing H<sub>2</sub> penetrations, with particular attention to their uneven distribution across the network. Standard physical

parameters are observed, including the higher heating value (HHV), the specific gravity and the Wobbe index (WI).

According to several National legislations, all the above-mentioned fluid-dynamic and gas quality parameters must be kept within specific boundaries to ensure safety and reliability of supply, compatibility with the end users' appliances, and proper metering of energy consumptions. Hydraulic operational constraints for Italian distribution infrastructures have been illustrated in Chapter 3. In the case of 4<sup>th</sup> *species* MP networks – i.e., the class under investigation – pressures should be kept between 1.5 – 5 barg, while gas velocities in pipes should not exceed 25 m/s. As for the quality of the natural gas mixtures, boundaries of the thermophysical properties have been previously illustrated within this chapter, as indicated by [94]. The restrictions listed in Table 12 apply.

On a fluid-dynamic level, the outputs of the simulations are used to evaluate the effect of hydrogen injection on average and minimum nodal pressures, and on average and maximum flow velocities. The values are compared against the legislative operational boundaries. On a gas quality level, the higher heating value, specific gravity and Wobbe index are observed in correspondence of the consumption node receiving the H<sub>2</sub>-richest blend. Attention is given to the occurrence of violations with respect to the ranges of values of Table 12.

The results are separately illustrated and discussed for the cases with constrained location (i.e., close to the source of NG) and free location of the hydrogen injection node.

### **5.3.1 Case A: effect of hydrogen injection nearby the NG source**

The effects of injecting hydrogen in proximity of the source of NG are uniformly observable across the grid. The simulated steady-state operations of the networks in presence of H<sub>2</sub> are illustrated in Figure 37. In most cases, the upstream hydrogen injection provides homogeneity to the gas composition across the grid, for all the penetration levels of H<sub>2</sub>. This is also visible in the chart of Figure 36 which, for each hydrogen penetration level, indicates the average fraction of consumption nodes whose received molar concentration of H<sub>2</sub> exceeds a given value. Variabilities among the different simulated networks are accounted by including the standard deviation (shaded areas) around the average lines. Average network responses indicate that more than 80% of the consumption

nodes receive blends with comparable hydrogen fractions, that are very close to the targeted network-wide hydrogen penetration level. The sudden fall of the average curves indicates that only a small fraction of points of consumption is provided with high H<sub>2</sub> concentrations. In a few cases, these concentrations can however be sensibly higher than the system-wide targeted H<sub>2</sub> penetration.

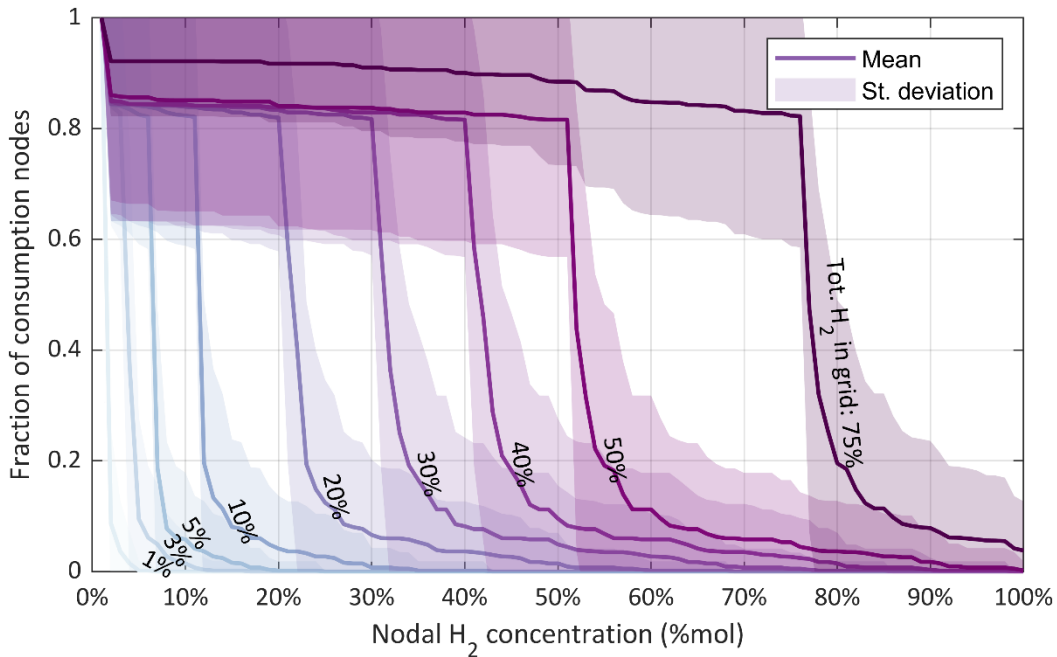


**Figure 36. Distribution of H<sub>2</sub> concentrations received by consumption nodes: fraction of load nodes for which the received H<sub>2</sub> molar concentration exceeds a given value. Hydrogen injection is constrained close to NG source.**

Statistical results on the network responses are also represented with boxplots in Figure 38, Figure 39 and Figure 40, focusing hydraulic and gas quality aspects. Boxes in the charts span from the 25<sup>th</sup> to the 75<sup>th</sup> percentile of the observations, and whiskers (dashed lines) cover the remaining data not detected as outliers. Every point corresponds to one observation and outliers are included.

Introducing hydrogen close to the NG source produces a general increase in the velocities of the blend (see Figure 38). Nevertheless, thanks to the high capacity of the pipelines surrounding the citygate, the effect remains negligible for hydrogen penetrations lower than 40%vol. From this level on, velocity violations are more likely to occur, but are still recorded in a minority of cases. With extreme admixtures of 75%vol of H<sub>2</sub>, the maximum observed velocity amounts to 37 m/s. These velocity levels constitute a violation of the current legislative indications and raise concerns in terms of mechanical stress on the pipelines, dragging of impurities and noise. Nevertheless, values may still result technically

tolerable for some sections of the grid, given that recommended gas velocities in the legislation of other Countries, like UK, foresee wider admitted velocity ranges, up to 40 m/s for MP networks [32].

Another evident effect caused by the introduction of hydrogen is represented by a general reduction in the pressure across the network (Figure 39). This trend is driven by an increase in the volume flow rates across the network, due to the lower density of hydrogen with respect to natural gas (partly compensated by a lower viscosity). Despite this trend, no violations in the minimum pressure (1.5 bar<sub>g</sub>) are recorded. Minimum pressures amount to 4 bar<sub>g</sub> on average with 100% NG, and linearly decrease to 3.7 bar<sub>g</sub> when grids run with 75%vol of hydrogen. The results suggest that the hydraulics of the distribution system should not be significantly impacted by the presence of H<sub>2</sub>, even in large quantities. It is worth pointing out that, however, the simulated networks are oversized by assumption and consequently feature large operational margins with respect to the minimum pressure of 1.5 bar<sub>g</sub>. Different vulnerabilities to the presence of hydrogen may be observed in cases with lower degrees of oversizing, with possibly higher risks of violating both minimum pressure and maximum velocity constraints. A sensitivity of the results to the utilization coefficient  $u$  – assumed 0.4 based on experience on other network models – may be analyzed in future work.

Charts in Figure 40 depict the evolution of the gas quality parameters at the most disadvantaged consumption node, i.e. the node with non-zero gas demand which receives the blend with the highest percentage of hydrogen. Comparable trends are observable for the HHV, the specific gravity and the Wobbe index. No violations are recorded for all the parameters at H<sub>2</sub> concentrations up to 3%vol. Injecting 10%vol of hydrogen in proximity of the NG source does not lead to quality issues in most (84%) of the cases, while gas quality violations become systematic (100% of cases) when blends of 20% or higher are targeted.

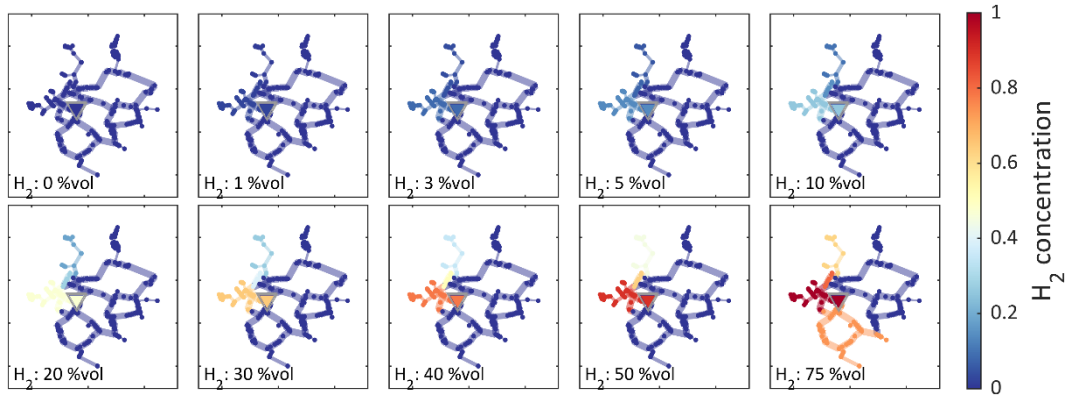
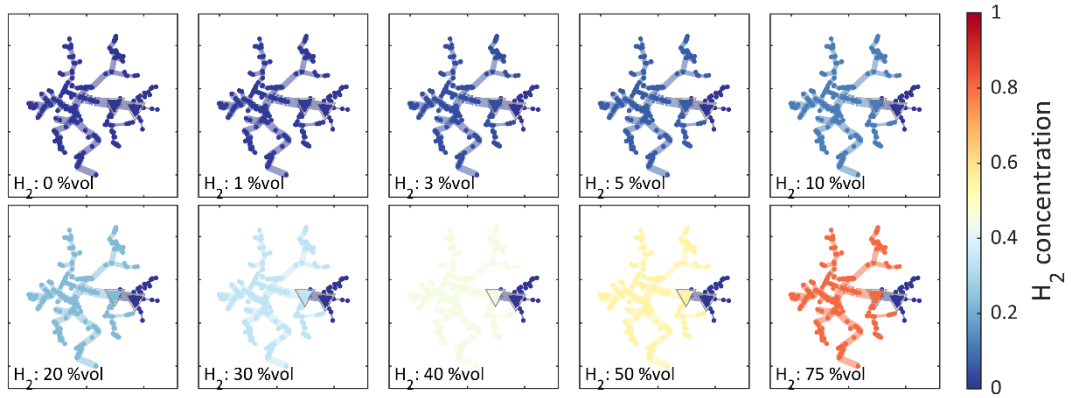
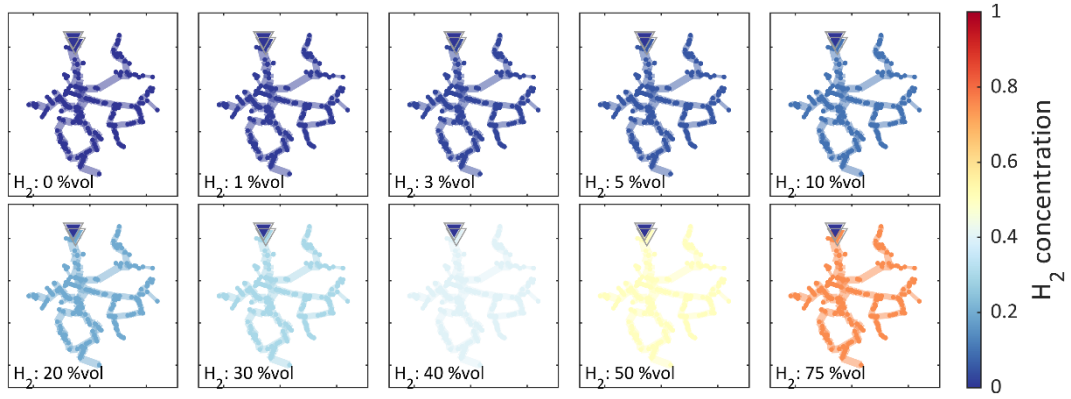
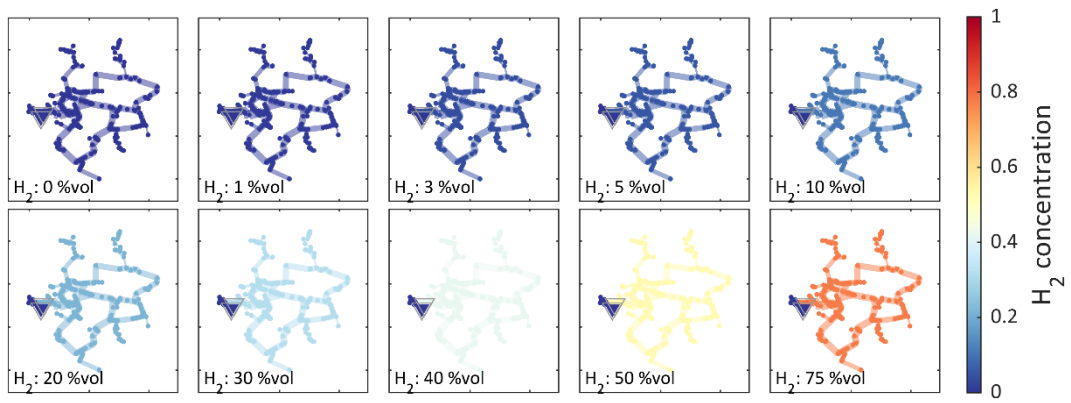


Figure 37. Tracking of gas quality for four sample networks featuring increasing levels of H<sub>2</sub> injections. H<sub>2</sub> injection point is constrained close to the source of NG.

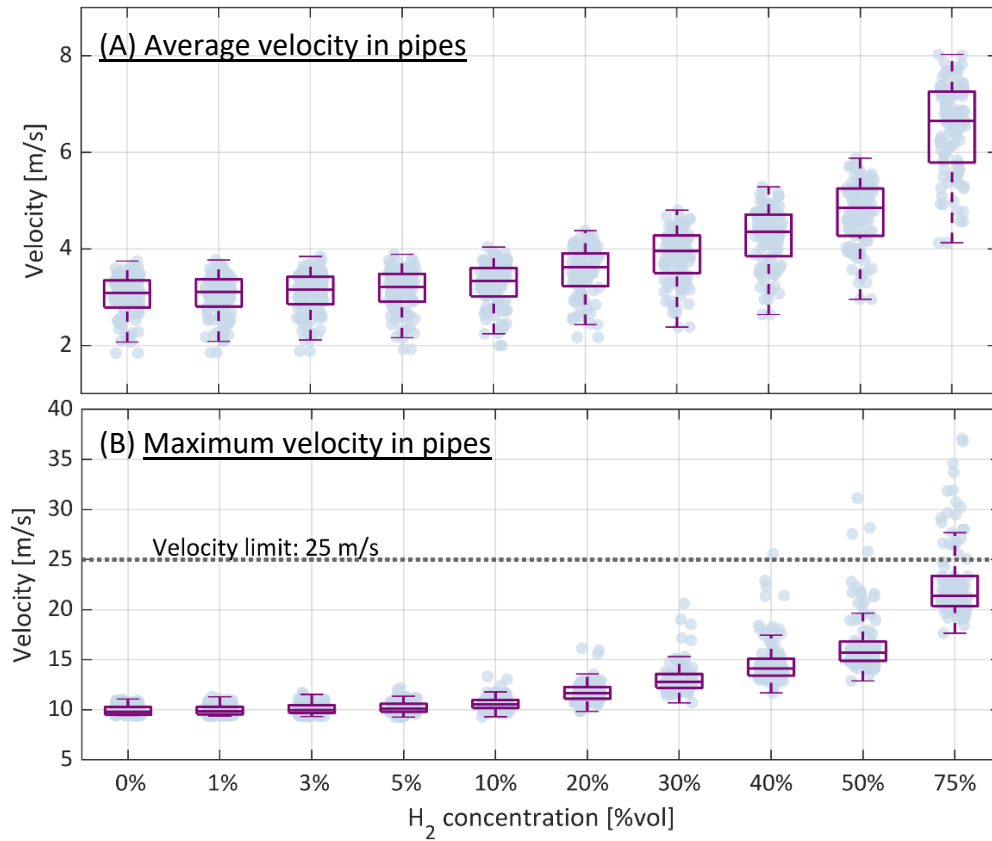


Figure 38. Evolution of average (panel A) and maximum (panel B) gas velocity in pipelines with increasing H<sub>2</sub> concentrations. H<sub>2</sub> injection point is constrained close to NG source.

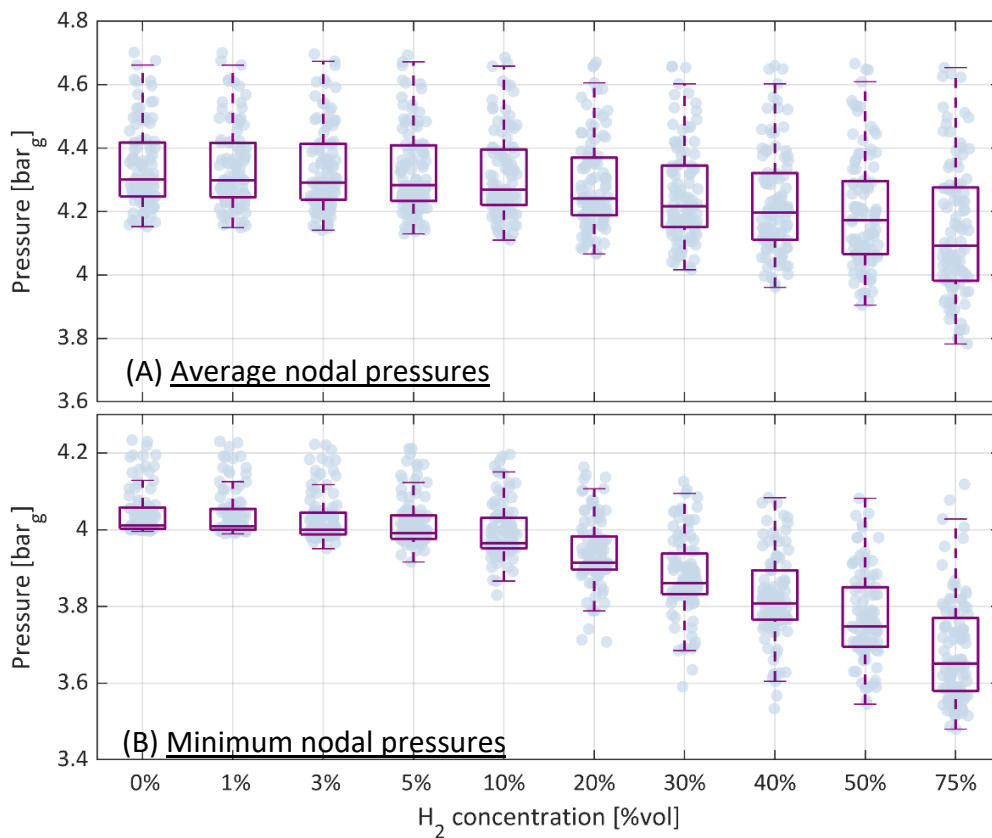
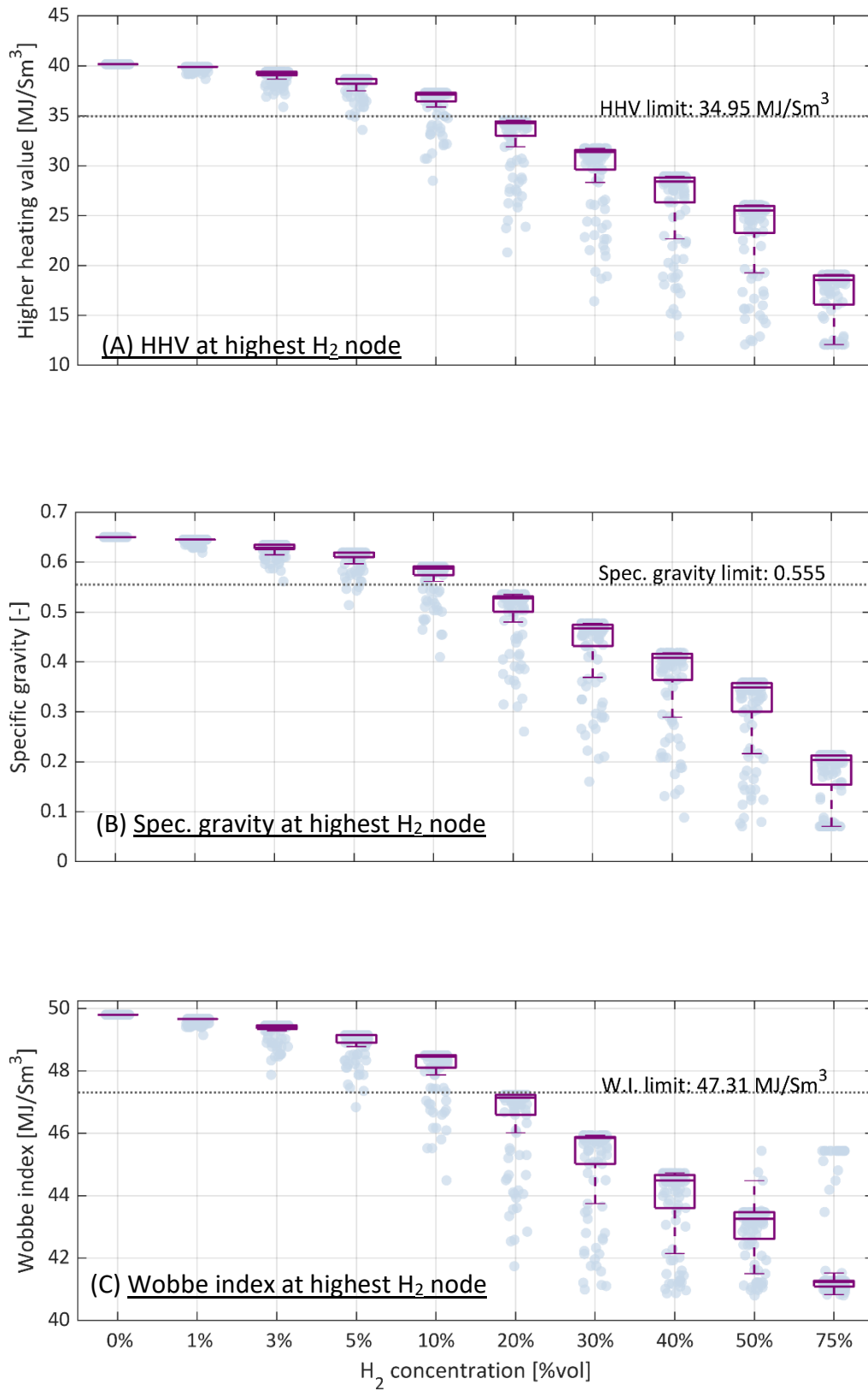


Figure 39. Evolution of average (panel A) and minimum (panel B) nodal pressures with increasing H<sub>2</sub> concentrations. H<sub>2</sub> injection point is constrained close to NG source.



**Figure 40. Evolution of higher heating value (panel A), specific gravity (panel B) and Wobbe Index (panel C) of blend with highest concentration of H<sub>2</sub> received by load nodes. H<sub>2</sub> injection point is constrained close to NG source.**

### 5.3.2 Case B: effect of hydrogen injection at arbitrary locations in the grid

Intuitively, a lower uniformity in the quality of gas is obtained when the hydrogen injection occurs at arbitrary locations within the network. The point of injection may be found close to the NG source or in remote areas of the distribution grid. The resulting stationary patterns of the H<sub>2</sub> concentrations at increasing penetration levels are depicted in Figure 42. The establishment of regions with uneven concentration levels is considerably more frequent than in the previous case. More critically, even at low H<sub>2</sub> penetration levels, clusters of nodes surrounding the point of injection receive pure hydrogen or H<sub>2</sub>-rich blends, while the remaining regions of the network receive natural gas in predominant shares or pure form. The distributions of the H<sub>2</sub> concentrations delivered to consumption nodes (Figure 41) highlight that an increased number of users receive higher concentrations than the targeted levels with respect to the case of upstream H<sub>2</sub> injection.

As in the previous case, the injection of H<sub>2</sub> causes a general increase in the gas velocities (Figure 43). Risks of exceeding the velocity limits of 25 m/s are higher than in case A. Violations are recorded starting from H<sub>2</sub> penetrations of 30%vol and result to be more frequent at higher penetration levels. Limits are exceeded in more than half the networks when hydrogen accounts for the 75%vol of the distributed blend. Even in these cases, however, the maximum velocities are higher than 40 m/s only in rare (12%) observations.

The injection of hydrogen in free locations of the grid has a two-fold effect on the pressures. In some cases, it causes a drop in the minimum pressure of the grid, as it was previously observed. In most cases, however, H<sub>2</sub> is supplied in peripheral regions of the network (i.e., not nearby the source of NG) which generates the opposite effect of sustaining the local pressure levels. Accordingly, the effect on the pressures of the grid sensibly depends on the location of the hydrogen injection. While minimum pressure constraints are never violated, overpressures are recorded starting from penetrations of 40%vol of H<sub>2</sub> (2% of cases) and become more frequent for higher penetration levels (12% of occurrences at 50%vol H<sub>2</sub> and 53% of occurrences at 75%vol H<sub>2</sub>).

When the injection of H<sub>2</sub> occurs at random and peripheral nodes of the grid, gas quality is very sensibly affected at nodes in the near surroundings. Due to the uneven distribution of the H<sub>2</sub> concentrations, even small quantities of hydrogen can produce violations of the quality constraints (Figure 45). Violations are recorded starting from targeted blends of 1%vol onwards, while a targeted H<sub>2</sub> penetration of 3%vol generates quality violations of HHV, specific gravity and Wobbe index in more than half the networks. Similarly as in the previous case, blend qualities become systematically not compliant to legislative restrictions (100% of observations) when admixtures equal or higher than 20%vol are targeted.

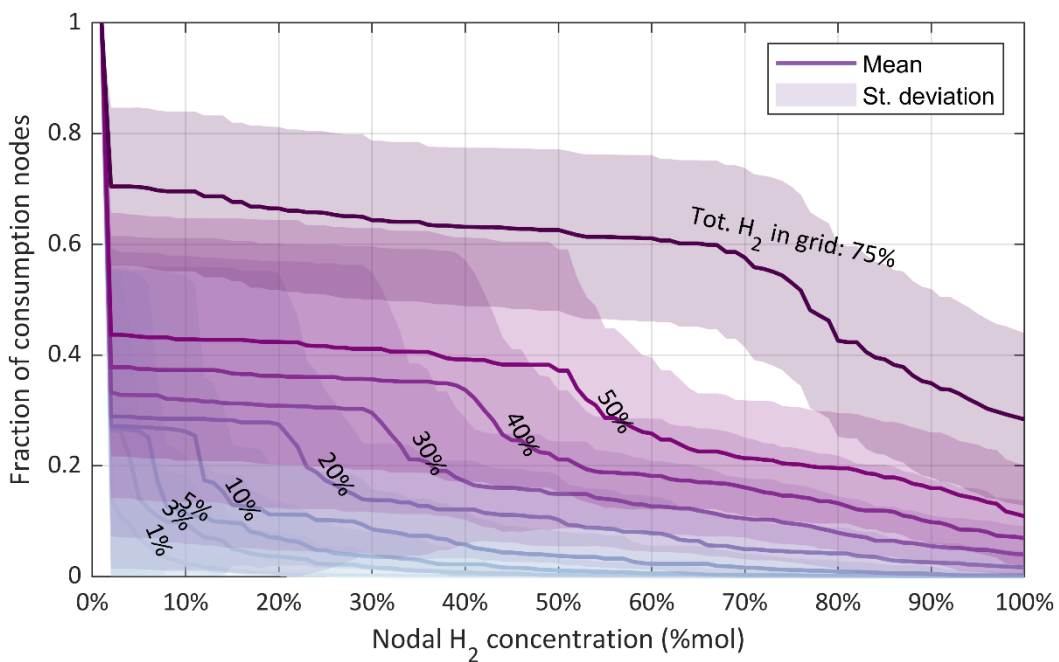


**Figure 41. Distribution of H<sub>2</sub> concentrations received by consumption nodes: fraction of load nodes for which the received H<sub>2</sub> molar concentration exceeds a given value. H<sub>2</sub> injection point is freely placed in the grid.**

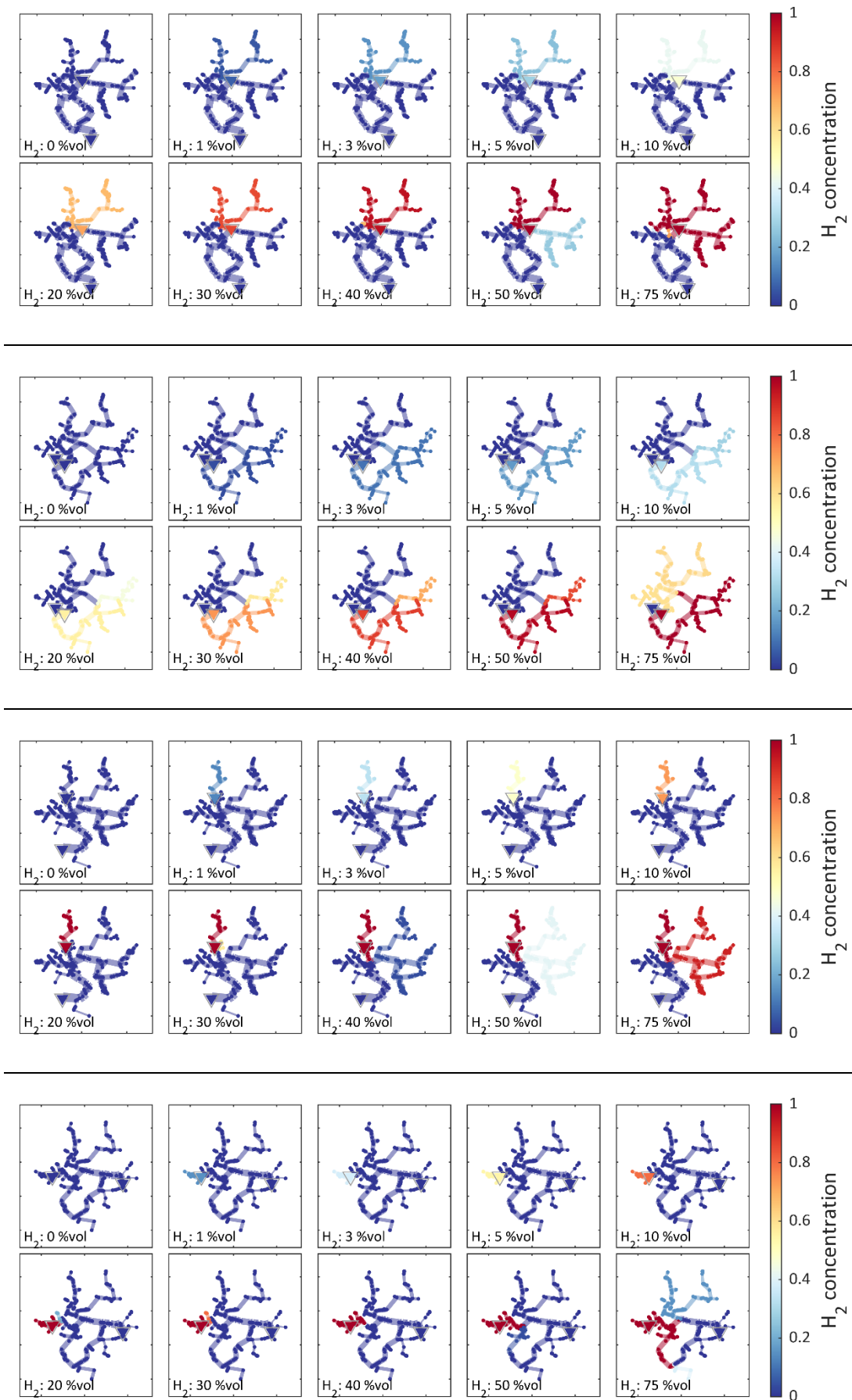


Figure 42. Tracking of gas quality for four sample networks featuring increasing levels of H<sub>2</sub> injections. H<sub>2</sub> injection point is freely placed close to the source of NG.

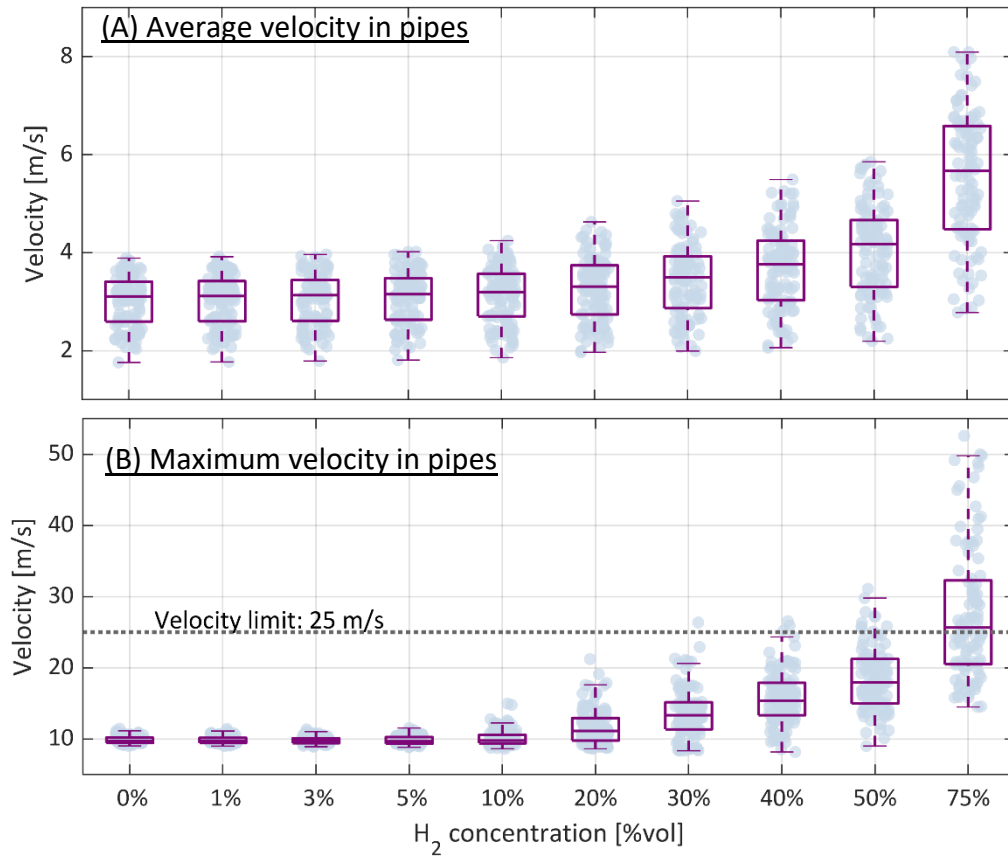


Figure 43. Evolution of average (panel A) and maximum (panel B) gas velocity in pipelines with increasing hydrogen concentrations. H<sub>2</sub> injection point is freely placed in the grid.

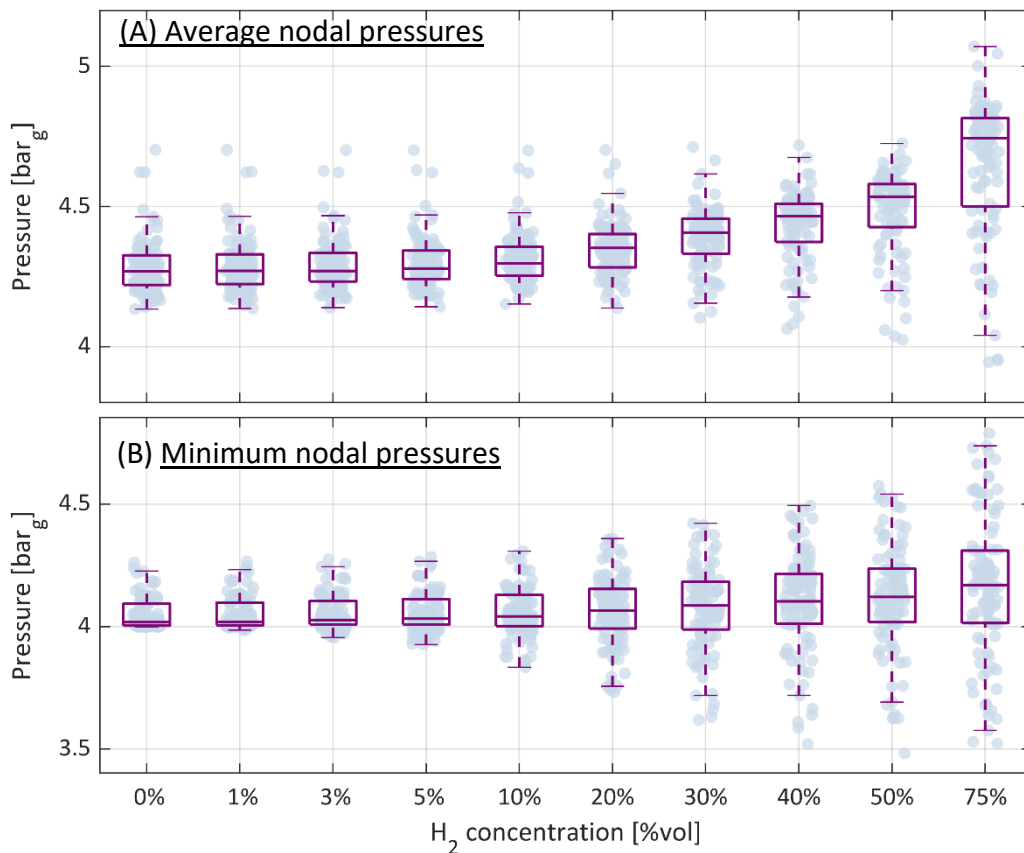


Figure 44. Evolution of average (panel A) and minimum (panel B) nodal pressures with increasing hydrogen concentrations. H<sub>2</sub> injection point is freely placed in the grid.

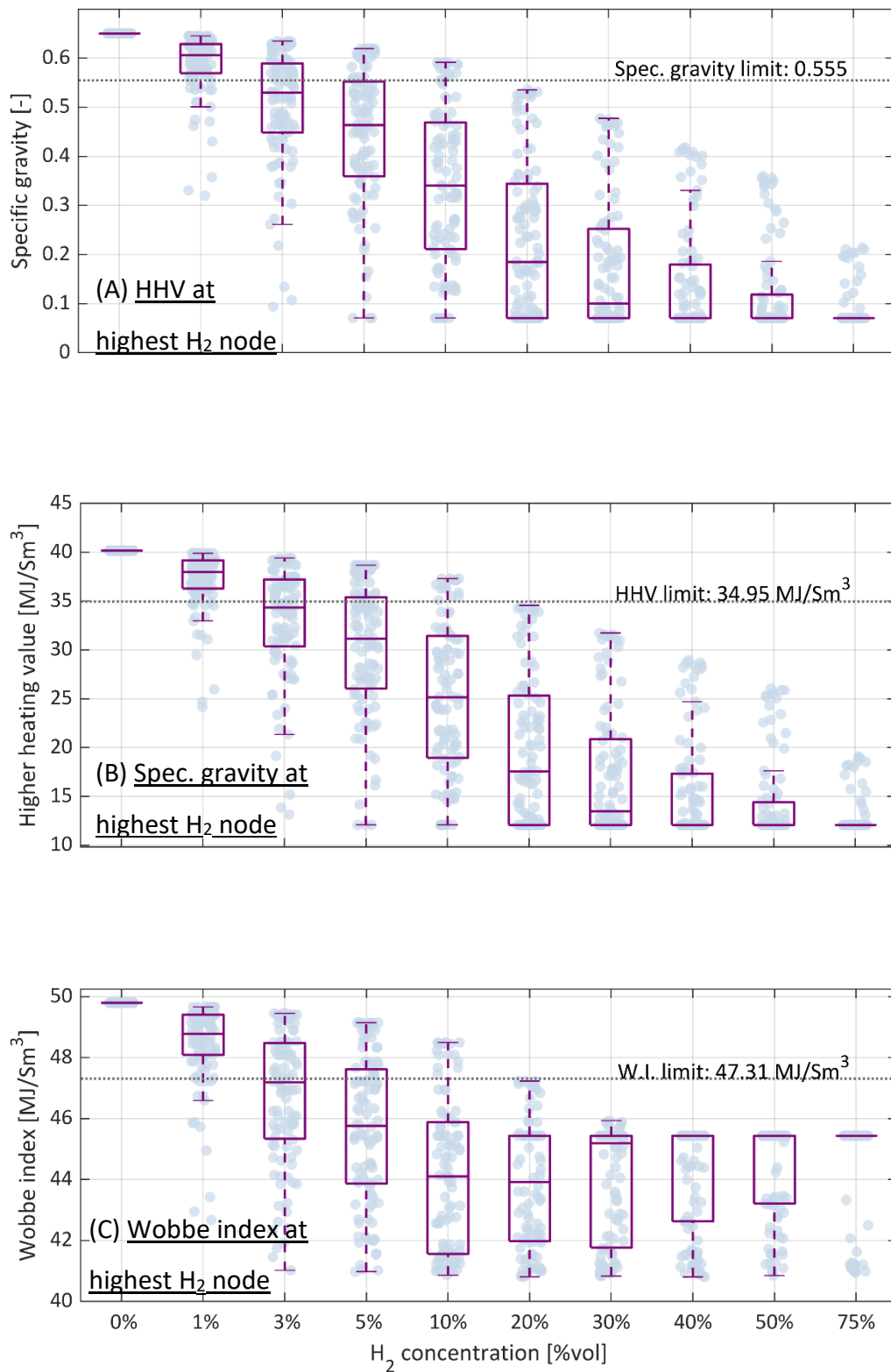


Figure 45. Evolution of higher heating value (panel A), specific gravity (panel B) and Wobbe Index (panel C) of blend with highest concentration of H<sub>2</sub> received by load nodes. H<sub>2</sub> injection point is freely placed in the grid.

## 5.4 Concluding remarks

With increasing momentum gained by the deployment of alternative fuels in gas networks, the proposed study has analysed the impact of the direct injection of increasing quantities of hydrogen in one hundred gas networks. Two main cases have been investigated, the first of which constrained the location of the injection facility close to the NG citygate (desirable option for more uniform H<sub>2</sub> concentrations) and the latter using free locations for the H<sub>2</sub> injection (realistic scenario in the case of power-to-gas plants at the service of the electrical grid).

The responses of the networks have been compared against operational and quality limits set by the Italian law. Results evidence that the principal criticalities linked to the use of H<sub>2</sub> are on the quality of gas, while no violations on the system hydraulics are recorded in most cases, unless for significant hydrogen penetration levels (around 50% of the total volume).

Larger H<sub>2</sub> contributions to the total demand are obtainable when hydrogen is injected close to the source of NG. In these conditions, effects are mitigated both on the velocities and on the quality of the blend (higher heating value, specific gravity, Wobbe index) distributed to the users. Hydrogen penetrations of 10%vol cause quality violations in 16 networks out of 100, while penetrations of 20%vol lead to non-compliance issues in all (100%) the cases. Velocities are never violated before H<sub>2</sub> penetrations of 40%vol (1% of cases) and are still observed in a minority of cases for higher injection levels.

The sensitivity of the networks is significantly higher when hydrogen is injected in free and peripheral regions. Serious quality issues are already encountered at low hydrogen injections: H<sub>2</sub> penetrations of 3%vol lead to gas quality violations in more than 50% of the cases. In rare occurrences, maximum velocities are exceeded already at for 30%vol of H<sub>2</sub>, but violations remain limited in number and entity also for higher penetration levels.

Minimum pressures are never violated in all the cases, partially due to the original assumption regarding the oversizing of the system. It has been observed that an upstream injection of H<sub>2</sub> (close to NG source) leads to higher pressure drops in the system, therefore causing lower average pressures. On the other hand, injecting hydrogen in peripheral regions can even support the network operations, producing an increase in the pressure profiles. It also emerged that, in

the latter case, some networks undergo overpressure contingencies ( $p > 5 \text{ bar}_g$ ) in order to guarantee the targeted injection rates, when  $\text{H}_2$  penetrations are equal or higher than 40%vol.

Hydrogen is distributed in different shares among the network users, even when the injection is carried out at upstream network sections. Results showed that, on average, around 10-20% of users receive significantly higher  $\text{H}_2$  concentrations than the desired system-wide levels, at penetrations higher than 10%vol. Blend uniformities are not fully achieved at lower injection levels either.

The findings evidence that medium-pressure distribution systems offer an overall adequate structural readiness to accommodate even significant shares of hydrogen. The main barrier to a massive deployment of  $\text{H}_2$  is constituted by quality requirements (specific gravity in first place). Transitional and demonstrational applications of hydrogen injections with total contributions up to 10%vol can however take place with low risks of non-compliance to the legislative thermophysical properties of the gas, as long as attention is given to the location of the injection facility. Since  $\text{H}_2$  concentrations received by the users are not uniform in most of the cases, particular care should be devoted to the metering of gas for billing purposes. Gas quality tracking and energy-based billing systems should be integrated even for modest decentralized hydrogen injections.

A significant renovation of the portfolio of end-user appliances (especially the older ones), of the minor non-pipeline elements of the distribution networks and, finally, of the legislative framework, will be needed to scale the deployment of  $\text{H}_2$ . If these conditions are met, a full exploitation of the above demonstrated structural capacity of the grids will offer a realistic option for the decarbonization of district-level gas networks, for the widespread adoption of power-to-gas technologies with direct  $\text{H}_2$  grid injection, and for the establishment of integrated and low-carbon distribution systems.

# Chapter 6

## Conclusions

The overall contribution of this thesis is the development of a methodology for the creation of synthetic gas network models and their deployment for assessing the injection of hydrogen in distribution gas grids. The work responds to the identified scarceness of publicly available gas network data, which constitutes a limitation to the research in the field. In fact, the generation of several realistic network models can enable systematic investigations onto a high number of case studies, with evident benefits in terms of validity and extendibility of the results. While synthetic network models are already acknowledged as a powerful support to the assessment of electricity grids, no similar methodologies have ever been applied to gas network systems.

A topological characterization of distribution gas networks has been undertaken, focusing degree-related properties, network loops, clustering of nodes, average path lengths and length of the pipelines. The intrinsic differences existing among different hierarchical pressure tiers have been suitably highlighted.

The topological information on real gas grids has been deployed as a benchmark to validate a novel algorithm for the establishment of synthetic network topologies. The tool replicates the spatial and topological characteristics of an arbitrary reference input network. As demonstrated, a high number of unique network topologies can be generated, as the probabilistic nature of the tool ensures that each execution leads to a different output network. Furthermore, it has been highlighted how the tool can handle complex networks with multiple

pressure tiers. A suitable calibration of the model parameters for every pressure level has provided a satisfactory agreement between the real and the synthetic network properties. The comparison has been carried out over the degree distributions, the pipeline length distributions, the clustering coefficient and the average path lengths.

The following step has addressed the need to assign technical specifications to the grids generated as from above. For this purpose, a rigorous automated tool for the technical design of distribution grids has been created. The tool offers a high flexibility, as it addresses the sizing of distribution systems with arbitrary topology and design parameters, including nominal and limit pressure and velocity values.

The application of the technical designer to 10,000 synthetic medium-pressure network models has evidenced the accuracy of the tool, which ensures that the target design parameters are always respected (i.e., the synthetic networks operating at design conditions never violate minimum pressures and maximum velocities). The structural and hydraulic properties of these networks have been observed in a statistical perspective. Despite their general correctness and realism, substantial variations in the network properties have been observed, highlighting the limit of studies carried out over a single network, which cannot gather these differences.

In a final application, the work has addressed the hydraulic and gas quality effect of injecting hydrogen in distribution gas grids. The analysis has been executed over 100 synthetic networks and results have been derived in a statistical fashion. What emerged is that most networks offer the structural capacity to receive even extreme admixtures of up to 75% vol, especially when pure hydrogen is injected nearby the city-gate that supplies natural gas to the system. Risks of exceeding maximum velocities due to increased volume flow rates ( $H_2$  volumes are less energy-dense than natural gas) are limited, or zero, for  $H_2$  penetrations up to 30-40%, depending on the injection location. Minimum pressures are never violated, although it has been highlighted that criticalities may arise in weaker systems operating close to their maximum capacity. Gas quality issues represent the most limiting factors to blending  $H_2$  into distribution gas grids. Results are extremely sensitive to the location of the injection facility. When  $H_2$  is injected close to the gas city-gate, low risks (16%) of violating quality

limits are experienced for admixtures up to 10%vol. However, violations are already recorded in all the cases for hydrogen penetrations of 20%vol. When free locations for H<sub>2</sub> injection are considered (e.g., case of power-to-gas facility prioritizing electrical grid services) 3%vol admixtures may cause quality issues in more than 50% of networks.

The results provide evidence on the added value offered by the proposed tool: in opposition to traditional case-specific investigations, the network generator enables statistical studies on gas networks carried out over a large basis of synthetic and realistic grids, accounting for the variety of responses found in real-world systems. Further investigations may address its utilization in multi-gas systems involving other green fuels like biomethane.

Additionally, given the technical relevance and the policy interest in the topic, further research will be pursued for the statistical assessment of coupled distribution-level electricity and gas networks, taking advantage of existing companion models for the synthetization of electricity networks. In this framework, valuable generalized guidelines may be provided on the impacts and benefits of the integration of coupling technologies like power-to-gas, and on their best locations accounting for both gas and electrical grid operation.

As final remark, as highlighted throughout the thesis, while the synthetic gas network generator has been primarily developed to enable statistical studies on gas grids, several other applications and adaptations can be envisioned. Among these, its deployment for the anonymization of real-world sensible network data has been mentioned. Other purposes may rely in problems of optimal network design and expansions to accommodate larger shares of renewable gases.

# References

- [1] IRENA. Renewable Energy Statistics 2020. 2020.
- [2] British Petroleum. Statistical Review of World Energy 2020 | 69th edition. 2020.
- [3] UNFCCC Secretariat. Paris Agreement. 2015. <https://doi.org/10.1201/9781351116589-2>.
- [4] European Parliament. Directive (EU) 2018/2001 of the European Parliament and of the Council on the promotion of the use of energy from renewable sources. vol. 2018. 2018.
- [5] European Commission. Clean energy for all Europeans. 2019. <https://doi.org/10.2833/9937>.
- [6] European Commission. Stepping up Europe's 2030 climate ambition - COM(2020) 562 final. 2020.
- [7] RAGWITZ JWBBMMMSC, HARMELINK M. Renewable energy directive target - Study for the ITRE committee. n.d.
- [8] International Energy Agency. World Energy Outlook 2020 2020;2050:1–461.
- [9] KEMA Consulting GmbH, Imperial College. Integration of Renewable Energy in Europe. 2014.
- [10] Wang Y, Silva V, Lopez-Botet-Zulueta M. Impact of high penetration of variable renewable generation on frequency dynamics in the continental Europe interconnected system. IET Renew Power Gener 2016;10:10–6. <https://doi.org/10.1049/iet-rpg.2015.0141>.
- [11] Cheng M, Wu J, Galsworthy SJ, Ugalde-Loo CE, Gargov N, Hung WW, et al. Power system frequency response from the control of bitumen tanks. IEEE Trans Power Syst 2016;31:1769–78. <https://doi.org/10.1109/TPWRS.2015.2440336>.
- [12] Thomson M, Infield DG. Network power-flow analysis for a high

- penetration of distributed generation. *IEEE Trans Power Syst* 2007;22:1157–62. <https://doi.org/10.1109/TPWRS.2007.901290>.
- [13] Eltawil MA, Zhao Z. Grid-connected photovoltaic power systems: Technical and potential problems-A review. *Renew Sustain Energy Rev* 2010;14:112–29. <https://doi.org/10.1016/j.rser.2009.07.015>.
- [14] Aziz T, Ketjoy N. PV Penetration Limits in Low Voltage Networks and Voltage Variations. *IEEE Access* 2017;5:16784–92. <https://doi.org/10.1109/ACCESS.2017.2747086>.
- [15] Davis SJ, Lewis NS, Shaner M, Aggarwal S, Arent D, Azevedo IL, et al. Net-zero emissions energy systems. *Science* (80- ) 2018;360. <https://doi.org/10.1126/science.aas9793>.
- [16] Mancarella P. MES (multi-energy systems): An overview of concepts and evaluation models. *Energy* 2014;65:1–17. <https://doi.org/10.1016/j.energy.2013.10.041>.
- [17] International Energy Agency. *Key World Energy Statistics 2020*. vol. 33. 2020.
- [18] Odyssee-Mure project. Sectorial profile: Households n.d. <https://www.odyssee-mure.eu/publications/efficiency-by-sector/>.
- [19] Bertelsen N, Mathiesen BV. EU-28 residential heat supply and consumption: Historical development and status. *Energies* 2020;13. <https://doi.org/10.3390/en13081894>.
- [20] Eser P, Singh A, Chokani N, Abhari RS. Effect of increased renewables generation on operation of thermal power plants. *Appl Energy* 2016;164:723–32. <https://doi.org/10.1016/j.apenergy.2015.12.017>.
- [21] Vaccariello E, Cavana M, Leone P. Impact of Renewable Power Penetration on Back-Up Thermal Power Plants and Storage Capacity. XIII Res. Dev. Power Eng. 28 nov-1 Dec 2017, Warsaw, 2017.
- [22] European Commission. *Powering a climate-neutral economy: An EU Strategy for Energy System Integration - COM(2020) 299 final*. Brussels: 2020.
- [23] Navigant, Gas for Climate. *Gas for Climate. The optimal role for gas in a net-zero emissions energy system*. 2019.
- [24] Quarton CJ, Samsatli S. Power-to-gas for injection into the gas grid: What can we learn from real-life projects, economic assessments and systems

- modelling? *Renew Sustain Energy Rev* 2018;98:302–16.  
<https://doi.org/10.1016/j.rser.2018.09.007>.
- [25] Thema M, Bauer F, Sterner M. Power-to-Gas: Electrolysis and methanation status review. *Renew Sustain Energy Rev* 2019;112:775–87.  
<https://doi.org/10.1016/j.rser.2019.06.030>.
- [26] Speirs J, Balcombe P, Johnson E, Martin J, Brandon N, Hawkes A. A greener gas grid: What are the options. *Energy Policy* 2018;118:291–7.  
<https://doi.org/10.1016/j.enpol.2018.03.069>.
- [27] European Commission. A hydrogen strategy for a climate-neutral Europe - COM(2020) 301 final. Brussels: 2020.
- [28] Quarton CJ, Samsatli S. Should we inject hydrogen into gas grids? Practicalities and whole-system value chain optimisation. *Appl Energy* 2020;275:115172. <https://doi.org/10.1016/j.apenergy.2020.115172>.
- [29] International Energy Agency. Hydrogen Projects Database n.d. <https://www.iea.org/reports/hydrogen-projects-database> (accessed January 11, 2021).
- [30] Hydrogen Europe. Hydrogen in the EU’s Economic Recovery Plans. 2020.
- [31] Fuel Cell and Hydrogen Joint Undertaking. Hydrogen Roadmap Europe - A sustainable pathway for the European energy transition. 2019.  
<https://doi.org/10.2843/249013>.
- [32] Sadler D, Cargill A, Crowther M, Rennie A, Watt J, Burton S, et al. H21 Leeds City Gate Report. *Leeds City Gate* 2016:1–382.
- [33] Qadrdan M, Abeysekera M, Wu J, Jenkins N, Winter B. The future of gas networks. The role of gas networks in a low carbon energy system. 2020.
- [34] Melaina MW, Antonia O, Penev M. Blending Hydrogen into Natural Gas Pipeline Networks: A Review of Key Issues. vol. 303. 2013.
- [35] Rotunno P, Lanzini A, Leone P. Energy and economic analysis of a water scrubbing based biogas upgrading process for biomethane injection into the gas grid or use as transportation fuel. *Renew Energy* 2017;102:417–32.  
<https://doi.org/10.1016/j.renene.2016.10.062>.
- [36] European Biogas Association. EBA Statistical report 2019. 2019.
- [37] European Biogas Association, Gas Infrastructure Europe. The ‘European Biomethane Map 2020 ’ shows a 51 % increase of biomethane plants in Europe in two years. 2020.

- [38] Guidehouse, Climate G for. Setting a binding target for 11 % renewable gas. 2021.
- [39] CEN. EN 16723-1. Natural gas and biomethane for use in transport and biomethane for injection in the natural gas network - Part 1: Specifications for biomethane for injection in the natural gas network 2016.
- [40] Ministero dello Sviluppo Economico. Decreto 2 marzo 2018 (“Decreto biometano”) (Italian). 2018.
- [41] Gestore dei Servizi Energetici (GSE). CONTATORE DM 2 MARZO 2018 n.d. <https://www.gse.it/contatore-biometano> (accessed April 12, 2021).
- [42] Altfeld K, Pinchbeck D. Admissible hydrogen concentrations in natural gas systems. *Gas Energy* 2013;March/2013:1–16.
- [43] de Vries H, Mokhov A V., Levinsky HB. The impact of natural gas/hydrogen mixtures on the performance of end-use equipment: Interchangeability analysis for domestic appliances. *Appl Energy* 2017;208:1007–19. <https://doi.org/10.1016/j.apenergy.2017.09.049>.
- [44] Alliat I, Heerings. Assessing the durability and integrity of natural gas infrastructures for transporting and distributing mixtures of hydrogen and natural gas. n.d.
- [45] Abeysekera M, Wu J, Jenkins N, Rees M. Steady state analysis of gas networks with distributed injection of alternative gas. *Appl Energy* 2016;164:991–1002. <https://doi.org/10.1016/j.apenergy.2015.05.099>.
- [46] Pellegrino S, Lanzini A, Leone P. Greening the gas network – The need for modelling the distributed injection of alternative fuels. *Renew Sustain Energy Rev* 2017;70:266–86. <https://doi.org/10.1016/j.rser.2016.11.243>.
- [47] Gondal IA. Hydrogen integration in power-to-gas networks. *Int J Hydrogen Energy* 2019;44:1803–15. <https://doi.org/10.1016/j.ijhydene.2018.11.164>.
- [48] Osiadacz AJ, Chaczykowski M. Modeling and Simulation of Gas Distribution Networks in a Multienergy System Environment. *Proc IEEE* 2020;108:1580–95. <https://doi.org/10.1109/JPROC.2020.2989114>.
- [49] Cavana M, Leone P. Biogas blending into the gas grid of a small municipality for the decarbonization of the heating sector. *Biomass and Bioenergy* 2019;127:105295. <https://doi.org/10.1016/j.biombioe.2019.105295>.
- [50] Cavana M. Gas network modelling for a multi-gas system. Politecnico di

Torino, 2020.

- [51] Cavana M, Mazza A, Chicco G, Leone P. Electrical and gas networks coupling through hydrogen blending under increasing distributed photovoltaic generation. *Appl Energy* 2021;290:116764. <https://doi.org/10.1016/j.apenergy.2021.116764>.
- [52] Qadrdan M, Abeyssekera M, Chaudry M, Wu J, Jenkins N. Role of power-to-gas in an integrated gas and electricity system in Great Britain. *Int J Hydrogen Energy* 2015;40:5763–75. <https://doi.org/10.1016/j.ijhydene.2015.03.004>.
- [53] Guandalini G, Campanari S, Romano MC. Power-to-gas plants and gas turbines for improved wind energy dispatchability: Energy and economic assessment. *Appl Energy* 2015;147:117–30. <https://doi.org/10.1016/j.apenergy.2015.02.055>.
- [54] Abeysinghe S, Wu J, Sooriyabandara M, Abeyssekera M, Xu T, Wang C. Topological properties of medium voltage electricity distribution networks. *Appl Energy* 2018;210:1101–12. <https://doi.org/10.1016/j.apenergy.2017.06.113>.
- [55] Prettico G, Gangale F, Mengolini A, Lucas A, Fulli G. Distribution System Operators Observatory - From European Electricity Distribution Systems to Representative Distribution Networks. 2016.
- [56] Resources | PES Test Feeder n.d. <https://site.ieee.org/pes-testfeeders/resources/> (accessed January 11, 2021).
- [57] Power Systems Test Case Archive - UWEE n.d. <https://labs.ece.uw.edu/pstca/> (accessed January 11, 2021).
- [58] Postigo Marcos F, Mateo Domingo C, Gómez San Román T, Palmintier B, Hodge B-M, Krishnan V, et al. A Review of Power Distribution Test Feeders in the United States and the Need for Synthetic Representative Networks. *Energies* 2017;10:1896. <https://doi.org/10.3390/en10111896>.
- [59] Transmission network datasets - wiki.openmod-initiative.org n.d. [https://wiki.openmod-initiative.org/wiki/Transmission\\_network\\_datasets](https://wiki.openmod-initiative.org/wiki/Transmission_network_datasets) (accessed April 13, 2021).
- [60] DiNeMo | JRC Smart Electricity Systems and Interoperability n.d. <https://ses.jrc.ec.europa.eu/dinemo> (accessed April 16, 2021).
- [61] Grzanic, Flammini, Prettico. Distribution Network Model Platform: A First

- Case Study. *Energies* 2019;12:4079. <https://doi.org/10.3390/en12214079>.
- [62] Gershenson D, Rohrer B, Lerner A. Predictive model for accurate electrical grid mapping 2019. <https://engineering.fb.com/2019/01/25/connectivity/electrical-grid-mapping/> (accessed January 11, 2021).
- [63] Lichtinghagen J, Sieberichs M, Moser A, Kübler A. Medium voltage network planning considering the current network and geographical restrictions. 2017 6th Int. Conf. Clean Electr. Power Renew. Energy Resour. Impact, ICCEP 2017, Institute of Electrical and Electronics Engineers Inc.; 2017, p. 689–93. <https://doi.org/10.1109/ICCEP.2017.8004765>.
- [64] Soltan S, Zussman G. Generation of synthetic spatially embedded power grid networks. *IEEE Power Energy Soc Gen Meet 2016;2016-Novem*:1–5. <https://doi.org/10.1109/PESGM.2016.7741383>.
- [65] Soltan S, Loh A, Zussman G. A learning-based method for generating synthetic power grids. *IEEE Syst J* 2019;13:625–34. <https://doi.org/10.1109/JSYST.2018.2825785>.
- [66] Birchfield AB, Xu T, Gegner KM, Shetye KS, Overbye TJ. Grid Structural Characteristics as Validation Criteria for Synthetic Networks. *IEEE Trans Power Syst* 2017;32:3258–65. <https://doi.org/10.1109/TPWRS.2016.2616385>.
- [67] Almeida D, Abeysinghe S, Ekanayake MP, Godaliyadda RI, Ekanayake J, Pasupuleti J. Generalized approach to assess and characterise the impact of solar PV on LV networks. *Int J Electr Power Energy Syst* 2020;121:106058. <https://doi.org/10.1016/j.ijepes.2020.106058>.
- [68] Abeysinghe S. A statistical assessment tool for electricity distribution networks. Cardiff University, 2018.
- [69] Schweitzer E, Scaglione A, Monti A, Pagani GA. Automated Generation Algorithm for Synthetic Medium Voltage Radial Distribution Systems. *IEEE J Emerg Sel Top Circuits Syst* 2017;7:271–84. <https://doi.org/10.1109/JETCAS.2017.2682934>.
- [70] Sadeghian H, Wang Z. AutoSynGrid: A MATLAB-based toolkit for automatic generation of synthetic power grids. *Int J Electr Power Energy Syst* 2020;118:105757. <https://doi.org/10.1016/j.ijepes.2019.105757>.

- [71] Mikolajková M, Haikarainen C, Saxén H, Pettersson F. Optimization of a natural gas distribution network with potential future extensions. *Energy* 2017;125:848–59. <https://doi.org/10.1016/j.energy.2016.11.090>.
- [72] Torkinejad M, Mahdavi I, Mahdavi Amiri N, Seyed Esfahani M. Topology Design and Component Selection in an Urban Gas Network: Simultaneous Optimization Approach. *J Pipeline Syst Eng Pract* 2019;10:04018035. [https://doi.org/10.1061/\(asce\)ps.1949-1204.0000359](https://doi.org/10.1061/(asce)ps.1949-1204.0000359).
- [73] Fayez O, El-Mahdy M, Ezz M, Ahmed H, Metwalli S. Computer aided optimization of natural gas pipe networks using genetic algorithm. *Appl Soft Comput* 2010;10:1141–50. <https://doi.org/10.1016/j.asoc.2010.05.010>.
- [74] Hansen CT, Madsen K, Nielsen HB. Optimization of pipe networks. *Math Program* 1991;52:45–58. <https://doi.org/10.1007/BF01582879>.
- [75] Zhang J, Zhu D. A bilevel programming method for pipe network optimization. *SIAM J Optim* 1996;6:838–57. <https://doi.org/10.1137/S1052623493260696>.
- [76] Han F, Zio E, Kopustinskas V, Praks P. Quantifying the importance of elements of a gas transmission network from topological, reliability and controllability perspectives, considering capacity constraints. *Risk, Reliab. Saf. Innov. Theory Pract. - Proc. 26th Eur. Saf. Reliab. Conf. ESREL 2016, 2017*, p. 419. <https://doi.org/10.1201/9781315374987-389>.
- [77] Wang P, Yu B, Sun D, Ao S, Zhai H. Study on Topology-Based Identification of Sources of Vulnerability for Natural Gas Pipeline Networks. *Lect. Notes Comput. Sci. (including Subser. Lect. Notes Artif. Intell. Lect. Notes Bioinformatics)*, vol. 10862 LNCS, Springer Verlag; 2018, p. 163–73. [https://doi.org/10.1007/978-3-319-93713-7\\_13](https://doi.org/10.1007/978-3-319-93713-7_13).
- [78] Genschuh AF, Hiller B, Humpola J, Koch T, Lehmann T, Schwarz R, et al. Gas Network Topology Optimization for Upcoming Market Requirements 2011;09.
- [79] Benner P, Grundel S, Himpe C, Huck C, Streubel T, Tischendorf C. Gas Network Benchmark Models, Springer, Cham; 2018, p. 171–97. [https://doi.org/10.1007/11221\\_2018\\_5](https://doi.org/10.1007/11221_2018_5).
- [80] Lloyd EK, Bondy JA, Murty USR. *Graph Theory with Applications*. vol. 62. 1978. <https://doi.org/10.2307/3617646>.
- [81] Ho CW, Ruehli AE, Brennan PA. The Modified Nodal Approach to

- Network Analysis. IEEE Trans Circuits Syst 1975;22:504–9. <https://doi.org/10.1109/TCS.1975.1084079>.
- [82] Osiadacz AJ. Method of steady-state simulation of a gas network. Int J Syst Sci 1988;19:2395–405. <https://doi.org/10.1080/00207728808964126>.
- [83] Vaccariello E, Leone P, Canavero FG, Stievano IS. Topological modelling of gas networks for co-simulation applications in multi-energy systems. Math Comput Simul 2020;183:244–53. <https://doi.org/10.1016/j.matcom.2019.12.018>.
- [84] Ministero dello Sviluppo Economico. Decreto 16 aprile 2008 - Regola tecnica per la progettazione, costruzione, collaudo, esercizio e sorveglianza delle opere e dei sistemi di distribuzione e di linee dirette del gas naturale con densità non superiore a 0,8. n.d.
- [85] Ester M, Kriegel H-P, Sander J, Xu X. A Density-Based Algorithm for Discovering Clusters in Large Spatial Databases with Noise. 1996.
- [86] CEER. Ceer Benchmarking Report on the Quality of Electricity and Gas Supply-2016: Gas-Technical Operational Quality. 2016.
- [87] UNI 9165:2020, Gas Infrastructures - Pipelines for maximum operating pressure up to and including 0,5 MPa (5 bar) - Design, construction, testing, operation, maintenance and rehabilitation 2020.
- [88] IRENE Pro Gas Pipeline Analysis Software n.d. <https://www.kiwa.com/nl/en/products/irene-pro-network-calculation/> (accessed April 16, 2021).
- [89] Electric and Gas Network Design Software Solution n.d. <https://www.bentley.com/en/solutions/electric-and-gas-network-design> (accessed April 16, 2021).
- [90] Prim RC. Shortest Connection Networks And Some Generalizations. Bell Syst Tech J 1957;36:1389–401. <https://doi.org/10.1002/j.1538-7305.1957.tb01515.x>.
- [91] Vatankhah AR. Comment on “Gene expression programming analysis of implicit Colebrook-White equation in turbulent flow friction factor calculation.” J Pet Sci Eng 2014;124:402–5. <https://doi.org/10.1016/j.petrol.2013.12.001>.
- [92] C. F. Colebrook, C. M. White. Experiments with fluid friction in roughened pipes. Proc R Soc London Ser A - Math Phys Sci 1937;161:367–81.

<https://doi.org/10.1098/rspa.1937.0150>.

- [93] International Energy Agency. Current limits on hydrogen blending in natural gas networks and gas demand per capita in selected locations – Charts – Data & Statistics - IEA n.d. <https://www.iea.org/data-and-statistics/charts/current-limits-on-hydrogen-blending-in-natural-gas-networks-and-gas-demand-per-capita-in-selected-locations> (accessed April 17, 2021).
- [94] Decreto ministeriale 18 maggio 2018 - Gas combustibile, aggiornamento regola tecnica n.d. <https://www.mise.gov.it/index.php/it/normativa/decreti-ministeriali/2038129-decreto-ministeriale-18-maggio-2018-gas-combustibile-aggiornamento-regola-tecnica> (accessed April 17, 2021).
- [95] ISO 6976:2016 - Natural gas -- Calculation of calorific values, density, relative density and Wobbe indices from composition. n.d.
- [96] Segeler CG. Gas Engineers Handbook. Industrial Press, Inc.; 1965.
- [97] UNI EN 437:1995 + A1:1999 n.d. <http://store.uni.com/catalogo/uni-en-437-1995-a1-1999> (accessed April 12, 2021).